KINETICS OF LIPASE-CATALYSED FUNCTIONALISATION OF EPSILON-CAPROLACTONE MONOMER AND OLIGOMER WITH METHYL-D-GLUCOPYRANOSIDE

MUHAMMAD NAZIZ BIN SAAT

FACULTY OF SCIENCE
UNIVERSITY OF MALAYA
KUALA LUMPUR

2019

KINETICS OF LIPASE-CATALYSED FUNCTIONALISATION OF EPSILON-CAPROLACTONE MONOMER AND OLIGOMER WITH METHYL-D-GLUCOPYRANOSIDE

MUHAMMAD NAZIZ BIN SAAT

THESIS SUBMITTED IN FULFILMENT OF THE REQUIREMENTS FOR THE DEGREE OF DOCTOR OF PHILOSOPHY

INSTITUTE OF BIOLOGICAL SCIENCES
FACULTY OF SCIENCE
UNIVERSITY OF MALAYA
KUALA LUMPUR

2019

UNIVERSITY OF MALAYA

ORIGINAL LITERARY WORK DECLARATION

Name of Candidate: **MUHAMMAD NAZIZ BIN SAAT**
Matric No: **SHC140053**
Name of Degree: **DOCTOR OF PHILOSOPHY**
Title of Thesis:
KINETICS OF LIPASE-CATALYSED FUNCTIONALISATION OF EPSILON-CAPROLACTONE MONOMER AND OLIGOMER WITH METHYL-D-GLUCOPYRANOSIDE

Field of Study: **BIOTECHNOLOGY**

I do solemnly and sincerely declare that:

(1) I am the sole author/writer of this Work;
(2) This Work is original;
(3) Any use of any work in which copyright exists was done by way of fair dealing and for permitted purposes and any excerpt or extract from, or reference to or reproduction of any copyright work has been disclosed expressly and sufficiently and the title of the Work and its authorship have been acknowledged in this Work;
(4) I do not have any actual knowledge nor do I ought reasonably to know that the making of this work constitutes an infringement of any copyright work;
(5) I hereby assign all and every rights in the copyright to this Work to the University of Malaya ("UM"), who henceforth shall be owner of the copyright in this Work and that any reproduction or use in any form or by any means whatsoever is prohibited without the written consent of UM having been first had and obtained;
(6) I am fully aware that if in the course of making this Work I have infringed any copyright whether intentionally or otherwise, I may be subject to legal action or any other action as may be determined by UM.

Candidate's Signature Date:

Subscribed and solemnly declared before,

Witness's Signature Date:

Name:
Designation:

KINETICS OF LIPASE-CATALYSED FUNCTIONALISATION OF EPSILON-CAPROLACTONE MONOMER AND OLIGOMER WITH METHYL-D-GLUCOPYRANOSIDE

ABSTRACT

One-pot synthesis of oligomeric sugar ester was carried out by lipase-catalysed esterification of ε-caprolactone (ECL) with methyl-*D*-glucopyranoside (MGP) followed by chain elongation of ECL monomer/oligomer. Functionalisation was performed in a custom-fabricated glass reactor equipped with Rushton turbine impeller using *tert*-butanol as reaction medium. Two-level half-fractional factorial design was employed to analyse the effects of selected operating variables namely lipase (1.2-2.8 % *w*/*v*), initial ε-caprolactone (3.8-11.5 % *w*/*v*), initial methyl-*D*-glucopyranoside (0.04-0.14 % *w*/*v*), temperature (40-60 °C) and agitation rate (90-180 rpm) as a function of maximum dry weight (% *w*/*v*) of MGP-functionalised ECL oligomer (MGP-6-*O*-oligo-ECL). It was found that individual variables *viz.* lipase (X_{Lip}), initial ε-caprolactone (X_{ECL}) and temperature (X_{Temp}) significantly affect the maximum product formation ($p < 0.05$). Two-way interaction effects between variables *viz.* lipase with initial ECL ($X_{Lip}\,X_{ECL}$), lipase with temperature ($X_{Lip}\,X_{Temp}$), initial ECL with initial MGP ($X_{ECL}\,X_{MGP}$), and initial ECL with temperature ($X_{ECL}\,X_{Temp}$) were found to be significant ($p < 0.05$) on the final dry weight of functionalised oligomer. Significant two-way interaction between variables suggested the presence of confounding effect among the variables studied. From descriptive statistic of the half-fractional factorial model, the percentage of variation (R^2) of the regression model was observed at 99.8 %, which indicated good fitting between predicted and actual data. The model validation using residual analysis showed the variation among predicted and experimental data was normally distributed. From the output of response optimizer program, the best conditions for maximum functionalised oligomer production are as follows: lipase loading of (2.8 % *w*/*v*), initial ECL (11.46 %

w/*v*), initial MGP (0.04 % *w*/*v*), temperature (60.0 °C), and agitation rate (90 rpm). The proposed mechanism for the functionalisation includes MGP esterification of ECL monomer/oligomer followed by chain elongation with free 6-hydroxyhexanoate monomer units, and both steps are catalysed by lipase. A ping-pong bi-bi mechanism without ternary complex was proposed for esterification of ECL with MGP with apparent values of kinetic constants namely maximal velocity (V_{max}), Michaelis constant for MGP (K_{mMGP}) and Michaelis constant for ECL (K_{mECL}) at 3.848×10^{-3} M h^{-1}, 8.189×10^{-2} M and 6.050 M, respectively. Chain propagation step of MGP-functionalised ECL oligomer exhibits the behavior of living polymerization mechanism. The apparent rate constant (r_{App}) of chain elongation showed highest value when ECL concentration was increased. Synthesized functionalised oligomer showed narrow range of molecular weight from 1,400 to 1,600 (g mol^{-1}) with more than 90 % ECL conversion achieved. Spectroscopic data established the presence of covalent bonding between terminal hydroxyl group in MGP and terminal carboxyl end group of ECL monomer/oligomer. Thermal analysis indicated three degradation stages of functionalised oligomer as compared to two stages of degradation in neat ECL oligomer. The current study highlighted significant potential for enzyme-mediated, one-pot synthetic process in the production of carbohydrate-functionalised bio-oligomer with controllable molecular weight as platform chemicals.

Keywords: enzyme reactor, functionalisation, lipase, kinetic model, one-pot synthesis.

KINETIK BERMANGKIN-LIPASE TERHADAP PENGFUNGSIAN MONOMER DAN OLIGOMER EPSILON-KAPROLAKTON DENGAN METIL-D-GLUKOPIRANOSIDA

ABSTRAK

Sintesis satu-reaktor oligomer ester gula telah dihasilkan melalui pengesteran bermangkin-lipase di antara epsilon-kaprolakton (ECL) dengan metil-*D*-glukopiranosida (MGP) diikuti oleh tindakbalas pemanjangan rantai monomer/oligomer ECL. Tindak balas pengfungsian dilakukan di dalam reaktor kaca yang dilengkapi dengan pengaduk turbin Rushton menggunakan *tert*-butanol sebagai medium reaksi. Reka bentuk pemfaktoran pecahan digunakan untuk analisis pembolehubah operasi terpilih iaitu lipase (1.2-2.8 % *w*/*v*), kepekatan awal epsilon-kaprolakton (3.8-11.5 % *w*/*v*), kepekatan awal metil-*D*-glukopiranosida (0.04-0.14 % *w*/*v*), suhu (40-60 °C) dan kadar agitasi (90-180 rpm) terhadap berat kering maksimum (% *w*/*v*) MGP-6-*O*-oligo-ECL. Pemboleh ubah individu seperti lipase (X_{Lip}), kepekatan awal epsilon-kaprolakton (X_{ECL}) dan suhu (X_{Temp}) memberi kesan yang signifikan kepada pembentukan maksimum produk ($p < 0.05$). Kesan interaksi dua hala di antara pemboleh ubah iaitu lipase dengan kepekatan awal ECL ($X_{\text{Lip}}\,X_{\text{ECL}}$), lipase dengan suhu ($X_{\text{Lip}}\,X_{\text{Temp}}$), kepekatan awal ECL dengan kepekatan awal MGP ($X_{\text{ECL}}\,X_{\text{MGP}}$), dan kepekatan awal ECL dengan suhu ($X_{\text{ECL}}\,X_{\text{Temp}}$) adalah signifikan ($p < 0.05$) pada penghasilan berat kering oligomer terfungsi. Nilai *p* yang signifikan bagi interaksi dua hala di antara dua pemboleh ubah menunjukkan kewujudan kesan korelasi di antara pemboleh ubah yang dikaji. Berdasarkan analisis statistik deskriptif bagi model pemfaktoran pecahan, peratusan variasi (R^2) bagi model regresi adalah sebanyak 99.8% di mana ia menunjukkan ketepatan padanan yang baik antara data ramalan dan data eksperimen. Pengesahan model menggunakan analisis pembakian menunjukkan variasi di antara taburan sampel adalah normal. Berdasarkan program pengoptimum respon, keadaan terbaik untuk penghasilan berat kering maksimum

oligomer terfungsi adalah seperti berikut: lipase (2.8 % *w*/*v*), kepekatan awal ECL (11.46 % *w*/*v*), kepekatan awal MGP (0.04 % *w*/*v*), suhu (60.0 °C) dan kadar agitasi (90 rpm). Mekanisma yang dicadangkan untuk langkah-langkah tindak balas pengfungsian termasuklah pengesteran di antara MGP dan monomer/oligomer ECL diikuti oleh pemanjangan rantai oleh unit monomer 6-hidroksihexanoat bebas di mana kedua-dua tindak balas menggunakan tindakbalas bermangkin-lipase. Mekanisma ping-pong bi-bi tanpa kompleks bertiga telah dicadangkan untuk tindak balas pengesteran ECL dan MGP dengan nilai ketara seperti pemalar kinetik iaitu halaju maksima (V_{max}), pemalar Michaelis untuk MGP (K_{mMGP}) dan pemalar Michaelis untuk ECL (K_{mECL}) masing-masing pada 3.848×10^{-3} M h^{-1}, 8.189×10^{-2} M dan 6.050 M. Tindak balas pemanjangan rantai oligomer terfungsi menunjukkan ciri-ciri mekanisme pempolimeran hidup. Pemalar kadar ketara (r_{App}) rantai pemanjangan menunjukkan nilai tertinggi apabila kepekatan ECL meningkat. Oligomer yang terhasil menunjukkan berat molekul dalam julat yang kecil daripada 1,400 hingga 1,600 (g mol^{-1}) dengan lebih 90 % penukaran monomer dicapai. Analisis struktur NMR dan FTIR telah mengesahkan kehadiran ikatan kovalen antara kumpulan hidroksil terminal di MGP dengan kumpulan karboksil terminal monomer/oligomer di dalam ECL. Analisis terma menunjukkan tiga tahap degradasi bagi oligomer terfungsi berbanding dengan dua peringkat di dalam oligomer yang tidak terfungsi. Melalui kajian ini potensi tindak balas bermangkin-lipase menunjukkan potensi signifikan untuk proses sintetik satu-reaktor di dalam penghasilan karbohidrat terfungsi bio-oligomer dengan berat molekul terkawal sebagai pelantar kimia.

Kata Kunci: reaktor enzim, pemfungsian, lipase, model kinetik, sintesis satu-reaktor.

ACKNOWLEDGEMENTS

Alhamdulillah and Praise to ALLAH SWT and HIS messenger, Prophet Muhammad SAW. With HIS blessing and mercy, it is possible for me to finish this Ph.D study with great enthusiasm and determination

My most and foremost gratitude to my beloved family especially my parents, Haji Saat Buang and Hajah Hasnah Samaon for their infinite support, unending love and pray. Their love and support for me has always encourage me to stay determine and never give up despite difficulties and problem during this wonderful Ph.D journey. I would like to express my sincere gratitude to my advisor Prof. Dr Mohamad Suffian Mohamad Annuar for the continuous support of my Ph.D study and related research, for his patience, motivation, and immense knowledge. His guidance helped me in all the time of research and writing of this thesis. I could not have imagined having a better advisor and mentor for my Ph.D study.

My sincere thanks also goes to the current members of Bioprocess and Enzyme Technology (BET) Laboratory especially to Haziq, Syed, CB Ong, Siraj, Kak Suhayati and Pey Ling. Thank you to all BET member for the stimulating discussions, for the sleepless nights we were working together before deadlines, and for all the fun we have had in the last four years. Special gratitude to my former BET lab mates, Alimin, Nurul Nadiah, Faezah, Syairah and Ana for the experience of doing research under pressure.

Last but not the least, I sincerely thanks to Malaysian Government and University Technology MARA for sponsoring my entire Ph.D study through Skim Biasiswa Tenaga Pengajar Muda UiTM. I am also indebted to University of Malaya for allocating me research fund of PG003-2015A which was very helpful for my bench work experiment.

TABLE OF CONTENTS

LIST OF FIGURES

LIST OF TABLES

LIST OF SYMBOLS AND ABBREVIATIONS

df	:	Degree of freedom
F	:	F statistic
k	:	Reaction rate constant
KBr	:	Potassium bromide
K_{Cat}	:	Turnover number
K_i	:	Dissociation constant
K_m	:	Michaelis-Menten constant
K_{mECL}	:	Michaelis constant of e-Caprolactone
K_{mMGP}	:	Michaelis constant of methyl-*D*-glucopyranoside
M_n	:	Number average molecular weight
p	:	Significant level
R^2	:	Pearson Correlation coefficient
r^2	:	Correlation coefficient
r_{App}	:	Apparent rate constant
R_P	:	Rate of polymerization
S_0	:	Initial substrate concentration
S_{con}	:	Substrate consumption
S_t	:	Substrate concentration at time t
v	:	Rate of reaction
v_0	:	Initial velocity
V_{max}	:	Maximum reaction velocity
X	:	Variables
Abs	:	Absorbance
Adj. MS	:	Adjusted mean of squares

Adj. SS	:	Adjusted sum of squares
ANOVA	:	Analysis of variance
CalB	:	*Candida antarctica* lipase B
C_{ECL}	:	Concentration of ε-caprolactone
CI	:	Confidence interval
D_f	:	Desirability function
DOE	:	Design of experiment
DW	:	Dried weight
E	:	Enzyme
ECL	:	ε-caprolactone
ES	:	Enzyme-substrate
E_T	:	Total enzyme
FTIR	:	Fourier Transform Infrared
GPC	:	Gel permeation chromatography
LB	:	Lineweaver Burk plot
MGP	:	Methyl-*D*-glucopyranoside
MGP-6-*O*-ECL	:	Methyl-6-*O*-(hydroxyhexanoyl)-D-glucopyranoside
MGP-6-*O*-oligo-ECL	:	Methyl-6-*O*-(hydroxyhexanoyl)$_n$-D-glucopyranoside
NMR	:	Nuclear Magnetic Resonance

LIST OF APPENDICES

CHAPTER 1: INTRODUCTION

1.1 Introduction

Approximately 6,300 metric tons of plastic was generated in 2015 where only 9 % of the waste recycled, 12 % incinerated and 79 % disposed in landfills (Geyer et al., 2017). By 2050, it is projected that approximately 12,000 metric tons of plastic waste will be accumulated in landfills. The discharge of plastic waste into the environment without proper management can cause dangerous impact in marine ecosystem (Jahnke et al., 2017; Lamb et al., 2018), freshwater ecosystem (Li et al., 2018), soil (Scheurer & Bigalke, 2018) and food chain (Romeo et al., 2015).

Global increase in recalcitrant plastic material disposal and waste, alongside the instability in the prices of fossil-based resources has prompted the search for alternative and/or substitute materials. Dozens of polyester-based medical devices are commercially available with new inventions introduced to the market yearly. The needs for biodegradable polyester in niche applications have contributed significantly for the growth of technology-based enterprises. The current market for biodegradable materials in regenerative implantation surgeries, therapeutic cell culturing and tissue repair is approximately US $23 billion, and it is anticipated to reach US $94.2 billion by the end of 2025 (Manavitehrani et al., 2016). Improvement of hydrophilicity and biodegradability of polyester is often needed for intended biomedical applications. Specific polymer properties are required for specialized devices to be used in bone scaffolding, dental materials, drug delivery, etc. The modification of biodegradable polyester to meet such requirements can be achieved through functionalisation of the polymer with specific chemical groups.

Functionalisation is often associated with chemo-enzymatic synthesis. Functionalisation can be defined as a process where one or more chemical groups are

introduced into polymer molecule that imparts specific chemical, physical, biological, pharmacological or other functions. The chemical groups could be categorized as functional group in the form of small moieties, monomer and even copolymers. They are used in the functionalisation process to produce functionalised polymer. In general, there are two ways of implementing functionalisation *viz. in vivo* biological or *in vitro* synthetic approach which proper selection should be made according to the requirements. The *in vivo* functionalisation is a process using living organism to produce functionalised polymer through fermentation or biotransformation processes. *In vitro* functionalisation involves physico-chemical or chemo-enzymatic synthesis, and carried out in scales ranging from microfluidic reactor to large industrial volume.

Functionalised polymers with various functional groups had improved the targeted properties of original neat polymer initially lacking. Novel properties can also be introduced into the neat polymers *via* functionalisation. The functionalised polymer produced from the enzymatic process is often suitable for human consumption and application. Polymer with carbohydrate functionalities are of interest due to the special properties the attached moieties present. Carbohydrates contain functional group including hydroxyl (-OH), ethers (R-O-R'), aldehydes (R-C(=O)-H) and/or ketones (R-C(=O)-R'). Most of the carbohydrate functional groups are characterized by its non-ionic, biodegradable and surfactant properties. The amphiphilic nature of carbohydrate functionalities has promoted their versatility in food emulsifiers, detergents, cosmetic removal, biomedical and electronic appliances (Kang et al., 2015; Molinier et al., 2006; Varma et al., 2004). It is also possible to perform environmental-friendly enzymatic esterification process followed by chemical radical polymerization for the synthesis of carbohydrate-functionalised polymer.

In this study, polycaprolactone (PCL) was functionalised with methyl-*D*-glucopyranoside (MGP) in one-pot lipase-catalysed synthesis. Cyclic lactone i.e. ε-

caprolactone (ECL) was used as starting monomer for the functionalisation study. PCL was preferred for the functionalisation study due to its broad spectrum of compatibility with a wide range of polymers and functional groups (Dash and Konkimalla, 2012; Mohamed & Yusoh, 2016). Furthermore, synthesis of PCL from ECL monomer is advantageous with the presence of hydroxyl and carboxyl group at the terminal end of the PCL chain (Wilberth et al., 2015; Liu et al., 2016). Compared to other branched polymers, biodegradable PCL provides an excellent model for the study of lipase-catalysed functionalisation reaction without side reactions due to its linear chain structure.

The enzymatic functionalisation is a complex reaction with many physical and biochemical factors affecting overall functionalisation reaction. Investigation of selected key variables for the reaction is required for the enzymatic functionalisation at reactor scale. Kinetic mechanism studies in the enzyme-catalysed functionalisation are essential in the reactor design optimization for the improvement in yield of functionalized product. Hence, cost of functionalized product can be potentially lowered.

In this study, the effects of selected key variables on one-pot synthesis of MGP-functionalised ECL oligomer (MGP-6-*O*-oligo-ECL) in a bench-scale custom-fabricated enzymatic reactor were investigated. Screening of significant variables was carried out using design of experiment (DOE). Key variables including lipase amount, initial ECL concentration, initial MGP concentration, temperature and agitation rate were evaluated by using half fractional factorial design (2^{k-1}). The mechanism and kinetic of lipase-catalysed esterification of ECL by MGP and subsequent elongation of oligomeric sugar ester by free 6-hydroxyhexanoate monomer units as a model for functionalised oligomer production was investigated. Ping-pong bi-bi mechanism was proposed for the reaction between ECL and MGP molecules in the esterification step of the functionalisation reaction. For chain propagation step, living polymerization mechanism was investigated.

1.2 Research Objectives

1. To study the effects of selected reaction variables on the lipase-catalysed MGP functionalisation of ECL oligomer and its production in batch reactor;
2. To investigate the kinetic mechanisms of lipase-catalysed esterification of ECL monomer/oligomer by MGP, and elongation of the esterified compound by free 6-hydroxyhexanoate units;
3. To characterize the functionalised oligomer based on the chemical structure authentication, molecular weight analysis and thermal properties.

CHAPTER 2: LITERATURE REVIEW

2.1 Polycaprolactone

Polycaprolactone (PCL) is biodegradable aliphatic polyester, composed of repeating hexanoate units. The chemical structure of PCL features the ester functional group, hydroxyl and carboxyl end group, and repeating unit of methylene group (Figure 2.1). The majority of PCL is mainly synthesized either from ring opening polymerization of ε-caprolactone (ECL) or polycondensation of 6-hydroxycaproic (6-hydroxyhexanoic) acid.

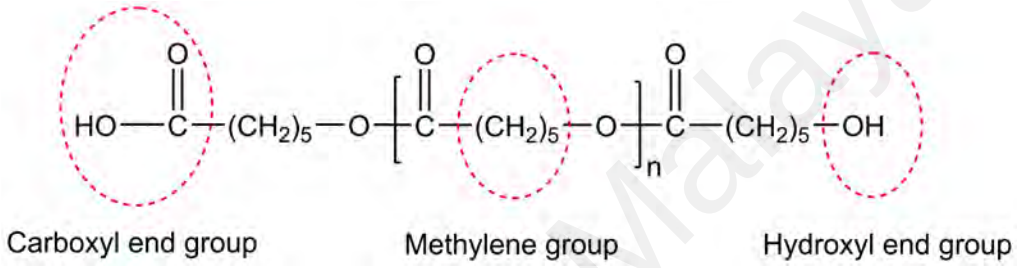

Figure 2.1: Chemical structure of neat PCL (Modified from Bosworth & Downes, 2010)

The semicrystalline polymer (up to 70 % of crystallinity) has a wide range of properties in terms of physical, thermal and mechanical. The properties of PCL are depending on the molecular weight and its degree of crystallinity (Table 2.1) (Labet & Thielemans, 2009). The average molecular weight of PCL depend on the molecular weight of repeat unit ECL monomer at 114.14 g mol^{-1}. Natta et al. (1934) has published the first article on the synthesis of PCL with high molecular weight from ECL monomer. The melting point of the PCL is around 60 °C with glass transition temperature of -60 °C. At room temperature, PCL exhibits good solubility in non-aqueous medium such as chloroform, dichloromethane, toluene, etc. In contrast, PCL displays poor solubility in alcohols, petroleum ether and water. As a result, PCL has been widely employed in the organic synthesis for the production of new polymers.

Table 2.1: Properties of biodegradable PCL.

Properties	Range	Reference
Molecular weight of monomer, M_n (g.mol^{-1}).	114.14	Duda et al. (2002).
Density, ρ (g.cm^{-3}).	1.073 1.110 1.140 1.141	Wang et al. (2005), Van de Velde & Kiekens (2002), Estelles et al. (2008), Ketelaars et al. (1997).
Glass transition temp, T_g (°C).	-61.5 -64.3 -60.0 -67.0	Averous et al. (2000), Wang et al. (2005), Cava et al. (2007), Avella et al. (2000).
Melting temp, T_m (°C).	62.0 58.0 60.0	Avella et al. (2000), Van de Velde & Kiekens (2002), Tokiwa et al. (2009).
Decomposition temp, (°C).	350	Lam et al. (2007).
Tensile strength, σ (MPa).	14 – 300 27.3 – 378.0 16.9 – 429.1 20.7 – 42.0	Granado et al. (2008), Correlo et al. (2005), Rosa et al. (2004), Van de Velde & Kiekens (2002).
Young modulus, E_Y (GPa).	0.21 – 0.44	Van de Velde & Kiekens (2002).
Elongation at break, ε (%).	300 - 1000	Van de Velde & Kiekens (2002).

PCL exhibits unique properties due to their excellent miscibility when blending with different polymers including polyvinyl chloride, polycarbonate, polystyrene, etc. The ability of PCL to blend with other polymers have further increased the interest on new materials for application in the drug delivery systems (Fereshteh et al., 2016), packaging materials (Ortega-Toro et al., 2015), bone scaffolding (Yao et al., 2017), etc.

PCL polymer is degradable in nature. PCL biodegrades within several months to years depending on the molecular weight, crystallinity degree and degradation conditions (Woodruff & Hutmacher, 2010). A wide range of aerobic and anaerobic microorganisms has been studied for their biodegradation activities on PCL which including *Pseudomonas* sp. (Uscategui et al., 2016), *Penicillium* sp. (Li et al., 2012), *Clostridium* sp. (Abou-Zeid et al., 2001), *Ralstonia* sp. (Shah et al., 2015), etc. In addition to microbial degradation, PCL can be degraded by enzymes such as lipase and esterase (Lin et al., 2013).

PCL has received much attention due to the concern on toxicity effects of the chemical-based polymers. It is synthesized from monomers obtained from microorganisms by using wide range of catalysts such as organic-, metal- and enzyme-based (Leisch et al., 2011). Due to the wide range of catalyst suitable for the ring opening polymerization of PCL, the effects of different catalytic systems influence the properties of synthesized PCL. Organic catalyst can be highly effective for the ring opening polymerization of macrolactone such as polypentadecalactone (PDL) and the copolymerization of PDL and ECL except it may produces PCL with moderate molecular weight (Bouyahyi et al., 2012). In other hand, the metal-based catalyst including aluminium, tin and zinc has been reported to produce low molecular weight PCL (Bouyahyi & Duchateau, 2014).

The used of biocatalyst has improved the biocompatibility and biodegradability of synthesized PCL for advanced biomedical applications. Furthermore, the environment for biocatalysis only requires mild reaction condition without toxicity effects. Biomedical applications of PCL synthesized from lipase-catalysed polymerization has been reported which includes scaffolds fabrication (Korzhikov et al., 2013) and drug delivery system (Piotrowska & Sobczak, 2015). The enzyme-substrate specificity, mild reaction condition and toxic free catalysts are the main features of biocatalyst reaction system for sustainable process (Champagne et al., 2016; Kobayashi, 2015).

2.2 Ɛ-Caprolactone Monomer

Seven-membered ring of ε-caprolactone (ECL) or simply caprolactone is a cyclic ester categorized in lactone family group. ECL usually forms colourless liquid miscible with most organic solvents. ECL has been extensively used as monomer for the production of biocompatible and biodegradable PCL. Various factors that influence the ability of these monomer to polymerize are related to the strain of the rings, Gibbs free energy of ring opening polymerization and the conformational linear model of the corresponding

homopolyester (Aleman et al., 2009). The Gibbs free energy of the ring opening polymerization calculated for ECL, an exergonic process, was found to be within -0.1 to -3.8 kcal.mol^{-1} (Aleman et al., 2009; Duda et al., 2005; Save et al., 2002).

Although lactone rings are widely distributed in nature in the form of building blocks, lactone can be synthesized through the intra-molecular esterification. ECL is usually prepared through the oxidation of cyclic ketones based on the Baeyer–Villiger oxidation (Chen et al., 2009). Enzyme-mediated synthesis of ECL monomer *via* Baeyer-Villiger oxidation has been widely used in the production of biodegradable PCL suitable for human consumption (Bucko et al., 2016; Drozdz et al., 2013).

2.3 Methyl-*D*-glucopyranoside

Methyl-*D*-glucopyranoside or methylglucoside (MGP) is a derivative of glucose, which contain methoxy group in carbon one (C1). MGP can be prepared by the acid-catalysed methylation of glucose with methanol. The general structure of MGP is classified as anomer with different configuration of C1 known as anomeric carbon (Figure 2.2). MGP is widely used for the reaction in a non-aqueous medium as compared to glucose. In the presence of methoxy group (-OCH_3) in C1, the poor solubility of glucose with hydroxyl group in C1 can be reduced. The presence of methoxy group in C1 of MGP, has increased its potential application in non-aqueous synthetic reaction. Currently, MGP is used as intermediate in the production of emulsifiers, surfactants, resins, etc. (Belmessieri et al., 2017; Charoensapyanan et al., 2016).

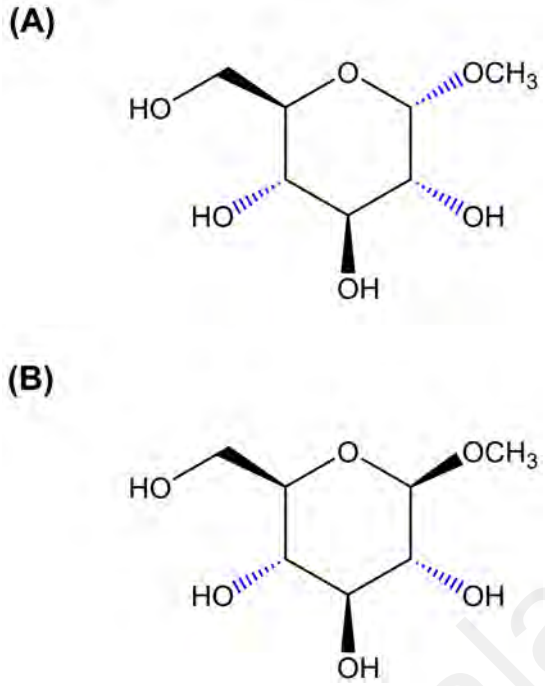

Figure 2.2: (A) Methyl α-*D*-glucopyranoside; (B) Methyl β-*D*-glucopyranoside (Adapted from Aguilar & Guareno, 2000)

2.4 Synthesis of Polycaprolactone

In 1934, Natta and co-workers published the first paper on synthesis of biodegradable high molecular weight polycaprolactone (PCL) by heating a reaction mixture containing monomer ε-caprolactone (Natta et al., 1934). As described in the literature, biodegradable PCL is synthesized *via* polycondensation and ring opening polymerization. Another feasible route of synthesizing biodegradable PCL is *via* polycondensation of 6-hydroxyhexanoic acid (Braud et al., 1998; Stanley et al., 2014). However, a high molecular weight and low dispersity PCL can be synthesized through ring opening polymerization of the cyclic ester (Sisson et al., 2013).

2.5 Ring Opening Polymerization

According to International Union of Pure and Applied Chemistry (IUPAC), ring opening polymerization is a polymerization in which a cyclic monomer yields a monomeric unit which is acyclic or contains fewer cycles than the monomer (Penczek &

Moad, 2009). If the monomer is polycyclic, the opening of a single ring is sufficient to classify the reaction as ring-opening polymerization. The general scheme of ROP involves opening of cyclic ring system and its polymerization into a longer chain. ROP mechanism can be classified into four different mechanisms namely anionic, cationic, monomer-activated and coordination-insertion. The classified mechanisms are dependent on the type of catalyst. Due to the high polarity of lactone monomer in nature, numerous nucleophiles can react to initiate ROP process. The presence of co-initiator for ROP of lactone monomer is required for certain nucleophilic initiator. As previously reported, the driving force for the ROP processes is the effect of ring strain of the cyclic monomer. Thermodynamically, the opening of cycling ring shows the relief of ring strain that enables the system to overcome the standard entropy state (Elling & Xia, 2015). The enthalpy change in the ROP processes is negative suggests the overall ROP processes is exergonic (Darensbourg & Yeung, 2014; del Rosal et al., 2015).

2.6 Mechanisms of Ring Opening Polymerization

Generally, there are four main mechanisms for ring opening polymerization of polycaprolactone (PCL) that depends on the type of catalyst. The four mechanisms of ROP are anionic, cationic, monomer activated and coordination-insertion (Table 2.2). Anionic and cationic mechanisms are considered as the simplest form of ROP mechanism which require initiator either nucleophile or electrophile to initiate ring opening of cyclic lactone into either anionic species or cationic species, respectively. Despite the wide range of nucleophiles available, the anionic and cationic mechanism have several drawbacks. One of the significant drawbacks is the occurrence of intra-molecular transesterification or "back-biting reaction" causing the formation of low molecular weight polymers and formation of cyclic oligomers (Jeon et al., 2016; Labet & Thielemans, 2009; Neitzel et al., 2016; Xia et al., 2016).

Table 2.2: Different reaction mechanisms of ring opening polymerization.

Mechanism	Catalyst/Initiator	Reaction Mechanism
Anionic (Endo, 2009)	**Initiator**: Nucleophilic reagents (Nuc^-), organometals, alcohols, water, etc.	• **Initiation**: Nucleophilic attack of Nuc^- towards functional group of monomer • **Propagation**: Nucleophilic attack of growing chain end towards functional group of monomer
Cationic (Endo, 2009)	**Initiator:** Electrophilic reagents (E^+), Bronsted acid, Lewis acid, alkyl esters, etc.	• **Initiation**: nucleophilic attack of functional group of monomer towards the E^+ initiated overall reaction • **Propagation**: Nucleophilic attack of lone electron pair of monomer towards the cationic centre due to ring opening
Activated monomer (Zhang et al., 2018)	**Catalyst**: Enzyme, metal based alkaline, Bronsted acid **Initiator**: Alcohol, water	• **Activation**: Nucleophilic attack of Nuc^- towards functional group of a monomer to produce activated monomer, (AM) • **Propagation**: Further nucleophilic attack of AM towards another monomer resulting in formation of anionic species (propagating species) • **Further activation:** Propagating species is acting as base for another monomer activation cycle
Coordination insertion (Mezzasalma et al., 2017)	**Initiator**: Metal alkoxides initiators (Stanium, titanium, zinc and aluminium)	• **First Transition State (TS1)**: Nucleophilic attack of metal alkoxide initiator (acting as active centre) towards carbonyl group of monomer to produce TS1 • **Second Transition State (TS2)**: Rearrangement of metal alkoxide ligand with oxygen atom of monomer (Sn-O) *via* acyl-oxygen bond cleavage resulting in second transition state (TS2)
Enzyme-catalysed synthesis (Barrera-Rivera et al., 2009)	**Catalyst**: Lipase **Initiator**: Alcohol, water	• **Initiation**: Nucleophilic attack of OH group in the enzyme active site towards carbonyl group of cyclic monomer • **Propagation**: Nucleophilic attack of terminal hydroxyl group of enzyme-substrate complex or propagating species towards carbonyl group of cyclic monomer

By contrast, the activated monomer of ROP (Figure 2.3) is characterized by the insertion of initiator molecules into monomer resulting in monomer activation (Ajellal et al., 2010; Albertsson & Varma, 2003). As previously studied, the activated monomer mechanism is initiated by nucleophilic attack of OH group to produce activated monomer (Ajellal et al., 2010). Moreover, metal triflates including aluminium triflate, zinc triflate, magnesium triflate and calcium triflate have been used as initiator with alcohol as co-initiator in the production of aliphatic polyester (Ajellal et al., 2010). Despite the potential for PCL production, most of the initiators in activated monomer mechanism are considered highly toxic and non-environmental friendly for the biomedical application. Thus, the biological catalyst such as lipase is preferred for PCL production. The application of lipase-catalysed ROP is considered to proceed *via* activated monomer mechanism; published reports suggested that the rate-determining step is the formation of enzyme-activated monomer (Panova & Kaplan, 2003; Zhang et al., 2018).

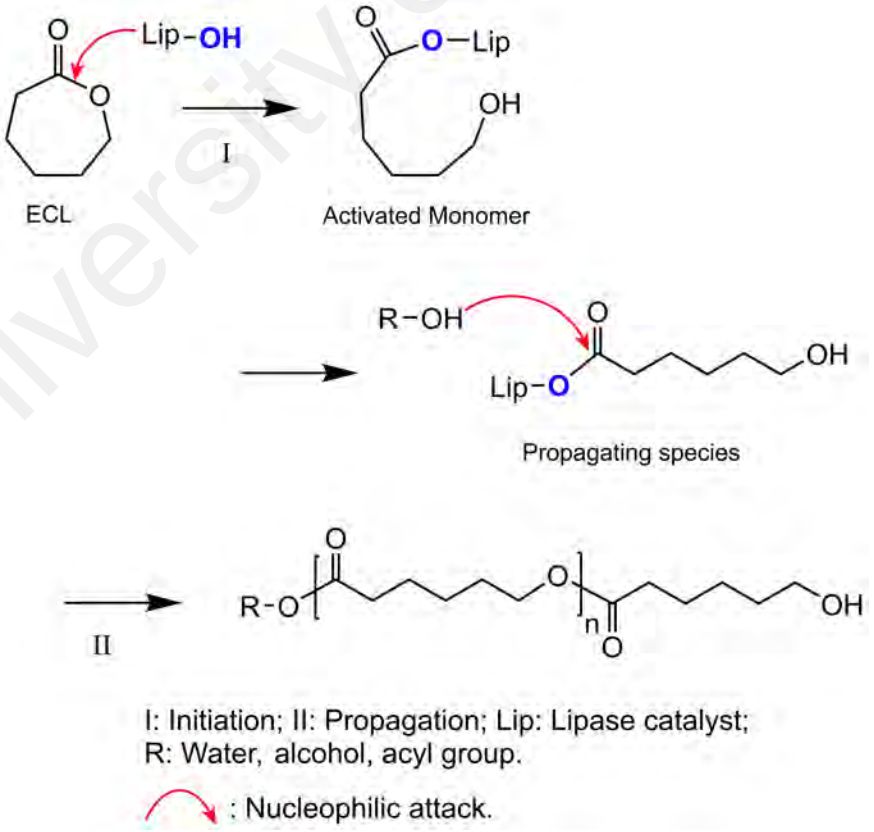

Figure 2.3: Activated monomer mechanism of lipase-catalysed ring opening polymerization (Adapted from Jerome & Lecomte, 2008)

The coordination insertion mechanism of ROP has been well documented for their high molecular weight and controllable stereochemistry properties. Different kinds of metal alkoxides including tin alkoxides, titanium alkoxides, zinc alkoxides and aluminium alkoxides have been used as initiator. The coordination insertion mechanism is characterized by the formation of ligand between metal alkoxide and monomer (Sn-O) *via* acyl-oxygen bond cleavage (Figure 2.4). Generally, the reaction coordinates of the mechanism involve several steps and states, which specifically depends on the type of metal alkoxides used. For example, the used of Sn alkoxides as initiator requires six steps with seven states which can be explained from transition state theory (Sattayanon et al., 2015). However, the used of metallic initiators for ROP requires high temperatures and longer reaction time that lead to the intra-molecular transesterification process (Mezzasalma et al., 2017; Sun et al., 2015).

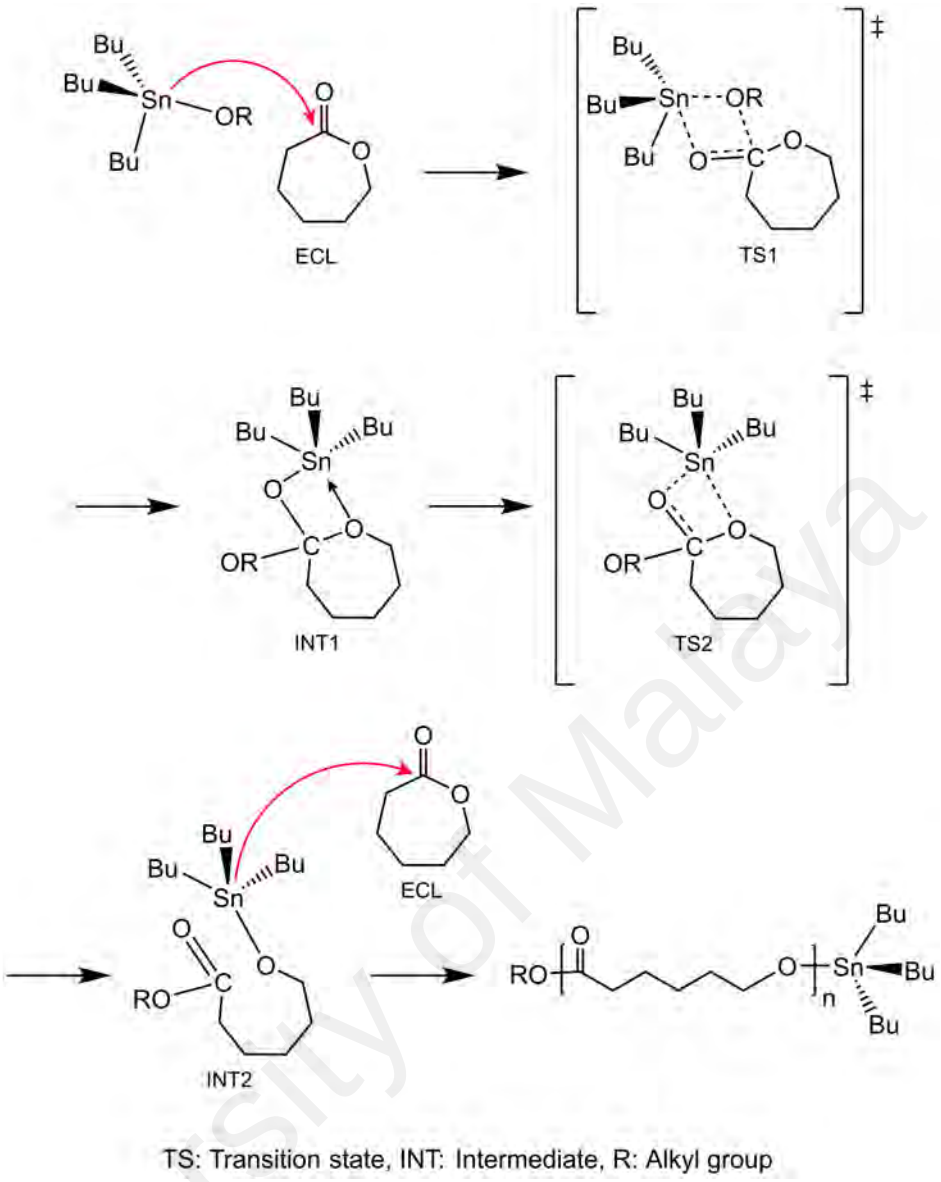

Figure 2.4: Coordination insertion mechanism of ring opening polymerization (Adapted from Sattayanon et al., 2015)

2.7 Enzyme-Catalysed Ring Opening Polymerization

Enzymes are biocatalyst that accelerates biochemical process by converting substrate into products. The macromolecular biocatalyst is mainly globular protein classified into oxidoreductase, transferases, hydrolases, lyases, isomerases and ligases. Enzyme activity can accelerate reactions by lowering the activation energy. Although enzyme role in nature is mostly involving *in vivo* system, its *in vitro* application is not limited per se. Enzymes have been isolated from the cells to be used *in vitro* either in aqueous or organic

medium for a specific reaction. Currently, enzymes have been applied in various biotechnological applications at industrial scale. Among the benefits of using enzymes include (i) highly selective with regards to chemoselectivity, enantioselectivity and regioselectivity, (ii) requires mild reaction conditions, (iii) environmental-friendly process due to non-toxic property of biocatalyst, etc.

Lipase enzyme is well known biocatalyst responsible for fatty acid esters hydrolysis in the aqueous media. Lipase has unique features since the enzyme can be used in organic solvent. In the non-aqueous media, lipase undergoes esterification by catalysing the formation of ester bond. The importance of lipase-catalysis in organic synthesis has provided opportunity in the preparation of wide range of chemical compounds. Tremendous progress in enzymology, enzymatic engineering and process development has contributed into the production of tailor-made enzymes making it possible to avoid disadvantages of natural enzymes for specialized catalysis.

2.7.1 Lipase

Lipase (triacyl glycerol hydrolases, EC 3.1.1.3) is well recognized as remarkable enzyme that catalyses wide range of substrates in hydrolytic and synthetic reactions. Lipase is primarily responsible for the hydrolysis of substrates in aqueous medium (Ferrario et al., 2011; Guo et al., 2015; Marten et al., 2003; Tsai & Chang, 1993) whereas in non-aqueous medium, lipase-catalyses synthesis reaction. At equilibrium, a substrate is hydrolysed by lipase in the presence of high water activity in aqueous media, but this equilibrium reaction shifts towards synthesis when reaction is performed in non-aqueous media with low water activity (Chamouleau et al., 2001; Humeau et al., 1998). Lipase catalyse reversible reaction between hydrolysis and synthesis. However the reversible reaction of lipase depends on the reaction conditions, solvent polarity, by-product formation, etc. (Champagne et al., 2016).

Lipase has been successfully used as biocatalyst for the ROP of a wide range of lactone monomer at different ring sizes suggesting its broad substrate specificity. Lipase-catalysed ROP has gained much attention since the backbone chain of synthesized polymer inherits the heteroatoms and functional groups of its corresponding monomers (Endo & Sudo, 2016). The application of lipase-catalysed ROP is considered important for the development of well-defined and tuneable biopolymer for applications in pharmaceutics, advanced biomaterials, electronics, and etc. Lipase abilities in the production of well-defined PCL with targeted end-functionalities become a major attraction. The ability to incorporate a wide range of different end-functional groups on the PCL has received much attention from its resulting biodegradability and biocompatibility, as well as the characteristic of end groups (Albertsson & Varma, 2003; Zhu et al., 2015).

PCL with a wide range of molecular weight from 500 to more than 100,000 g mol^{-1} has been synthesized with lipase as biocatalyst. Various organisms have been reported to be able to produce significant quantities of lipase. Commercially available lipases are isolated from animals, plants and microorganisms. The production of pancreatic lipase from porcine has been widely commercialized due to its economical preparation. Although it has been used to a lesser extent relative to microbial lipase, porcine pancreatic lipase (PPL) exhibits high stability in anhydrous medium (Mendes et al., 2012).

Lipases isolated from various microbial sources are the most significant ones. Lipases from various microbial species have been extensively studied due to their versatility in catalytic activities, high yield, ease of genetic manipulation, rapid production, regular supply as well as inexpensive microorganism growth media (Hasan et al., 2006; Singh et al., 2016). Microbial enzymes are also more stable and their production is more expedient and safer (Matsumura, 2006). Microbial species including *Candida antarctica, Pseudomonas fluorescens, Aspergillur niger*, *Burkholderia cepacia* and etc., are among

the lipase-producer microorganisms (Hasan et al., 2006; Namekawa et al., 1998; Shoda et al., 2016). Lipase ability to synthesize PCL with high molecular weight depends on the type of monomer and reaction condition. By comparison, microbial lipases have advantages over animal lipases due to their wide variety of catalytic activities. Investigation on lipases of different origins in the ROP of ε-caprolactone monomer for the production PCL is summarized in Table 2.3.

Table 2.3: PCL from enzyme-catalysed ring opening polymerization of ECL.

Source of Enzyme	M_n (g mol^{-1})	Reference
Aspergillus niger	780	Kobayashi et al. (1998)
Candida antarctica	2,900	Sobczak (2012)
	4,500	Kikuchi et al. (2002)
Candida cylindracea	1,000	Kobayashi et al. (1998)
Pseudomonas cepacia	3,900	Sobczak (2012)
Pseudomonas fluorescencs	3,000	Sobczak (2012)
	7,000	Uyama et al. (1997)
Rhizopus japonicus	840	Namekawa et al. (1999)
Trichosporon laibacchii	2,168	Zhang et al. (2018)
Yarrowia lipolytica	10,700	Barrera-Rivera & Martinez-Richa (2017)

2.7.2 *Candida antarctica* Lipase B

Lipase isolated from yeast *Candida antarctica* (CalB) is made up of 317 amino acids with molar mass of 33 kDa. The active site of CalB consists of amino acid residues $Serine_{105}$, $Histidine_{224}$ and $Aspartate_{187}$ which are protected by the amphiphilic lid structure. During the interfacial activation, the lid structure undergoes conformational changes allowing micellar substrates to penetrate enzyme active site. Within the catalytic site, the Ser_{105} residue of the active site will bind to the substrate to form the enzyme-substrate intermediate. There is evidence to suggest that region of the lid, a mobile amphipathic structure which covers the catalytic active site of most lipases play significant role in modulating the enzyme activity, specificity, enantio-selectivity and stability of the enzymes (Secundo et al., 2006; Stergiou et al., 2013).

Lipases (EC 3.1.1.3; triacylglycerol hydrolases) are thought to be activated when they encounter the water–lipid interface causing a "lid" region to move and expose the catalytic site (Cheng et al., 2012; Ericsson et al., 2008; Skjold-Jorgensen et al., 2015). The presence of lid region in the lipase structure enhance enzyme stability at low water content. The moveable lid region protects the enzyme active site at the interface between hydrophobic solvent and hydrophilic region. There is evidence that suggest that the region of the lid, a mobile amphipathic structure which covers the catalytic active site of most lipases play significant role in modulating the enzyme activity, specificity, enantioselectivity and stability of the enzymes (Secundo et al., 2006; Stergiou et al., 2013).

2.8 Reaction Parameters in Lipase-Catalysed Ring Opening Polymerization

2.8.1 Effect of Reaction Medium

Products from the non-aqueous reaction system have received much attention due to their applications in cosmetics, fine chemicals, pharmaceuticals, food ingredients and recently in advanced biomedical. In the case of PCL, lipase-catalysed ring opening polymerization is carried out in the non-aqueous medium due to low solubility of PCL in the aqueous medium. The non-aqueous media include organic solvent system, ionic liquids, supercritical fluid system, bulk substrates, etc. have been previously reported for the lipase-catalysed ring opening polymerization (Deng & Gross, 1999; Polloni et al., 2017; Zhao, 2018; Zhao et al., 2017).

The rate of polymerization in different non-aqueous media depends on the polarity of the solvent. Solvents with different polarities are measured *via* solvent log *P*. It is suggested that higher log *P* of a particular solvent will results in better activation of the enzyme active site (Romero et al., 2012; Yadav & Devendran, 2012). The used of deuterated solvent as reaction medium in lipase-catalysed ROP shortened the reaction

time to less than 8 hours with conversion more than 90 % (Mei et al., 2002). However, solvent with high log *P* value does not always correlate with high lipase catalytic activity when a substrate exhibits poor solubility in a particular solvent. These factors resulted in varied catalytic activities of lipase for solvents with different log *P* values. The effects of different functional group for solvents with same log *P* values also exhibit varied behaviour of catalytic activities for lipase; it shows higher relative activities in solvents with functional groups of nitrile and carbonyl (Yang et al., 2012).

2.8.2 Effect of Reaction Temperature

The role of temperature in lipase-catalysed ring opening polymerization is crucial since it influences lipase stability, solubility of reactants and products, rate of polymerization and thermodynamic equilibrium of the system. Lipase from *Candida antarctica* is the most common enzyme used in ROP of lactone with various ring sizes since it is stable at temperature between 60 to 80 ºC (Yoshida et al., 2006). It has been reported that temperature clearly influence the molecular weight of synthesized PCL and their degree of crystallinity (He et al., 2015). It has also been shown that PCL synthesized at lower temperature of 37 ºC is suitable for the growth of fibroblast cell due to the biocompatibility of the synthesized polymer (García-Argüelles et al., 2015). Furthermore, the percentage of monomer conversion increases as with temperature. The formation of enzyme-substrate complex increases as thermodynamic equilibrium is shifted towards product formation at higher temperature.

When reaction time is increased from 24 to 48 hours at higher temperature, it reduces the molecular weight of synthesized PCL due to predominant side reaction such as backbiting mechanism and β-scission (Liu et al., 2014; Yang et al., 2011). Temperature elevation up to 90 ºC in the ROP significantly altered the properties of polypentadecanolide with respect to its molecular weight and the crystallinity (Herrera-

Kao et al., 2015). Furthermore, the issues regarding enzyme denaturation and deactivation as well as the non-enzymatic thermal initiation could arise from high reaction temperature. Low crystallinity of PCL is due to the build-up in the number of terminal hydroxyl group which disrupt the crystalline structure of the polymer (Herrera-Kao et al., 2015). Specifically, higher temperature promotes backbiting mechanism and β-scission resulting in significant generation of terminal hydroxyl group (Liu et al., 2014). Table 2.4 summarizes the temperature effects on selected variables in lipase-catalysed ROP of ε-caprolactone.

Table 2.4: Effect of temperature on molecular weight and conversion in lipase-catalysed ring opening polymerization of ECL.

Medium	Temp. (°C)	Time (h)	M_n (g mol^{-1})	Conv. (%)	Reference
Sc-CO_2	35	24	50,000	100	Thurecht et al. (2006)
Toluene-d8	20	7	17,800	97	Mei et al. (2002)
Toluene	60	24	15,600	55	Marcilla et al. (2006)
sc-CO_2	65	2	7,400	-	He et al. (2015)
Toluene	40	460	15,600	98	Zhang et al. (2012)
Toluene	80	24	1257	98	Todea et al. (2018)

Temp.: Temperature; M_n: molecular weight, Conv.: conversion, Sc-CO_2: supercritical CO_2

2.8.3 Effect of Substrates

One of the major concerns in lipase-catalysed ring opening polymerization is the effect of unwanted side reaction(s). To overcome it, there should be an excess concentration of acyl donor i.e. ε-caprolactone monomer. The molecular weight of polymerized PCL depends on the effect of hydrolysis and cyclization governed by thermodynamics equilibrium. The excess amount of ε-caprolactone increases the ratio of acyl donor to acyl acceptor resulting in increased formation of oligomers. According to ring-chain equilibrium principle, high concentration of acyl donor is required to obtain high molecular weight PCL. Thus, polymerization with bulk substrate is preferred since the reaction mixture is saturated with acyl donor substrate (Habeych et al., 2011). Lipase-catalysed ring opening polymerization of ECL in bulk substrates has been widely

reported. Several important considerations regarding the lipase-catalysed ring opening polymerization in bulk substrates including the amount of water in reaction medium and solubility of other reactants and products have been highlighted in previous studies (Marcilla et al., 2006; Uyama et al., 1997).

In the case of multi-substrate reaction, bulk concentration of a single substrate may reduce the solubility of other substrates. Thus, the probability of reaction moving forward will depend on the substrate availability to penetrate enzyme active site. Poor solubility of certain substrates may hinder the polymerization of desired product. To overcome this problem, the use of solvent with appropriate log *P*, is important not only to solubilize the reactants but also to maintain the enzyme catalytic activity. Alternatively, the application of ionic liquids also provide a greener and sustainable process in the face of toxicity issue for many organic solvents (Marcilla et al., 2006). The application of new reaction environment such as supercritical system has emerge as another alternative to the conventional system (Matsumura et al., 2001). Finally, separate consideration relating to low water content in bulk substrate system on the catalytic activity of lipase should be made, since a small amount of water is required for enzyme hydration. Therefore, proper selection of reaction medium is crucial to obtain desired product(s) (Kobayashi, 2010).

2.9 Functionalised Polycaprolactone

Modification of biodegradable polyesters has received great attention due to the requirements of advanced biomedical applications in recent years. Functionalisation introduces a chemical group into polymer molecule to exert specific chemical, physical, biological, pharmacological or other functions. The chemical groups in the form of small moiety, monomer and even copolymer are used in the functionalisation of polymer. Improvement of desired properties such as degradation rate, mechanical strength and stimuli-responsive capability towards environmental changes are important in the

development of novel materials with biocompatible characteristic (de Gracia Lux et al., 2012; Tian et al., 2012). Biodegradable polycaprolactone (PCL) has received much attention in the past few years due to its superior rheological and viscoelastic properties. Furthermore, its manufacturing process is relatively inexpensive, in addition to being easily manipulated physically, chemically and biologically. Functionalised PCL is a potential candidate for various applications due to its biodegradability and biocompatibility.

Biodegradability of PCL suggests the polymer can be degraded in nature through microbial activities. However previous studies indicated that PCL are not biodegradable in animal and human bodies (Vert, 2009). The slower degradation rate of functional PCL in mammalian environment makes the polymer more suitable for longer period *in vivo* applications (Labet & Thielemans, 2009). Evaluation of the biodegradation of functionalised PCL based on results from haematology, clinical chemistry and histology studies demonstrated that functionalised PCL polymers are biocompatible and safe for human consumption (Pulkkinen et al., 2009).

Biocompatibility of PCL refers to the ability of a material to perform with an appropriate host response in a specific application (Williams, 2003). Host responses such as immunogenic, carcinogenic and thrombogenic have been conducted for functionalised PCL in *in vivo* system. Biocompatibility of functionalised PCL has received much attention for the application of bone regeneration. The use of PCL scaffold in animals for the formation of new bone at the region of scaffold, and defect sites of human bodies have been widely accepted (Reichert et al., 2011). Long-term study of biocompatibility of functionalised PCL is crucial in view of scaffold implantation in human bodies for the regeneration of new tissues. It requires almost three years for complete clearance of implant (Meek & Jansen, 2009).

2.10 Ring Opening Polymerization in Functionalised Polycaprolactone

The role of ring opening polymerization in the production of functionalised polycaprolactone (PCL) showed complex lactone can be polymerized with simultaneous addition of functional group(s). Ring opening polymerization for functionalised lactones production has been investigated on lactones with different ring size including β-propiolactones, valerolactones, lactides and glycolides (Lou et al., 2003). Among the advantages of ring opening polymerization are the ability to achieve controlled molecular weight, lower polydispersity and higher monomer conversion. The main structure of PCL consists of ester units and inert ethylene group which are required for the reaction with functional group. A functionalised PCL can be synthesized *via* terminal end group and block copolymerization.

2.10.1 Terminal End Group Functionalisation

Terminal end group functionalisation could proceed *viz.* initiation and/or termination routes. Functionalisation *via* initiation route involves nucleophilic agent to initiate the polymerization (Figure 2.5A). Agents include water, alcohol, amine or thiol have been widely used for terminal end functionalisation of polyester (Dzienia et al., 2017; Medina et al., 2018; Zhu et al., 2015). Most common terminal end functionalisation is also initiated using a metal-based initiator e.g. stannous, aluminium, magnesium, zinc, etc. (Sarvari et al., 2017; Wang et al., 2012). There have been several reports on the application of enzyme catalyst for terminal end functionalisation *via* initiator routes. Lipase-catalysed ring opening polymerization for terminal end functionalisation is an alternative method to the chemical method using organometallic catalyst. Biocatalyst such as lipase has technical advantages such as regio-selectivity and stereo-selectivity; the whole polymerization is comparable with living polymerization using metal catalyst (Thurecht et al., 2006; Zhu et al., 2018).

In the case of termination route for terminal end functionalisation, terminating agents including vinyl methacrylic acid and divinyl sebacate are used for single step acylation of hydroxyl end group of biodegradable polyester (Carrot et al., 1999; Uyama et al., 1995). The agents are responsible for termination of chain propagation with the addition of functional group at terminal hydroxyl group (Figure 2.5B). Compared to initiation route, termination route of terminal end functionalisation is not favourable due to low yield and molecular weight of functionalised polyester at higher concentration of terminating agent.

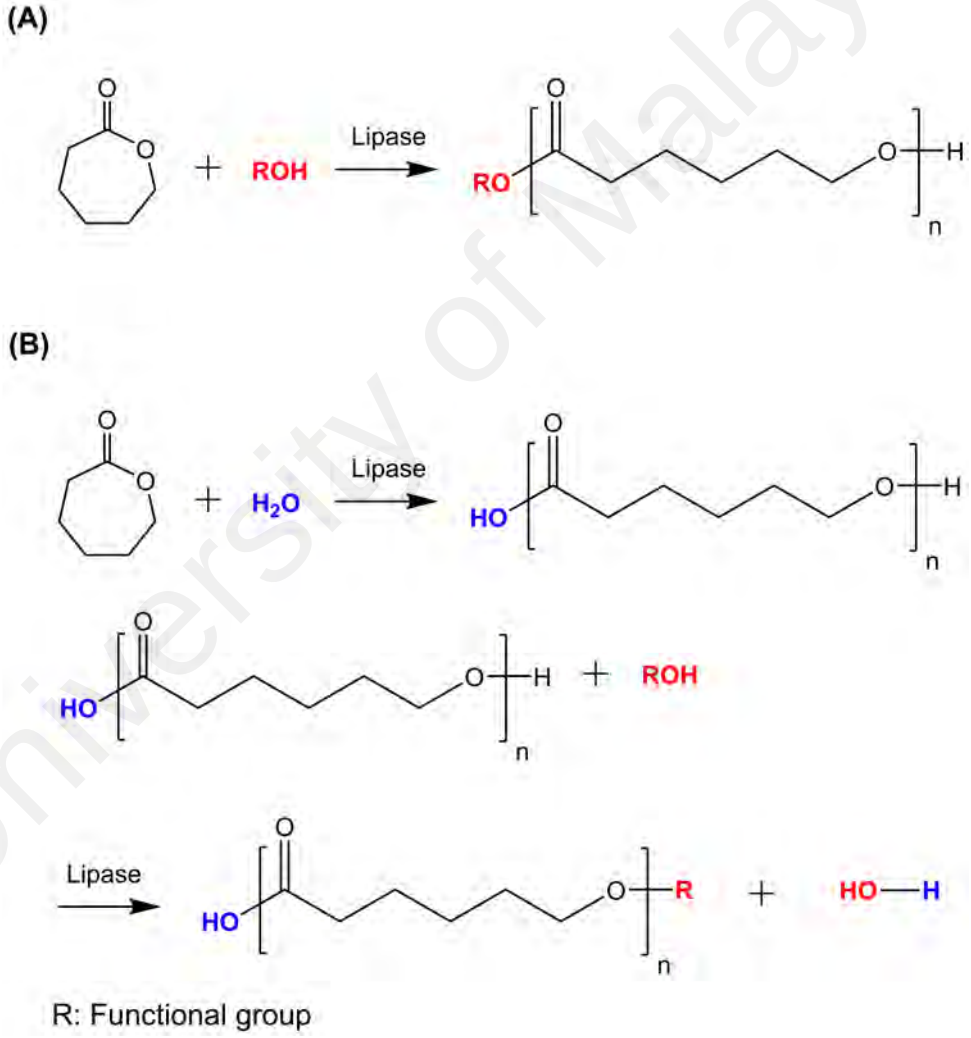

Figure 2.5: Terminal end functionalised PCL (A) Initiation; (B) Termination (Adapted from Yang et al., 2014)

2.10.2 Block Copolymerization of Functionalised Polycaprolactone

Functionalisation of polycaprolactone (PCL) can be carried out with high molecular weight functional group for the synthesis of AB block copolymers. Initially, macro initiator is used to initiate the ring opening polymerization of PCL allowing the polymerization of functionalised multi-block PCL copolymer (Alamri et al., 2014; Huang et al., 2011). Besides, functionalised PCL can be inversely synthesized by polymerizing the neat PCL before being subjected to functionalisation *via* end capping method; with this method, the functional group is grafted onto the neat PCL at the terminal end of molecules.

The role of living polymerization on the production of block copolymerization of functionalised PCL has been reported (Liu et al., 2001; Qi et al., 2013). By using this approach, a defined block copolymer can be polymerized under living polymerization mechanism without chain termination step. The synthesized functionalised PCL block copolymers contain high molecular weight with narrow range of polymer dispersity index values (Qi et al., 2013; Yao et al., 2014).

2.11 Enzymatic Functionalisation of Polycaprolactone

The application of chemical catalysis for transferring active functional groups onto the polyester has become a major issue due to possible toxicity effects when intended for human consumption. Thus, there is a critical need for enzyme as biocatalyst in the production of functionalised polymer following its biological nature (Bhangale et al., 2012; Detrembleur et al., 2000; Zhu et al., 2015). Functional groups including fatty acids, aromatic compounds, unsaturated compounds and glycoside have been used widely studied for production of functionalised polyester using lipase from *Candida antarctica* (CalB) as biocatalyst (Bhangale et al., 2012; Srivastava & Albertsson, 2006).

The application of immobilized enzyme in catalysing the synthesis of functionalised polymer has been developed for biotransformation at industrial scale (Liese & Villela Filho, 1999; Zaks, 2001). The sustainability of functionalisation process can be achieved since most of the enzymes are produced from renewable resources, free of heavy metals. However, the application of enzymatic functionalisation has been limited due to its higher cost, instability in organic solvent and availability in analytical amount. Therefore, several strategies have been employed in order to improve the application of enzyme in functionalisation process (Hudson et al., 2005). Table 2.5 shows several examples of enzymatic functionalisation of polymer.

Table 2.5: Lipase-catalysed functionalisation of lactone monomers.

Lipase	Monomer	Functional Polymer	Reference
Novozyme 435 (CalB)	1,5-dioxepan-2-one (DXO) + ε-caprolactone (ECL)	Poly(1,5-dioxepan-2-one) (PDXO)	Srivastava & Albertsson (2006)
Pseudomonas cepacia	5-methyl-5-carboxyl-1,3-dioxan-2-one (MCC) + trimethylene carbonate (TMC)	Poly(Trimethylene carbonate-co-5-methyl-5-carboxyl-1,3-dioxan-2-one)	Al-Azemi Talal & Bisht Kirpal (2002)
Novozyme 435 (CalB)	2-Hydroxyethyl methacrylate (HEMA) + g-Pentadecalactone (PDL) + ε-caprolactone (ECL)	Methacrylation of PCL and PPDL	Takwa et al. (2008)
Novozyme 435 (CalB)	Benzyl alcohol + ε-caprolactone	Benzyle ester end functionalised PCL	Bhangale et al. (2012)
Candida sp. 99-125	6-mercapto-1-hexanol + ε-caprolactone	Thiol-terminated end PCL	Zhu et al. (2015)
Novozyme 435 (CalB)	Poly(ethylene glycol) Methyl Ether (MPEO) + ε-caprolactone (ECL)	MPEOx-co-poly(ε-caprolactone)	Hans et al. (2006)

2.12 Michaelis-Menten Model for Enzymatic Functionalisation

Michaelis-Menten model is the simplest for describing reaction between enzyme and its substrate (Li et al., 2011). Namekawa et al. (1999) was the first to determine the kinetic parameters of Michaelis-Menten model for enzyme-catalysed ring opening

polymerization of polycaprolactone (PCL). The formation of acyl-enzyme intermediate is proposed as the rate determining step of overall reaction (Namekawa et al., 1999). In the presence of terminal carboxyl end group of acyclic lactone monomer, the reactivity of the intermediate is considered high and thus the subsequent steps proceed rapidly. Although the general reaction steps of enzyme-catalysed ring opening polymerization of PCL are well established, the elucidation of its detailed mechanism based on kinetic data is not entirely complete. Furthermore, there are only a few examples in literature using Michaelis-Menten model to predict the kinetic parameters of functionalisation process (Kobayashi, 2015).

2.12.1 Michaelis-Menten Model for Single Substrate

For single substrate reaction, Michaelis-Menten model is described by a two-step process that includes (i) reversible binding of enzyme (E) and substrate (S) in the formation of enzyme-substrate complex (ES) and (ii) irreversible breakdown of enzyme-substrate complex to free enzyme (E) and product (P) formation (Eq. 2.1).

$$E + S \rightleftharpoons ES \longrightarrow E + P \qquad \text{Eq. 2.1}$$

From the general stoichiometry (Eq. 2.1), the equation describing the Michaelis-Menten model is:

$$v_0 = \frac{V_{max}[S]}{K_m + [S]} \qquad \text{Eq. 2.2}$$

where v_0 is the initial velocity (M h^{-1}), V_{max} is the maximum reaction velocity (M h^{-1}), [S] is the substrate concentration (M) and K_m is the Michaelis-Menten constant (M) which correspond to a substrate concentration giving 50 % maximum reaction velocity. The relationship between substrate concentration and the initial velocity is described in Figure 2.6, where V_{max} and K_m can be determined using linear and non-linear regression analyses.

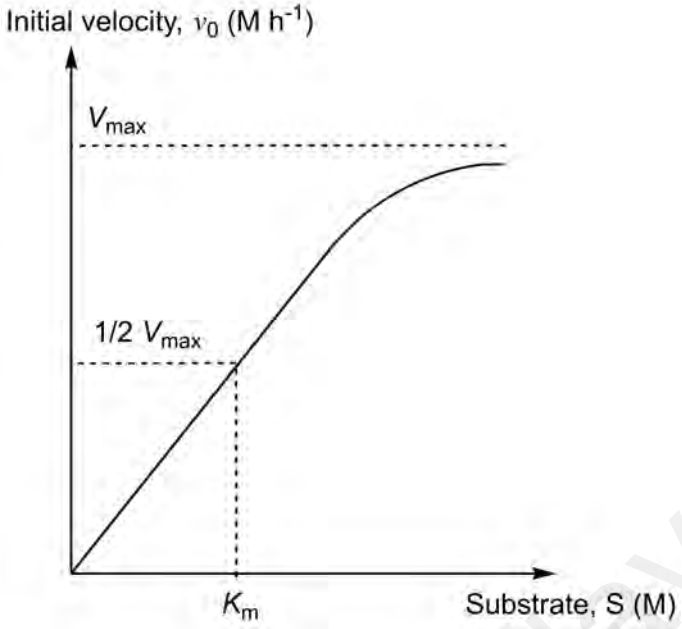

Figure 2.6: Michaelis-Menten plot of different substrate concentration

Significant kinetic studies using Michaelis-Menten model for *uni* substrate reaction has been carried out for the ring opening polymerization of PCL. Table 2.6 shows the values of V_{max} and K_m of lipase-catalysed ring opening polymerization of lactone monomer with different ring size and molecular weight. Ring opening polymerization utilizing different ring sizes of lactone monomer showed the V_{max} increases with ring size of lactone monomer (Namekawa et al., 1999). The ratio of V_{max}/K_m is the measure of polymerizability with lower ring size of monomer showing significantly higher polymerizability. van der Mee et al. (2006) observed that the V_{max} varies in non-specific trend when reaction is conducted at 45 °C in toluene. In addition to ring size, the effect of lipase from different sources on the ring opening polymerization of PCL has been reported. V_{max} value of lipase from *Candida antarctica* is the highest among other lipases such as from *Pseudomonas fluorescens* and *Fervidobacterium nodosum* (Table 2.7). Whilst lipase enzyme has been widely used in the ring opening polymerization for PCL production, Ma et al. (2009) on the other hand demonstrated esterase-catalysed PCL production along with the determination of its associated V_{max} and K_m.

Table 2.6: Effects of different lactone monomers on Michaelis-Menten kinetic parameters for *uni* substrate ring opening polymerization of PCL.

Lactone	Ring size	Enzyme	Temperature (°C)	Reaction Medium	V_{max}, (mol L^{-1} h^{-1})	K_m, (mol L^{-1})	$\frac{V_{max}}{K_m}$, (h^{-1})	Reference
ε-caprolactone	7	Lipase PF	60	Isopropyl ether	6.60×10^{-1}	6.10×10^{-1}	1.08	(Namekawa et al., 1999)
11-undecanolide	12				7.80×10^{-1}	5.80×10^{-1}	1.34	
12-dodecanolie	13				2.30	1.10	2.09	
15-pentadecanolide	16				6.50	8.00×10^{-1}	8.13	
16-hexadecanolide	17				7.20	6.30×10^{-1}	11.43	
δ-Valerolactone	6	Lipase CA	45	Toluene	9.50×10^{-1}	7.30×10^{-1}	1.30	(van der Mee et al., 2006)
ε-caprolactone	7				1.97	7.20×10^{-1}	2.74	
11-undecanolide	12				3.70×10^{-1}	3.30×10^{-1}	1.12	
12-dodecanolie	13				2.80	4.20×10^{-1}	6.67	
15-pentadecanolide	16				5.51	3.10×10^{-1}	17.77	

PF - *Pseudomonas fluorescens*; CA - *Candida antarctica*

Table 2.7: Effects of different enzymes in the ring opening polymerization of PCL.

Enzyme	V_{max}, (mol L^{-1} h^{-1})	K_m, (mol L^{-1})	$\frac{V_{max}}{K_m}$, (h^{-1})	Reference
Esterase AF	2.00×10^{-1}	9.30×10^{-2}	2.15	Ma et al. (2009)
Lipase FN	2.54×10^{-2}	3.20×10^{-1}	7.94×10^{-2}	Li et al. (2011)
Lipase PF	6.60×10^{-1}	6.10×10^{-1}	1.08	Namekawa et al. (1999)
Lipase CA	1.97	7.20×10^{-1}	2.74	van der Mee et al. (2006)
Lipase *Candida* sp. 99-125	1.46×10^{-4}	6.10×10^{-3}	2.40×10^{-2}	He et al. (2015)

AF: *Archaeoglobus fulgidus*; FN: *Fervidobacterium nodosum*; PF: *Pseudomonas fluorescens*; CA: *Candida antarctica*

2.12.2 Michaelis-Menten Model for Multiple Substrate Reaction

Many enzymes catalyse reaction between two or more substrates with the formation more than one product. The number of reactants and products in the reaction can be written in specific terms of *uni* (one), *bi* (two), *ter* (three) and *quad* (four). The discussion on multiple substrate reactions can be described based on the stoichiometric equation of enzyme-catalysed reactions (Eq. 2.3). The binding of two substrates with the formation of two products is called a "bi-bi" reaction. The binding of two substrates can occur through two mechanisms i.e. sequential mechanism and non-sequential mechanism.

$$A + B \rightleftharpoons P + Q \qquad \text{Eq. 2.3}$$

In the sequential mechanism, all substrates must bind with the enzyme before the reaction can take place for product formation. This mechanism can be further subdivided into random and ordered sequential mechanism. For random sequential mechanism, the substrates bind with the enzyme in random order (Figure 2.7A). However, in ordered sequential mechanism, substrates are bind with the enzyme in a subsequent order which the first substrate must bind before the second substrate is able to bind (Figure 2.7B). Similarly, the reversible binding of substrates and enzyme has resulted in the formation of intermediate EAB, which is identical by either mechanism.

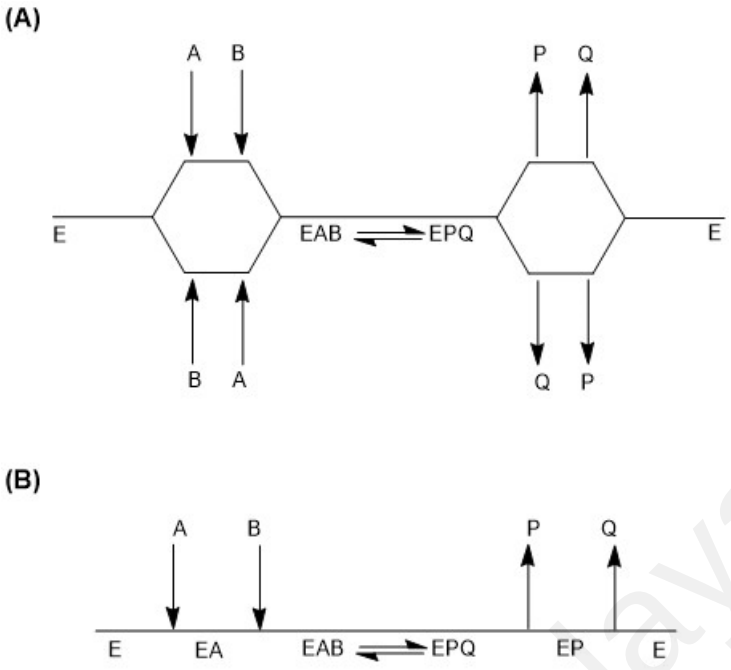

Figure 2.7: Cleland schematic reaction (A) Random sequential; (B) Ordered sequential (Adapted from Kooy et al., 2014)

Generally, a non-sequential mechanism is also known as ping-pong (double displacement) mechanism required at least one product is released before all substrates have bound. The following equation describes the stoichiometry of ping-pong bi-bi mechanism.

$$E + A \underset{k_{-1}}{\overset{k_1}{\rightleftharpoons}} EA \xrightarrow{k_2} E^*P + B \underset{k_{-3}}{\overset{k_3}{\rightleftharpoons}} E^*B \xrightarrow{k_4} E + Q \qquad \text{Eq. 2.4}$$

The first substrate (A) binds to enzyme (E) active site to form first intermediate enzyme-substrate complex (EA). During the formation of central complex (EA), the substrate (A) is converted into product (P) and the enzyme that covalently binds to product has become acylated (E*). Then, the released of the first product from acylated enzyme has resulted in the binding of second substrate (B), which followed by the formation of second intermediate acylated enzyme-substrate complex (E*B). As the second product released (Q), the free enzyme is regenerated from its acylated form. The process whereby the enzyme is bouncing back and forth from an intermediate state to its

standard state is called “ping-pong” mechanism. Figure 2.8 shows the Cleland schematic reaction corresponding to ping-pong bi-bi mechanism.

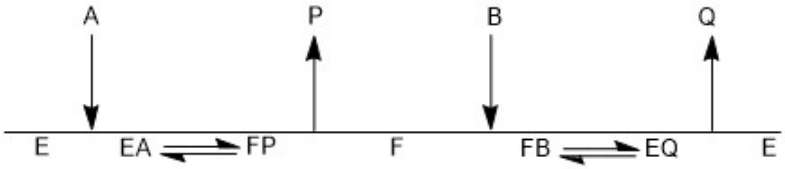

Figure 2.8: Cleland schematic reaction of ping-pong bi-bi mechanism (Adapted from Kooy et al., 2014)

2.12.3 Derivation of Initial Rate of Ping-pong Bi-bi Mechanism

The kinetic of double displacement ping-pong bi-bi mechanism can be described according to the general steady-state stoichiometric equation (Eq. 2.4). For simplicity, all of the enzyme kinetic equations have been derived assuming no products are present. From the steady-state equation, the rate equation (v), Michaelis-Menten constants (K_m) and enzyme mass balance can be developed. By considering the random sequential mechanism, the derivation of rate equation for ping-pong bi-bi mechanism is determined from the effective dissociation constant of reactant A. The two effective dissociation constants are K_{iA} and K_A. The first effective dissociation constant is K_{iA} constant which describes the binding constant of A to E. The second effective dissociation constant is K_A correspond to binding constant of A to EB. Thus, effective dissociation constant of bi-substrate can be written as:

$$K_{iA} = \frac{[E][A]}{[EA]} \qquad \text{Eq. 2.5}$$

$$K_{iB} = \frac{[E][B]}{[EB]} \qquad \text{Eq. 2.6}$$

$$K_A = \frac{[EB][A]}{[EAB]} \qquad \text{Eq. 2.7}$$

$$K_B = \frac{[EA][B]}{[EAB]} \qquad \text{Eq. 2.8}$$

The mass balance of total enzyme can be written as:

$$E_T = E + EA + EB + EAB \qquad \text{Eq. 2.9}$$

By rearranging the rate equations in Eq. 2.5 - 2.9, the following equation can be obtained:

$$EA = \frac{K_B[EAB]}{[B]};$$

$$EB = \frac{K_A[EAB]}{[A]}, \text{ and}$$

$$E = \frac{K_{iA}[EA]}{[A]} = \frac{K_{iA}K_B[EAB]}{[A][B]}.$$

Thus, the mass balance of total enzyme can be solved:

$$E_T = E + [EA] + [EB] + [EAB]$$

$$E_T = \frac{K_{iA}K_B[EAB]}{[A][B]} + \frac{K_B[EAB]}{[B]} + \frac{K_A[EAB]}{[A]} + [EAB]$$

$$E_T = \left(\frac{K_{iA}K_B}{[A][B]} + \frac{K_B}{[B]} + \frac{K_A}{[A]} + 1\right) EAB$$

Since $v_0 = K_{cat}[EAB]$;

$$E_T = \left(\frac{K_{iA}K_B}{[A][B]} + \frac{K_B}{[B]} + \frac{K_A}{[A]} + 1\right)\left(\frac{v_0}{K_{cat}}\right)$$

$$(v_0) = E_T(K_{cat})\left(\frac{[A][B]}{K_{iA}K_B} + \frac{[A][B]}{[A]K_B} + \frac{[A][B]}{[B]K_A} + 1\right)$$

and $V_{max} = K_{cat} E_T$:

$$(v_0) = \frac{V_{max}[A][B]}{(K_{iA}K_B + [A]K_B + [B]K_A + [A][B])} \qquad \text{Eq. 2.10}$$

By assuming rapid equilibrium, the K_{iA} and K_{iB} terms in Eq. 2.10 can be removed since the final EAB concentration is obtained from the identical path which either E to A to EAB or E to B to EAB. Therefore, the final equation describing the ping-pong bi-bi mechanism can be described as follows:

$$(v_0) = \frac{V_{max}[A][B]}{(K_B[A] + K_A[B] + [A][B])} \quad \text{Eq. 2.11}$$

2.13 Kinetics of Living Polymerization in Polymer Chain Propagation

In general, living polymerization can be defined as any reaction which does not undergo chain termination or chain transfer step, and the rate of monomer consumption in the propagation step follows a first-order rate law (van der Mee et al., 2006). According to IUPAC, the term living polymerization is reserved for polymerization that proceed without irreversible termination (Jenkins et al., 2010). The synthesized polymer *via* living polymerization mechanism has the ability to propagate under controlled molecular weight while the chain termination or chain transfer is negligible (Szwarc, 1998). The chain propagation step is characterized by the addition of a monomer unit at the chain-end that remain active. Without living polymerization mechanism, the propagation proceeds according to standard elementary steps of initiation, propagation and chain termination. The general mechanism of living polymerization requires an initiator and monomer whereas for complex living polymerization mechanism, the use of catalyst and chain end stabilizers are often needed.

Besides the ability to control molecular weight of polymer *via* sequential addition of monomer, living polymerization mechanism is also used to synthesize functionalised polymers through selective termination with appropriate functional reagents. As previously reported, living polymerization techniques for ring opening polymerization of functionalised PCL are shown in Table 2.8. The application of living polymerization mechanism in functionalised PCL production exhibits significant potential based on published literature. Living polymerization is a desirable process since it provides polymer population with narrow dispersity, facilitate excellent control over end group functionality, and incorporate a broad range of functional groups into polymer scaffolds and network materials.

Table 2.8: Living polymerization techniques in ring opening polymerization of functionalised PCL.

Living polymerization techniques	Reactants/Products			Reaction condition		Reference
	Catalyst/Initiator	**Substrates**	**Polymer**	**Medium**	**Temp (C°)**	
Anionic	**Initiator:** Aluminum tri(4-oxy-TEMPO)	ECL	TEMPO-functionalised PCL	Toluene	25–40	Yoshida & Osagawa (1998)
	Catalyst: $Sn(Oct)_2$; **Macroinitiator:** Poly(styrene)-b-Poly(ethyleneoxide)	ECL	ABC 3-miktoarm star-shaped terpolymers of Poly(styrene), Poly(ethylene oxide),and Poly(ε-caprolactone)	Toluene	110	Wang & Huang (2008)
	Catalyst: Phosphazene base (P_4-t-Bu); **Initiator:** Methanol, ethylene glycol, ethyl acetate	ECL, Methyl Methacrylate.	Hybrid copolymerized of Poly(CL-*co*-MMA)	Toluene	25	Yang et al. (2012)
Cationic	**Catalyst:** Diphenyl phosphate (DPP); **Initiator:** 3-phenyl-1-propanol (PPA).	GVL, ECL.	Block copolymerization Poly(VL-*co*-CL)	Toluene	27	Makiguchi et al. (2011)
	Catalyst: HCl diethylether (Et_2O.HCL); **Macroinitiator:** Poly(isobutyl vinyl ether) (PIBVE)	ECL.	Block copolymerization of Poly(IBVE-*co*-CL)	Toluene	50	Zaleska et al. (2009)
Monomer activated	**Catalyst:** Lipase CALB; **Initiator:** Water, alcohol.	ECL	PCL	Deuterated toluene	60	Mei et al. (2003)
	Catalyst: Lipase CALB; **Macroinitiator:** Poly(ethylene glycol)-methyl ether, 2000 ($MPEO_{2000}$)	ECL	Block copolymerization of Poly(ECL-b-$MPEO_{2000}$)	Bulk substrate	70	Yang et al. (2018)

ECL: ε-Caprolactone; GVL: δ-Valerolactone; PCL: Polycaprolactone

CHAPTER 3: MATERIALS AND METHODS

3.1 Materials

Monomers including ε-caprolactone (Cat: 802801) and methyl-*D*-glucopyranoside (Cat: 840024) were purchased from Merck (Germany). Immozyme CalB is an immobilized lipase B preparation from *Candida antarctica* was purchased from ChiralVision (Netherlands). *tert*-butanol (2-methylpropan-2-ol) (Cat: 16) was purchased from Ajax Chemical (Australia). Methanol (Cat: 106009), tetrahydrofuran (Cat: 109731), chloroform (Cat: 102445) were purchased from Merck (Germany). All chemicals were of analytical grade. Molecular sieve 3 Å (Cat: 208574) was purchased from Sigma-Aldrich (USA).

3.2 Reactor Assembly

Batch mode reactions were carried out in 500 mL round bottom glass vessel equipped with Rushton turbine impeller. The reaction temperature was kept constant by using digital control water bath (Memmert, Germany). Digital overhead stirrer (IKA Eurostar 60, USA) was used to control the impeller speed during the reaction. Complete schematic of enzyme batch reactor is illustrated in Figure 3.1.

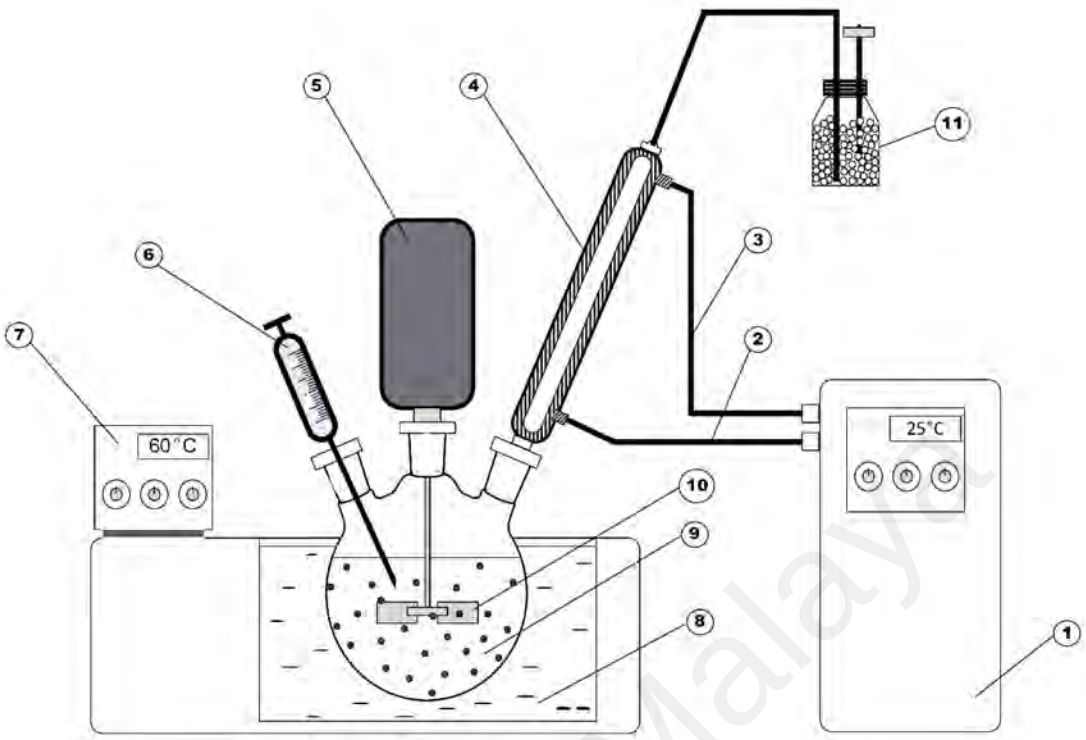

Figure 3.1: Schematic assembly of enzymatic batch reactor (1) Circulating water bath for circulating cooling water in exhaust condenser; (2) Cooling water outlet; (3) Cooling water inlet; (4) Exhaust condenser; (5) Overhead stirrer; (6) Sampling syringe; (7) Water bath controller; (8) Thermostatic water bath; (9) Reaction mixture; (10) Rushton turbine impeller; (11) Molecular sieve 3 Å

3.3 General Reaction Preparation

Batch mode reactions were performed in a bench-scale custom-fabricated enzymatic reactor according to schematic diagram in Figure 3.1. The overall general reaction was described in Figure 3.2. Dried *tert*-butanol was prepared by shaking with 30 % *w*/*v* of molecular sieve 3 Å for 24 hours. This was followed by adding an appropriate amount of MGP into 280 mL of dried *tert*-butanol and incubated at 80 °C for 24 hours prior to the addition of ECL. To initiate the functionalisation reaction immobilized lipase is added into the reaction mixture.

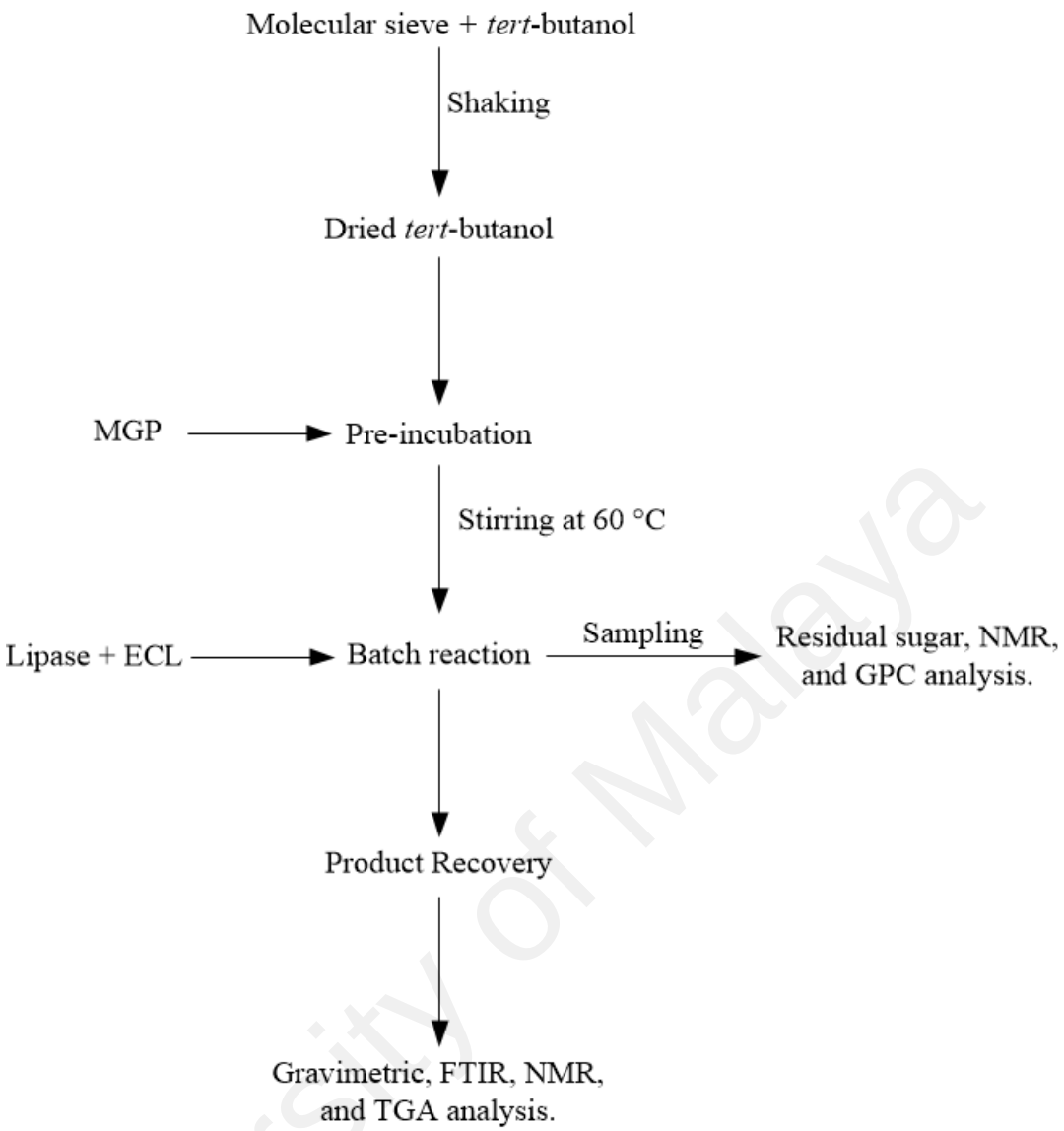

Figure 3.2: General steps of functionalisation reaction

3.4 Product Sampling

Periodically, about 2.0. mL of crude sample was withdrawn from the reaction mixture from the sampling port before subjected to filtration using 0.2 µm PTFE membrane filter. Sample filtrate was collected for product recovery and purification.

3.5 Product Recovery and Purification

Figure 3.3 summarizes the general steps in the recovery and purification of the functionalised oligomer. Chloroform was added to the batch reaction mixture in 1:1 ratio

to stop the reaction. Then, whole reaction mixture was filtered out using 90 mm of PTFE membrane filter (pore size 0.2 μm) (Sartorius) to remove lipase beads and solid particles before subjected to solvent removal using rotary evaporator (Rotavap) at 60 °C under reduced pressure. After solvent removal, cold methanol was added into the concentrated reaction mixture in ratio 1:10 *v*/*v* in order to precipitate the functionalised polymer before subjected to drying process at 40 °C under reduced pressure for 24 hours incubation.

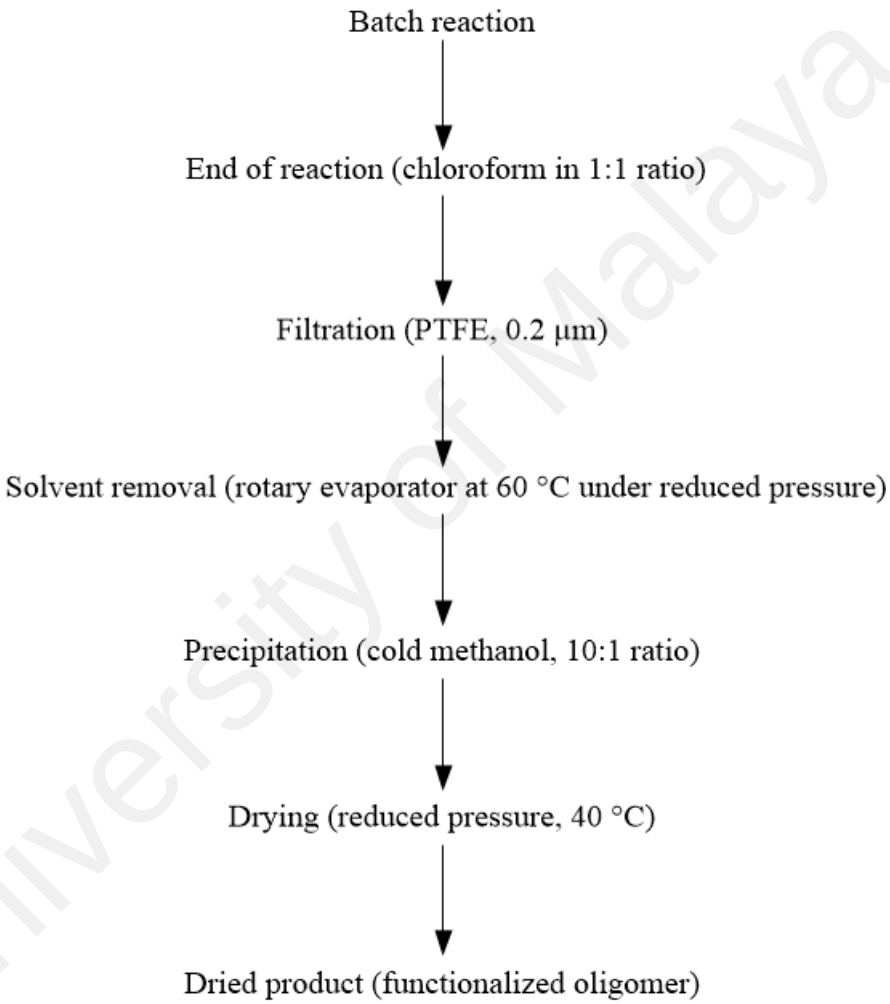

Figure 3.3: Steps in product recovery and purification

3.6 Dried Weight Analysis

Dried weight analysis was carried out using product recovered from the whole batch reaction at specified interval. Dried precipitates from the drying process under reduced pressure were incubated at room temperature before subjected to weight determination using analytical balance (Sartorius) (Figure 3.4).

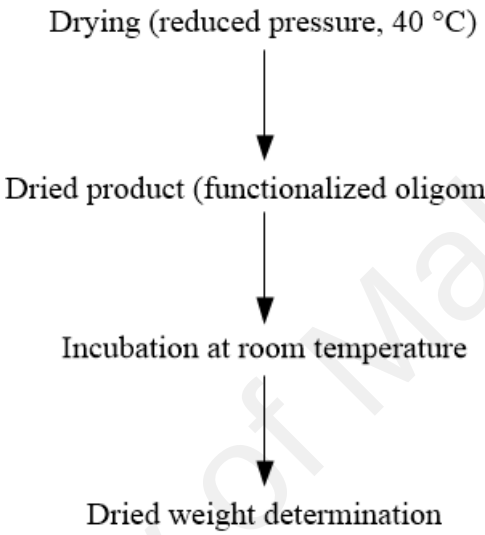

Figure 3.4: Steps in dried weight determination

3.7 Residual Sugar Analysis

Figure 3.5 showed the steps involved in residual sugar analysis. For measurement of residual sugar concentration, samples were withdrawn at specific intervals. Firstly, chloroform was added to the withdrawn samples in 1:1 ratio to terminate the reaction. Then, samples were filtered out using 0.2 µm PTFE membrane filter to remove lipase beads before being subjected to liquid-liquid separation according to Ariffin et al. (2014).

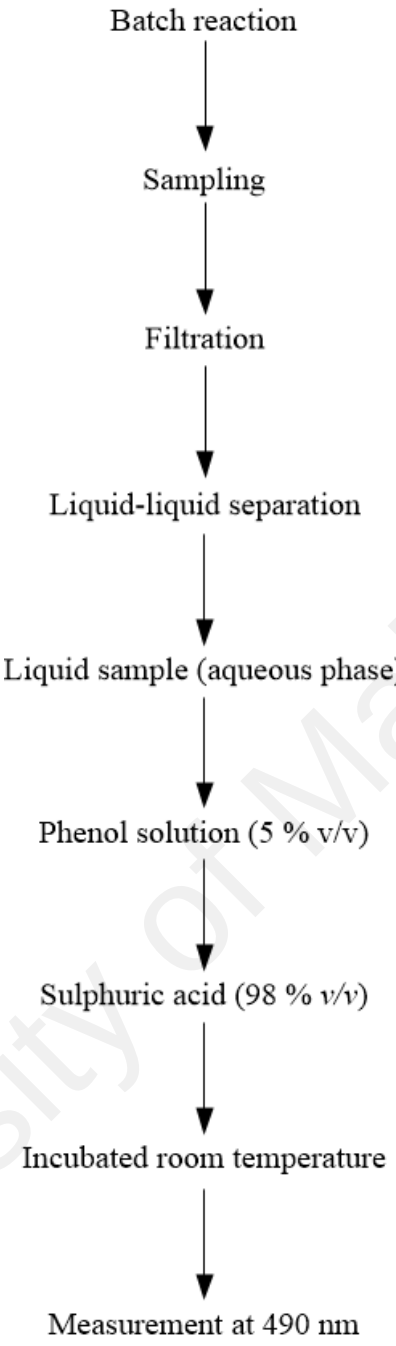

Figure 3.5: Steps in residual sugar analysis

About 450 µL of sample was recovered from the aqueous phase of liquid-liquid separation for residual sugar analysis. Sample was added into a test tube containing 50 µL of 5 % (*v*/*v*) phenol solution. Then, about 2,500 µL of concentrated 98 % (*v*/*v*) sulphuric acid was added into the mixture. Reaction between phenol and sample was facilitated by vigorous vortexing for a few seconds. Then, sample was cooled down to

room temperature by incubation in the water bath at 25 °C for 5 minutes. Absorbance reading at 490 nm was carried out in quartz cuvette using JASCO 630 UV/Vis spectrophotometer (Japan). The actual amount of residual carbohydrate was determined from the standard calibration plot of different concentrations methyl-*D*-glucopyranoside (MGP) as indicated in Table 3.1. Stock solution of MGP (1,000 mg L^{-1}) was dissolved in ultrapure water. Standard calibration plot was constructed based on the absorbance of each concentration.

Table 3.1: Preparation of methyl-*D*-glucopyranoside standards.

	Methyl-*D*-glucopyranoside						
in mM	0.515	0.773	1.030	1.287	1.545	1.802	2.060
in mg L^{-1}	100	150	200	250	300	350	400
Stock (mL)	0.045	0.068	0.090	0.113	0.135	0.158	0.180
dH_2O (mL)	0.405	0.382	0.360	0.337	0.315	0.292	0.270
Total volume	0.450	0.450	0.450	0.450	0.450	0.450	0.450

3.8 Monomer Conversion

The percentage of monomer conversion was calculated based on gravimetric analysis of dried sample weight (Henini et al., 2012). The dried weight of converted ECL (m_{ECL}) was calculated according to the mass balance equation (Eq. 3.1):

$$m_{Functionalized} = m_{ECL} + m_{MGP} \quad \text{Eq. 3.1}$$

where $m_{Functionalised}$ is final dry weight of functionalised oligomer (g), and m_{MGP} is converted dry weight of MGP (g) calculated from the residual sugar analysis as discussed in Section 3.7. The dried weight of functionalised oligomer was calculated based on gravimetric analysis (Section 3.6).

3.9 Gel Permeation Chromatography

Gel permeation chromatography (GPC) analysis was used to determine the molecular weight (g mol^{-1}) of the samples. Analysis was carried out using Agilent LC 1220 (Agilent,

USA) equipped with a refractive index detector (Model 1260). General steps in GPC analysis is summarized in Figure 3.6. GPC column i.e. Phenomenex Phenogel 5 µm Linear phase column (300 × 7.8 mm) was used for separation product with molecular weight range 100-10,000 kDa using tetrahydrofuran (THF) as a mobile phase at a flow rate of 1.0 mL min^{-1}. About 10 to 15 mg of dried samples were dissolved in 1.0 mL THF solvent and filtered out using 0.22 µm PTFE membrane filter prior to injection. GPC analysis was carried out at 35 °C with injection volume of 10.0 µL. A calibration plot employing commercial polystyrene standards, EasiVial PS-M (Agilent) with a medium range of molecular weights (162–500,000 Da) was used for the estimation of number average molecular weight (M_n) of product samples.

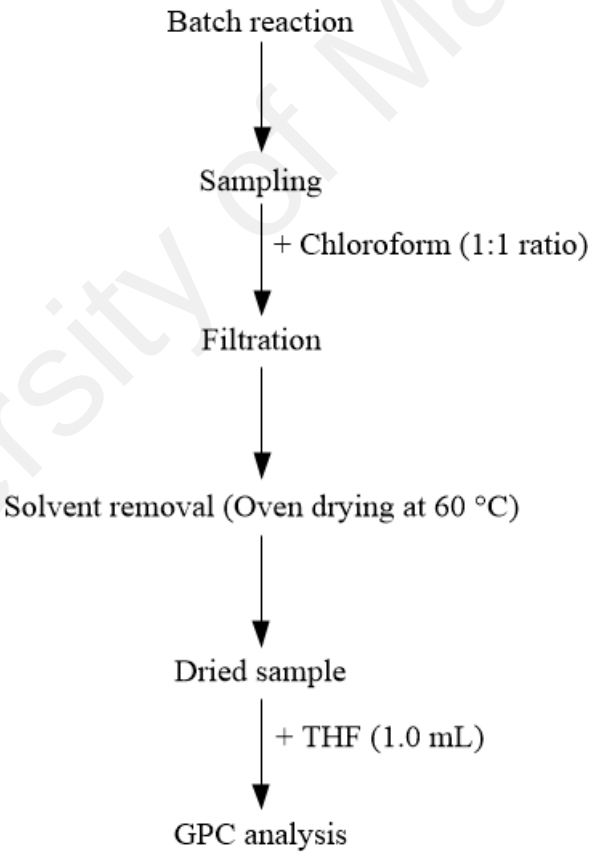

Figure 3.6: Steps in gel permeation chromatography analysis

3.10 Product Characterization

Product characterization was carried out using dried samples obtained after drying under reduced pressure unless stated otherwise. General steps for product characterization are shown in Figure 3.7. Analyses include Fourier Transform Infrared spectroscopy (FTIR), nuclear magnetic resonance (NMR) and thermal gravimetric analysis (TGA).

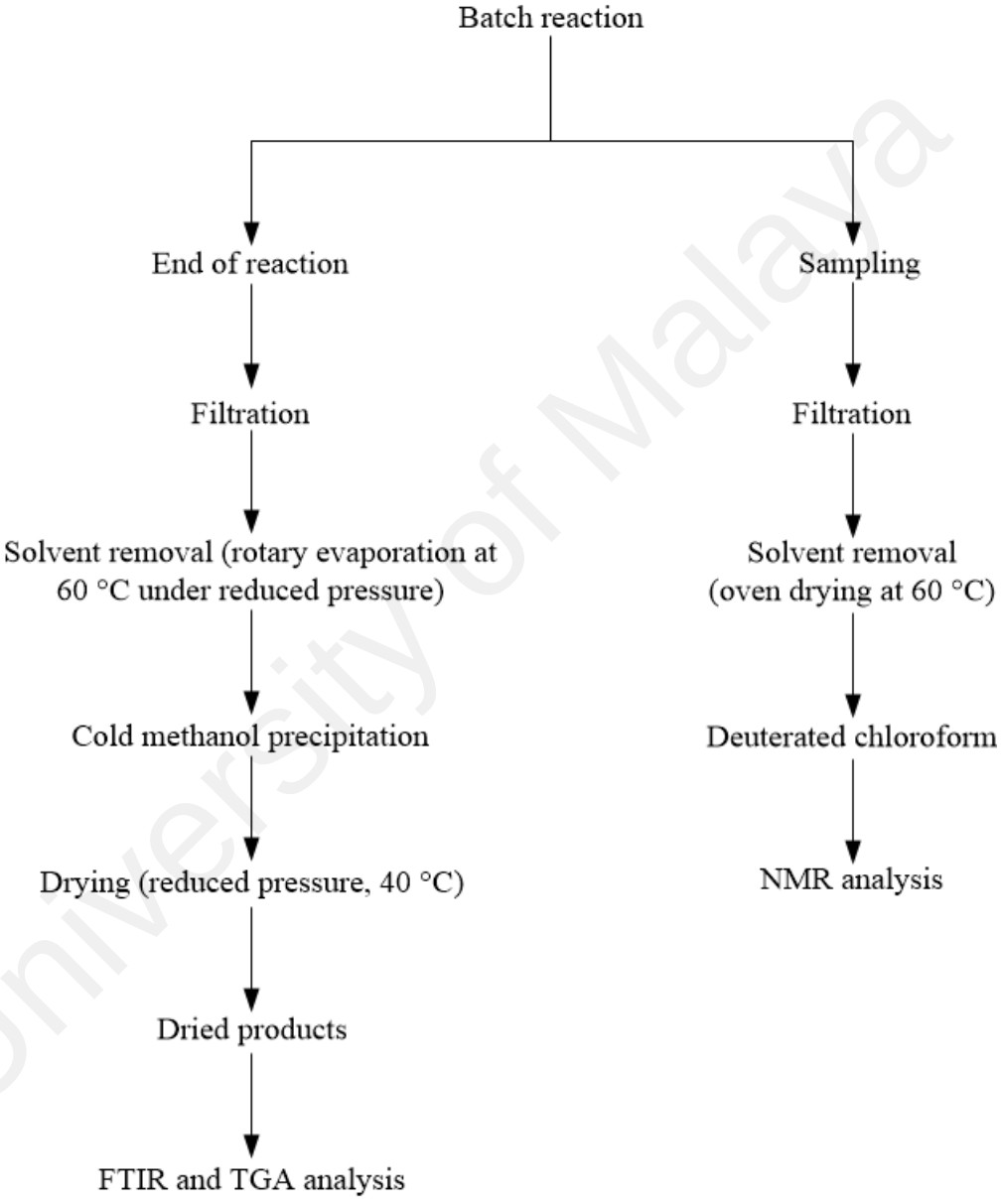

Figure 3.7: Steps in product characterization

3.10.1 Fourier Transform Infrared (FTIR)

For product characterization, the general steps in Figure 3.7 were followed. FTIR analysis was carried out using Perkin-Elmer FTIR RX-1 spectrometer (Perkin-Elmer). About 15.0 mg of dried sample was ground with 20.0 mg dried potassium bromide (KBr) pellets as carrier and casted on the FTIR sample carrier. Spectrum measurement was recorded at room temperature between 4,000 and 400 cm^{-1} with 4 cm^{-1} resolution with a total of ten running scans.

3.10.2 Nuclear Magnetic Resonance (NMR)

Sample for NMR was obtained according to Figure 3.7. NMR spectrum was recorded on ECA 400 FT-NMR system (JEOL) at 400 MHz. Deuterated chloroform with tetramethylsilane (TMS) as internal reference standard was used to dissolve 15.0 mg of dried sample. Prior to addition to the NMR tubes, sample mixture was filtered using 0.22 μm PTFE syringe filter.

3.10.3 Thermogravimetric Analysis (TGA)

Samples for thermogravimetric analysis was obtained according to Figure 3.7. The analysis was conducted by using TGA-4000 machine (Perkin-Elmer, USA). About 20 mg of dried sample was used for analysis. Samples were heated from 30 to 900 °C at scanning rate of 10 °C min^{-1} under constant nitrogen flow rate at 20 mL min^{-1}.

3.11 Screening of Selected Operating Variables

The effects of selected operating variables namely lipase, initial MGP concentration, initial ECL concentration, temperature and agitation rate were studied in a randomized two-level half factorial design (2^{k-1}). Statistical software, Minitab® 18 was used to design the factorial experiment for the screening of selected operating variable. A 2^{k-1} design was

employed since it requires fewer runs whereas in full factorial design (2^k), the number of runs increases significantly with the number of factors. From the study, the fractional factorial design experiment was used to screen significant parameters for the batch functionalisation in a new customized stirred tank reactor. The significant parameters from factorial screening can be used as reference for the optimization studies using response surface analysis. Furthermore, responses from factorial analysis can be used in the central composite design for the response surface analysis. The advantage of factorial design it requires fewer runs used only minimum and maximum level of each factor.

However, effects of some factors in 2^{k-1} design can lead to wrong conclusion from confounding effect. According to Jankowski et al. (2016), a confounding effect is defined as two or more effects that cannot be separated during data analysis. The observed effect cannot be ascribed solely to first variable without considering the effect of a second variable. The half factorial design is possibly the most used design for screening significant factors (Jiang et al., 2017; Junior et al., 2012; Santos et al., 2012; Wong et al., 2015). The design has the resolution V error with at least either main effect or two-way interactions effect is confounded with a three-way or more interactions. In the case of screening experiments, the experimental design with higher order interactions were negligible and the confounding factors can be omitted. Thus, a two-level half factorial design with resolution V is preferred since no confounding effects are observed between the main effects and two-way interactions.

The effects of main variables and interactions between variables were analysed using dried weight of functionalised oligomer (% *w*/*v*) as the response. In the study, the functionalisation in customized batch reactor was investigated based on the combination of selected key physical (agitation speed, temperature) and chemical factors (enzyme and substrates). Owing to the complex nature of physico-chemical interactions in lipase-catalysed functionalisation (Villadsen et al., 2011), factorial design experiment is an

effective and practical route for investigating the dynamics of the proposed reaction system. According to Walter & Pronzato (1997), establishing optimum condition using design of experiment (e.g. factorial design and response surface analysis) can maximise the confidence on the model parameters, thus increasing the confidence on the model prediction.

Table 3.2 showed factor levels and concentration range of selected operating variables. Analysis of variance (ANOVA) was used to analyse the response with significance level of $p < 0.05$ for each of selected operating variables. For model adequacy, residual analysis was carried out in order to determine the goodness-of-fit in regression model. Graphical analysis on the statistical data was applied to explore the behaviour of data distribution, error and assess relationship between variables.

Table 3.2: Two-level half factorial design levels and concentration.

Variables	Symbol	Levels	
		Low (-1)	High (+1)
Lipase (% *w*/*v*)	X_{Lip}	1.2	2.8
Initial ECL (% *w*/*v*)	X_{ECL}	3.8	11.5
Initial MGP (% *w*/*v*)	X_{MGP}	0.04	0.14
Temperature (°C)	X_{Temp}	40	60
Agitation rate (min^{-1})	X_{Agi}	90	180

3.12 Kinetic Studies

For the kinetic studies, the reaction conditions such as initial MGP concentrations, initial ECL concentrations, lipase, agitation rate and reaction temperature were summarized in Table 3.3. The concentration range for both substrates were chosen according to their solubility in *tert*-butanol and the ratio of percentage volume (% *v*/*v*) reactants to reaction mixture. In the case of solubility, MGP has poor solubility in *tert*-butanol. Furthermore, the volume of substrates used in the reaction was standardized so as not exceeding 10 % of the total reaction mixture volume. From the study, the maximum volume of ECL was calculated at 10.7 % *v/v* or 30 mL of the total 280 mL *tert*-butanol.

Table 3.3: Reaction condition for kinetic studies.

Parameter	Condition/Concentration
Agitation rate*	-
Temperature*	-
Lipase*	-
Initial MGP	1.84, 4.60 and 7.36 mM
Initial ECL	0.34, 0.50 and 1.00 M
Reaction Medium (*tert*-Butanol)	280 mL

*Determined from factorial design experiment

The initial rate of reaction, v_0 is the instantaneous rate was calculated from the slope of tangent line from origin on substrate consumption time profile. From Figure 3.8, the initial rate is determined from the region of constant substrate consumption rate with time where the curve represents a zero order reaction. Substrate consumption is calculated as $S_{Cons} = S_0 - S_t$ where S_{Cons} is molar substrate consumption (M), S_0 is initial substrate concentration (M) and S_t is residual substrate concentration (M) at t time (h). The initial rate is measured when substrate concentration is non-limiting and enzyme activity is at the maximum. The measured initial reaction rates were used to fit the initial velocity equation as a function of initial substrates concentration.

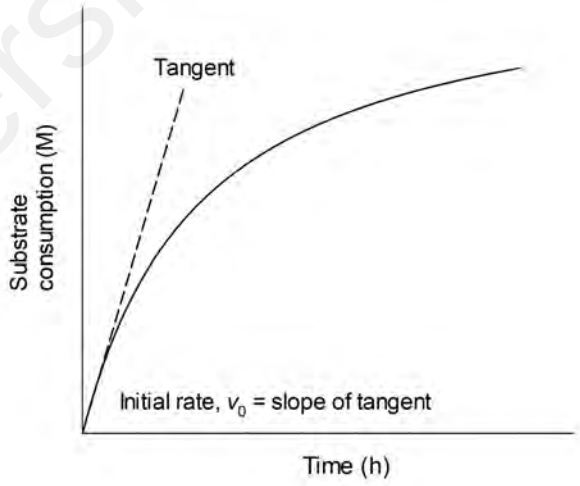

Figure 3.8: Initial rate determination

A ping-pong bi-bi mechanism without ternary complex formation was used to model lipase-catalysed MGP functionalisation of ECL according to Eq. (3.2):

$$(v_0) = \frac{V_{max}[\mathrm{ECL}][\mathrm{MGP}]}{\left(K_{mMGP}[\mathrm{ECL}] + K_{mECL}[\mathrm{MGP}] + [\mathrm{ECL}][\mathrm{MGP}]\right)} \quad \text{Eq. 3.2}$$

where v_0 is the initial rate of reaction (M h^{-1}), V_{max} is the maximum velocity (M h^{-1}), [ECL] is ε-caprolactone (M), [MGP] is methyl-*D*-glucopyranoside (M), K_{mECL} is the Michaelis constant for ε-caprolactone (M) and K_{mMGP} is the Michaelis constant for methyl-*D*-glucopyranoside (M). Kinetic parameters in the nonlinear equation (Eq. 3.2) were solved using Polymath® 6.0 software. The predicted kinetic parameters were validated using statistical analysis of 95 % confidence interval, correlation coefficient (R^2) and residual analysis.

For chain propagation step, kinetic mechanism of living polymerization was applied for the investigation. It is assumed that chain propagation proceeds at a constant rate. The equation describing the kinetic of chain propagation based on living polymerization mechanism can be written according to Eq. (3.3):

$$R_P = \frac{d(C_{ECL})}{d(t)} = r_{App}(C_{ECL}) \quad \text{Eq. 3.3}$$

where R_P denotes the rate of polymerization (M h^{-1}), r_{App} is the apparent rate constant of living polymerization mechanism (h^{-1}), C_{ECL} is monomer concentration (M) and t is reaction time (h). Model fitting was performed using linear and non-linear regressions (Polymath® 6.0).

CHAPTER 4: RESULTS AND DISCUSSION

4.1 Standard Calibration Plot of Methyl-*D*-glucopyranoside

Figure 4.1 showed the standard calibration plot for a series of methyl-*D*-glucopyranoside (MGP) concentrations.

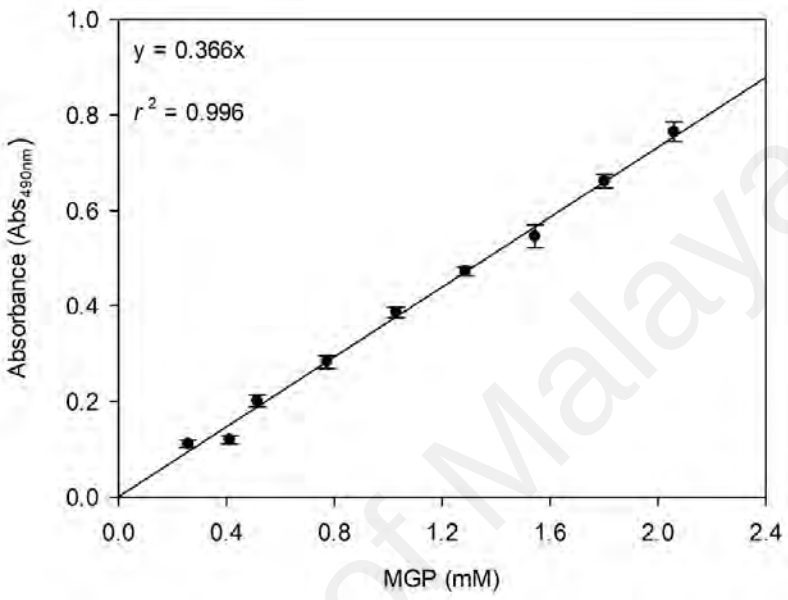

Figure 4.1: Standard calibration plot of MGP

4.2 Screening of Selected Operating Variables

Design of experiment (DOE) was used to analyse the half factorial model of screening selected operating variables. A total of 48 experimental runs were carried out according to design matrix with percentage dried weight of functionalised oligomer was used as experimental response (Table 4.1).

Table 4.1: Design matrix and the experimental response.

Run	Variables					DW
	X_{Lip}	X_{ECL}	X_{MGP}	X_{Temp}	X_{Agi}	
1	1.20	3.82	0.04	60.00	90.00	1.90
2	2.80	3.82	0.14	60.00	90.00	3.48
3	1.20	3.82	0.14	60.00	180.00	1.79
4	1.20	3.82	0.14	60.00	180.00	1.96
5	1.20	3.82	0.04	60.00	90.00	2.06
6	1.20	11.46	0.04	60.00	180.00	7.90
7	2.80	11.46	0.14	40.00	90.00	8.64
8	1.20	11.46	0.04	40.00	90.00	5.95
9	1.20	3.82	0.14	40.00	90.00	1.41
10	1.20	11.46	0.14	40.00	180.00	6.39
11	2.80	3.82	0.14	60.00	90.00	3.33
12	2.80	3.82	0.04	40.00	90.00	2.50
13	1.20	11.46	0.14	40.00	180.00	6.01
14	2.80	3.82	0.14	60.00	90.00	3.21
15	2.80	11.46	0.14	60.00	180.00	11.11
16	2.80	11.46	0.04	40.00	180.00	9.26
17	1.20	3.82	0.04	40.00	180.00	1.61
18	1.20	11.46	0.04	60.00	180.00	7.84
19	1.20	11.46	0.14	60.00	90.00	7.69
20	2.80	3.82	0.04	40.00	90.00	2.60
21	1.20	3.82	0.04	60.00	90.00	2.10
22	2.80	11.46	0.04	60.00	90.00	10.76
23	2.80	3.82	0.14	40.00	180.00	2.84
24	2.80	11.46	0.04	40.00	180.00	9.06
25	2.80	3.82	0.04	40.00	90.00	2.43
26	1.20	3.82	0.04	40.00	180.00	1.45
27	2.80	3.82	0.04	60.00	180.00	3.44
28	2.80	11.46	0.14	40.00	90.00	8.98
29	1.20	11.46	0.04	40.00	90.00	6.02
30	2.80	11.46	0.14	40.00	90.00	8.54
31	1.20	11.46	0.14	40.00	180.00	5.83
32	1.20	11.46	0.04	60.00	180.00	7.55
33	1.20	11.46	0.14	60.00	90.00	7.41
34	1.20	3.82	0.04	40.00	180.00	1.50
35	1.20	11.46	0.14	60.00	90.00	7.31
36	1.20	3.82	0.14	40.00	90.00	1.56
37	2.80	3.82	0.14	40.00	180.00	2.80
38	2.80	3.82	0.04	60.00	180.00	3.02
39	2.80	11.46	0.04	60.00	90.00	10.96
40	2.80	11.46	0.14	60.00	180.00	10.83
41	1.20	3.82	0.14	40.00	90.00	1.47
42	2.80	3.82	0.14	40.00	180.00	2.63

Table 4.1, continued.

Run	Variables					DW
	X_{Lip}	X_{ECL}	X_{MGP}	X_{Temp}	X_{Agi}	
43	2.80	11.46	0.14	60.00	180.00	10.59
44	1.20	3.82	0.14	60.00	180.00	1.90
45	2.80	11.46	0.04	60.00	90.00	11.26
46	2.80	3.82	0.04	60.00	180.00	3.27
47	1.20	11.46	0.04	40.00	90.00	6.15
48	2.80	11.46	0.04	40.00	180.00	8.86

X_{Lip}: Lipase (% *w*/*v*); X_{ECL}: Initial ECL (% *w*/*v*); X_{MGP}: Initial MGP (% *w*/*v*); X_{Temp}: Temperature (°C); X_{Agi}: Agitation rate (rpm); and DW: Dried weight of functionalised oligomer (% *w*/*v*)

4.3 Statistical Analysis of Screening Selected Operating Variables

The effects of selected operating variables on the dried weight of functionalised oligomer (% *w*/*v*) were analysed using analysis of variance (ANOVA) as indicated in Table 4.2. From the analysis, the percentage of correlation coefficient (r^2) of the regression model was observed at 99.8 %, which indicated good fitting between factorial model and experimental data. The effects of main variables of lipase (X_{Lip}), initial ECL (X_{ECL}) and temperature (X_{Temp}) were significant ($p < 0.05$) on the production of dried weight of functionalised oligomer. However, the effects of initial MGP (X_{MGP}) and agitation rate (X_{Agi}) were insignificant ($p > 0.05$) (Table 4.2).

In addition to main variables, the two-way interactions were also investigated in order to determine the relationship between variables. Interpreting the effects of main variables without considering the interaction effects may result in wrong conclusions. From the ANOVA, the interactions of lipase with initial ECL (X_{Lip} X_{ECL}), lipase with temperature (X_{Lip} X_{Temp}), initial ECL with initial MGP (X_{ECL} X_{MGP}), and initial ECL with temperature (X_{ECL} X_{Temp}) were found to be significant ($p < 0.05$) on the production of functionalised oligomer (expressed as dry weight amount) (Table 4.2). The significant effect of two-way interactions indicated the presence of confounding effect among the selected operating variables.

Table 4.2: Analysis of variance of selected operating variables.

Variables	df	Adj. SS	Adj. MS	*F*	*p*
X_{Lip}	1	55.49	55.49	1,772.25	0.00
X_{ECL}	1	435.93	435.93	13,922.07	0.00
X_{MGP}	1	0.06	0.06	1.98	0.17
X_{Temp}	1	16.53	16.53	527.90	0.00
X_{Agi}	1	0.06	0.06	1.98	0.17
X_{Lip} X_{ECL}	1	10.06	10.06	321.29	0.00
X_{Lip} X_{MGP}	1	0.02	0.02	0.50	0.48
X_{Lip} X_{Temp}	1	0.34	0.34	10.97	0.00
X_{Lip} X_{Agi}	1	0.00	0.00	0.07	0.79
X_{ECL} X_{MGP}	1	0.16	0.16	4.97	0.03
X_{ECL} X_{Temp}	1	4.60	4.60	146.93	0.00
X_{ECL} X_{Agi}	1	0.04	0.04	1.31	0.26
X_{MGP} X_{Temp}	1	0.03	0.03	0.94	0.34
X_{MGP} X_{Agi}	1	0.05	0.05	1.61	0.21
X_{Temp} X_{Agi}	1	0.11	0.11	3.47	0.07
Error	32	1.002	0.031		
Total	47	524.49			

X_{Lip}: Lipase (% *w*/*v*); X_{ECL}: Initial ECL (% *w*/*v*); X_{MGP}: Initial MGP (% *w*/*v*); X_{Temp}: Temperature (°C); X_{Agi}: Agitation rate (rpm); DF: Degree of freedom; Adj. SS: Adjusted sum of squares; Adj. MS: Adjusted mean of squares; *F*: *F* statistic; and *p*: *p* statistic (significance level at $p = 0.05$).

The main variable of initial ECL represents major contributing factor with highest *F* value followed by lipase and temperature. The interaction of lipase with initial ECL showed the greatest effect on dried weight of functionalised oligomer with the highest *F* value recorded, followed by interaction of initial ECL with temperature, interaction lipase with temperature and interaction initial ECL with initial MGP (Table 4.2).

4.4 Residual Analysis

Residual analysis was conducted using Minitab® 18 software in order to validate the regression model applied. Graphical analysis for the ANOVA of the selected operating variables is presented (Figure 4.2). The normal probability plot showed all standardized residual points followed normal distribution with data points falling on the straight line (Figure 4.2A). Furthermore, there was no clear evidence of outlier since the Grubb test showed all unusual data values come from the same normal population ($p > 0.05$). For the plot of standardized residual versus fitted value (Figure 4.2B), the residual points

showed non-identical pattern with all data points distributed rather equally within positive and negative boundaries indicating equal variance. The histogram (Figure 4.2C) showed the standardized residual followed approximately normal distribution with the highest frequency observed at the middle range of standardized residual value. The plot of standardize residual versus run order showed random scatter showing the absence of dependency between residual errors and the order of experimental runs (Figure 4.2D).

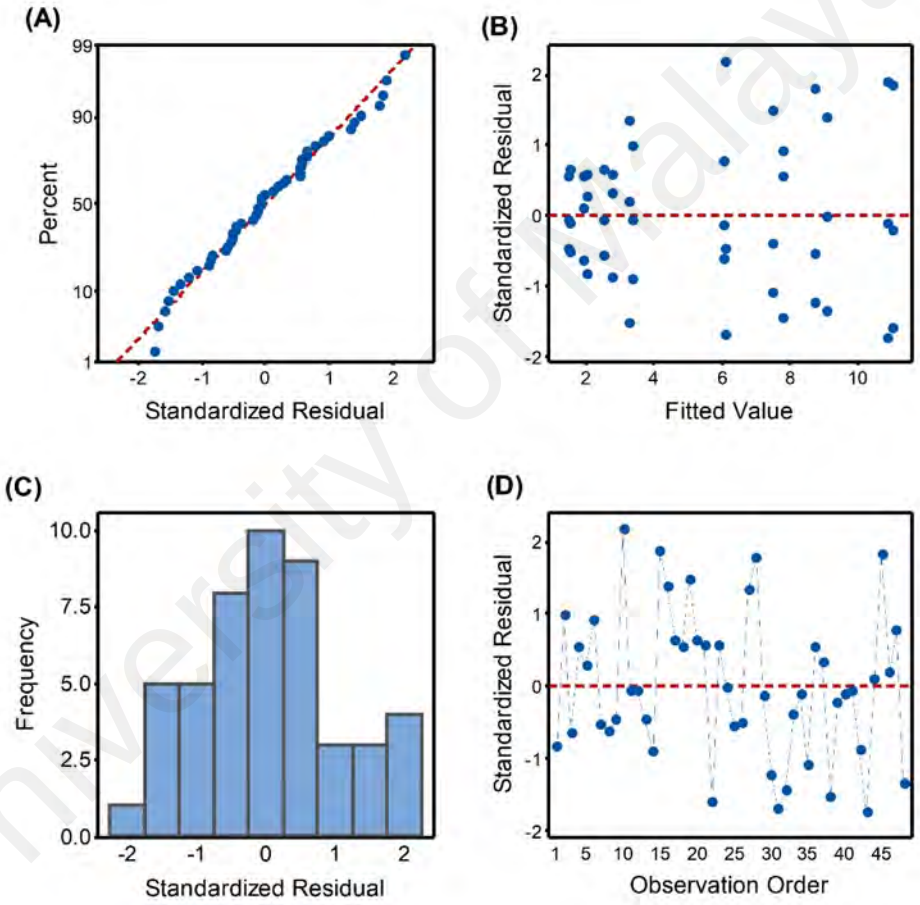

Figure 4.2: Residual plot analysis of half factorial design (A) Normal probability plot; (B) Standardized residual versus fitted plot; (C) Histogram; (D) Standardized residual versus run order plot

4.5 Main Effect Analysis

The main effect plot of selected operating variable on dried weight of functionalised oligomer is presented in Figure 4.3. The connected line between low and high level of each variable was used to analyse the relationship between the experimental response (mean dried weight, % *w*/*v*) and the selected variable. Steeper gradient of the connected line indicated greater influence of corresponding variable on the experimental response. Positive gradient indicated that the relationship between the variable level and experimental response is in the same direction.

High concentration of lipase should result in parallel increase in functionalised oligomer production. This is clearly shown when lipase concentration was increased from 1.2 to 2.8 % *w*/*v* (Figure 4.3A). Similar observation were made for the main effect of initial ECL and temperature as the levels of each variables were increased from 3.8 to 11.5 % and 40 to 60 °C, respectively (Figure 4.3B, 4.3D). The connected lines between low and high level of these variables showed positive gradient. However, the dried weight of functionalised oligomer were unaffected when initial MGP and agitation rate were increased from 0.04 to 0.14 % *w*/*v* and 90 to 180 rpm, indicated by the flat connected lines (Figure 4.3C, 4.3E).

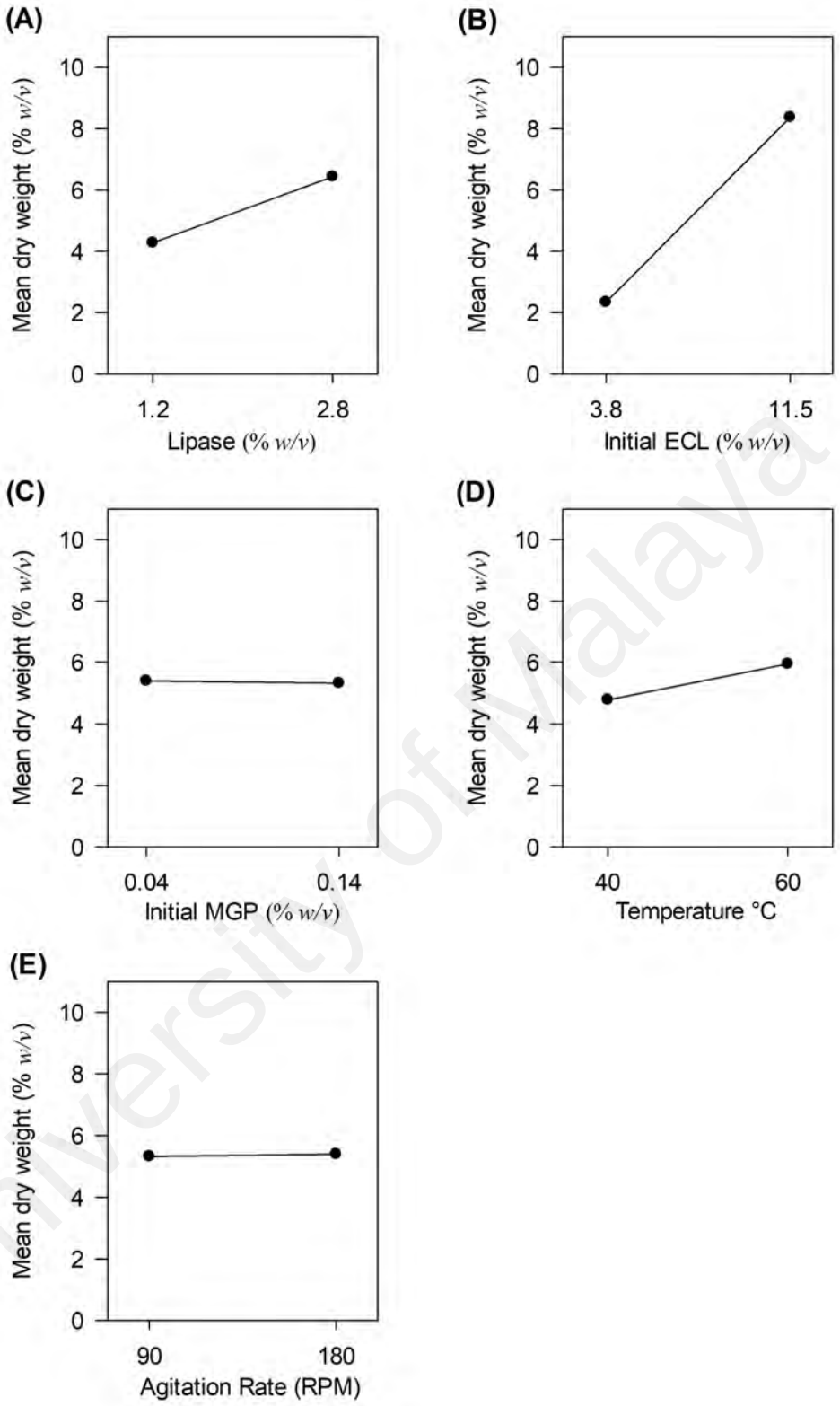

Figure 4.3: Main effect plot analysis (A) Lipase (% *w*/*v*); (B) Initial ECL concentration (% *w*/*v*); (C) Initial MGP concentration (% *w*/*v*); (D) Temperature (°C); (E) Agitation rate (rpm)

The interaction effect between the agitation rate and all other variables were found to be insignificant ($p > 0.05$). Thus, the insignificance of agitation rate variable was implicitly validated from the interaction effect analysis. On the other hand, whilst the main effect of initial MGP was insignificant ($p > 0.05$), the relationship observed between initial MGP with initial ECL suggests that the level of initial MGP somehow influenced the estimation of main effect of initial ECL.

4.6 Two-way Interaction Effect Analysis

Analysis on the two-way interaction was also conducted in order to determine the relationship between variables. Interpreting the effects of main variables without considering interaction effects may result in wrong conclusions. From the ANOVA (Table 4.2), the interactions of lipase with initial ECL ($X_{Lip}\,X_{ECL}$), lipase with temperature ($X_{Lip}\,X_{Temp}$), initial ECL with initial MGP ($X_{ECL}\,X_{MGP}$), and initial ECL with temperature ($X_{ECL}\,X_{Temp}$) were found to be significant ($p < 0.05$) corresponding to the dried weight of functionalised oligomer.

From the calculated F value in Table 4.2, the interaction of lipase with initial ECL ($X_{Lip}\,X_{ECL}$) showed the greatest effect on dried weight of functionalised oligomer with the highest F-value recorded ($F = 321.29$). This was followed by interaction of initial ECL with temperature ($X_{ECL}\,X_{Temp}$) ($F = 146.93$), lipase with temperature ($X_{Lip}\,X_{Temp}$) ($F = 10.97$) and initial ECL with initial MGP ($X_{ECL}\,X_{MGP}$) ($F = 4.97$). Therefore, the effect lipase and initial ECL showed highest correlation between variables.

4.7 Effects of Significant Operating Variables

4.7.1 Lipase

Based on Table 4.2, the effect of lipase was found to be significant ($p < 0.05$). According to Figure 4.3, it was clearly observed that dried weight of functionalised

oligomer increased from 4.3 to 6.4 % *w*/*v* when lipase loading increased from 1.2 to 2.8 % *w*/*v*, respectively. Increase in total concentration of lipase most likely affects both the reaction rate and product yield (Kim et al., 2004). The used of immobilized lipase is preferable in esterification as it improves thermal stability and catalytic activity as compared to its free form (Wang et al., 2017). By increasing lipase loading, the formation of acylated-enzyme substrate (AES) complex also increases due to more active site available for binding between substrates and nucleophiles resulting in higher conversion rate of the final product (Hans et al., 2009). With the formation of AES complex, lipase reduces the activation energy of reaction and increases the rate conversion of substrate into final product. Without lipase, a large amount of energy is required for a reaction to proceed. However, maximum reaction velocity was not favourable at low ratio of substrate to lipase concentration.

4.7.2 Initial ECL

According to ANOVA (Table 4.2), the effect of initial ECL was significant ($p < 0.05$). Initial ECL showed major contributing effect on dried weight of functionalised oligomer production with the highest *F* value of all variables (Table 4.2). Higher concentration of initial ECL was favourable in obtaining higher dried weight of functionalised oligomer. In the current study (Figure 4.3), an increase of initial ECL from 3.8 to 11.5 % *w*/*v* significantly enhanced the production of functionalised oligomer with the highest dried weight recorded above 11.0 % *w*/*v*. Reduction of initial ECL concentration was accompanied by the decrease in acylated-enzyme substrate (AES) complex formation from lipase-catalysed ring opening polymerization of ECL monomer; which subsequently polymerized into repeating unit of 6-hydroxyhexanoate of hydrophobic oligomer chain (Cooke & Whittington, 2016; Scherkus et al., 2016). By contrast, MGP consumption showed rapid decrease from the initial concentration within the first six hours of reaction

followed by a plateau until the end of experiment. Further conversion of MGP at a later stage was not observed since the nucleophilic attack of AES complex was no longer feasible at this point due to enzyme active site predominantly involved in chain propagation reaction (Ye et al., 2010).

4.7.3 Temperature

Based on the ANOVA in Table 4.2, the effect of temperature on the dried weight of functionalised oligomer was significant ($p < 0.05$). Its production was enhanced when reaction temperature increased from 40 to 60 °C (Figure 4.3). The highest dried weight of 6.0 % *w*/*v* was observed at 60 °C. At higher temperature, the chain propagation proceeds at a higher rate due to the fact that reactant molecules has sufficient kinetic energy to overcome the activation barrier for chemical reaction to occur (Wu et al., 2017). Higher reaction temperature also helps to increase the solubility of reactants in the reaction mixture (Lambermont-Thijs et al., 2010). The poor solubility of reactant is one of contributing factor of mass transfer resistance. In our case, both ECL and MGP were found to be completely dissolved in *tert*-butanol for the concentration and temperature ranges tested i.e. 3.8-11.5 % *w*/*v*, 0.04-0.14 % *w*/*v*, and 40-60 °C respectively. Further increase of temperature above 80 °C may reduce the lipase activity due to thermal inactivation (Wang et al., 2017).

4.7.4 Agitation Rate

Generally, an increase of agitation rate above 180 rpm will introduce higher shear force on the immobilized lipase which promotes enzyme leakage. Meanwhile agitation rate below 90 rpm was not suitable due to poor access of substrates to the active site within immobilize matrix (Gopinath & Sugunan, 2007). Based on the ANOVA, the effect of agitation rate was found to be insignificant ($p > 0.05$). The rate of reaction remain

unaffected when factor level agitation rate increased from 90 to 180 rpm (Figure 4.3). It is likely that the range of agitation rate applied in this study satisfies the interfacial mass transfer requirement for efficient process. From the factorial experiment, the agitation rate applied has the added advantage of minimising shear force impact on the labile immobilized lipase.

4.8 Establishment of Maximum Response

The combination of input variables setting for maximum response was determined based on the individual or multiple responses. In the current study, the maximum dried weight of functionalised oligomer was statistically determined according to its desirability function (D_f). Combinations of variables setting were investigated until D_f reaches maximum value indicating the settings are favourable for maximum response as a whole. Response optimizer program in Minitab® 18 software was used to maximize the experimental response corresponding to the selected operating variables.

The maximum value of dried weight of functionalised oligomer is predicted at 10.993 ± 0.100 % *w*/*v* with desirability function of 0.973, which is very close to 1.000 indicating successful optimization for obtaining maximum response target (Table 4.3). Validation experiments were carried out using selected significant variables with high-level settings for maximum functionalised oligomer production. On the other hand, the levels for insignificant variables were fixed at minimum settings. Half factorial design was validated experimentally using the combination of variables for maximum response determined using response optimizer of the software. The validation experiment showed dried weight production of 10.67 % *w*/*v* was achieved, which agreed well with the predicted response.

Table 4.3: Response optimizer of selected operating variables.

	Prediction	Experiment
Dried weight % *w*/*v* (± SE)	10.993 ± 0.102	10.673 ± 0.350

Variables	Best setting
Lipase loading (% *w*/*v*)	2.80
Initial ECL (% *w*/*v*)	11.46
Initial MGP (% *w*/*v*)	0.04
Temperature (°C)	60.0
Agitation rate (rpm)	90

SE: Standard error

4.9 Effect of Substrate Conversion on Molecular Weight

4.9.1 ε-Caprolactone

At fixed concentration of methyl-*D*-glucopyranoside (MGP) at 1.84 mM (Figure 4.4A), 4.60 mM (Figure 4.4B) and 7.36 mM (Figure 4.4C), the effect of ε-caprolactone (ECL) conversion on molecular weight of functionalised oligomer were plotted as function of time. For all cases, the conversion of ECL monomer increased steadily from the start of reaction and was found to be more than 80 % converted after 36 hours of reaction. Similar trend was observed for the increase in molecular weight of functionalised oligomers, which the observed molecular weight was found to increase more than 1,200 g mol^{-1} after 36 hours. The steady increase in molecular weight and ECL conversion for all cases during early stages of the reaction indicated that the polymer propagation rate was the dominating step (Huang et al., 2015; Sha et al., 2005). No observable reversion of the polymerization was recorded during the course of the reaction. It could be partly prevented due to continuous evaporation of water by product from the reaction liquid and subsequently adsorbed by molecular sieve bed indicated in Figure 3.1. Water molecules are produced as by product from esterification of MGP to ECL monomer and during chain propagation step of ECL oligomer.

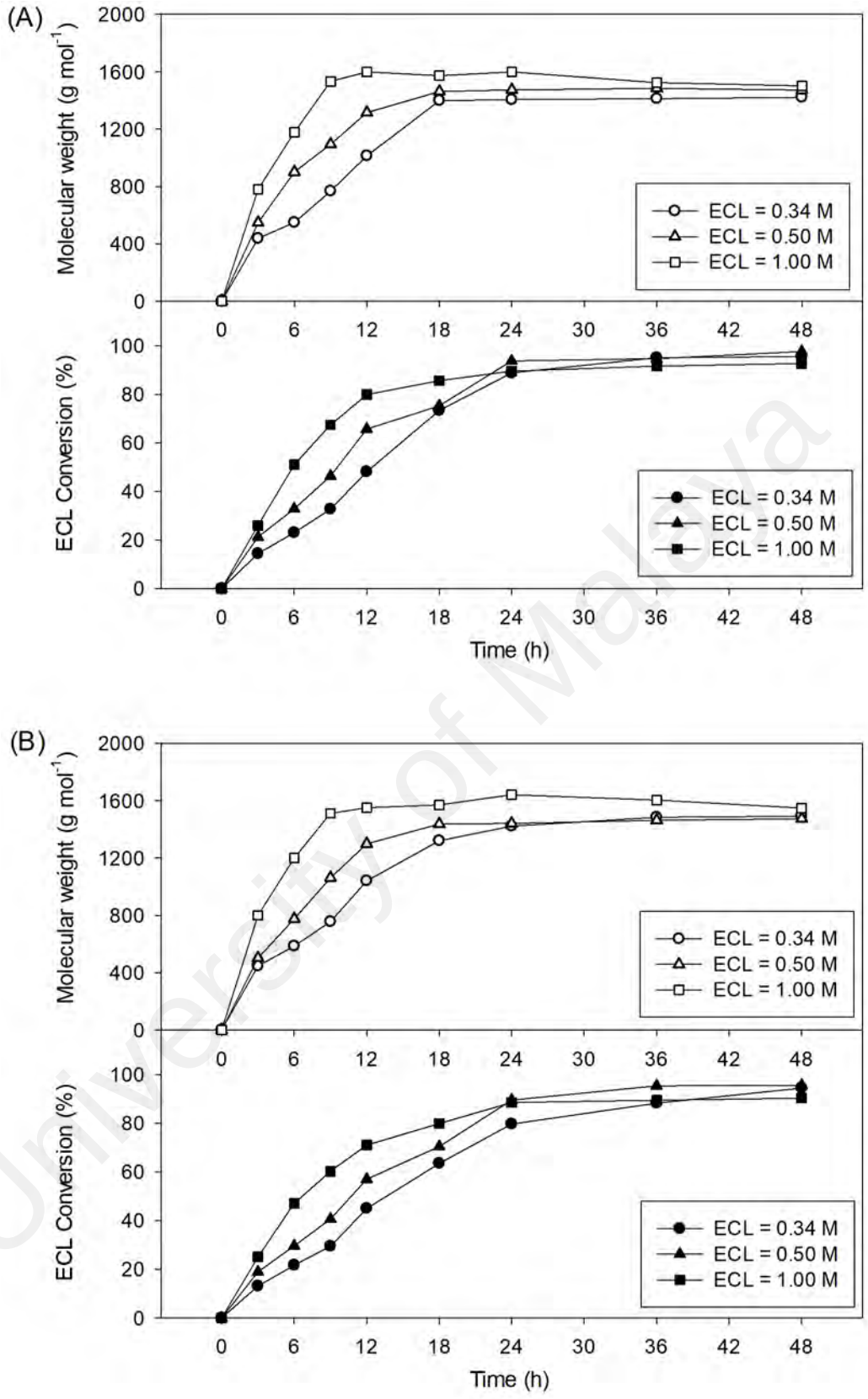

Figure 4.4: Effect of varied ε-caprolactone (ECL) conversion (%) on molecular weight (g mol^{-1}) of functionalised oligomer at fixed methyl-*D*-glucopyranoside (MGP) (A) 1.84 mM of MGP; (B) 4.60 mM of MGP; (C) 7.36 mM of MGP

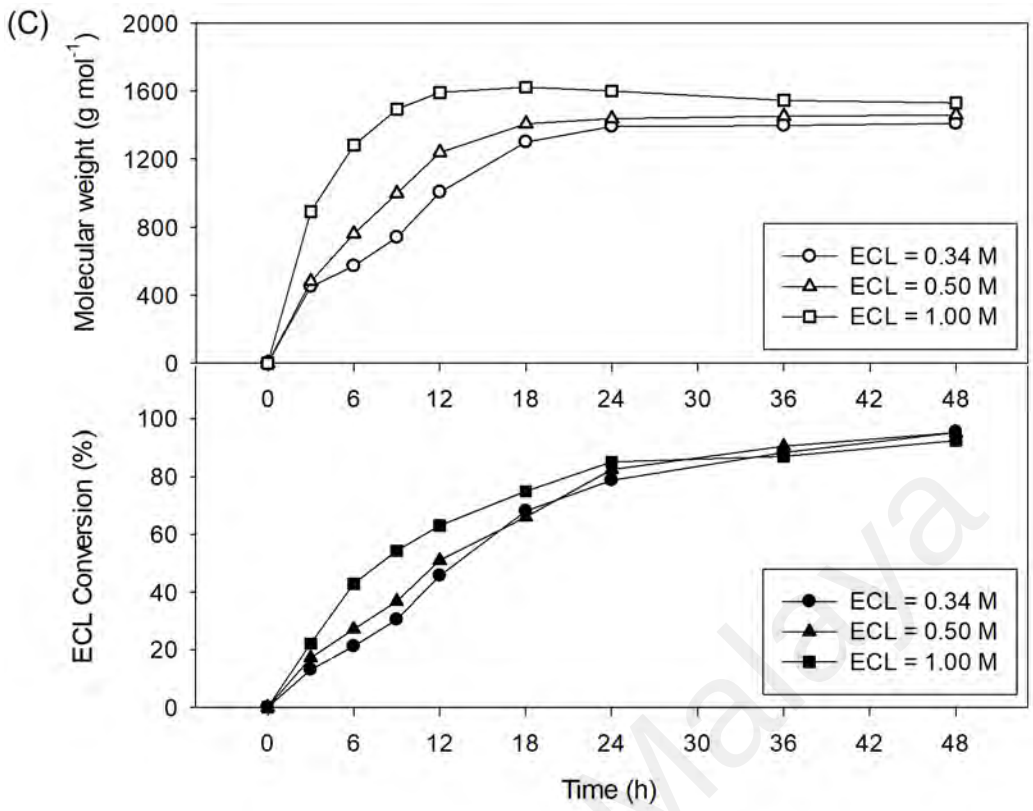

Figure 4.4, continued.

4.9.2 Methyl-*D*-glucopyranoside

At fixed concentration of ε-caprolactone (ECL) at 0.34 M (Figure 4.5A), 0.50 M (Figure 4.5B) and 1.00 M (Figure 4.5C), the effect of methyl-*D*-glucopyranoside (MGP) conversion on molecular weight of functionalised oligomer were plotted as function of time. Steady increase of MGP conversion at early reaction stage could be due to the esterification activities between acid (acyl donor) and alcohol (acyl acceptor), respectively (Yan et al., 2014). In this case, the carboxyl group of acylated enzyme-substrate (AES) complex of ECL monomer/oligomer is attributed to acyl donor whereas the hydroxyl group of C6 in MGP is the acyl acceptor. However, the MGP conversion showed constant profile after 6 hours reaction due to the chain propagation of functionalised oligomer.

The increase in molecular weight at constant MGP conversion rate was attributed to ECL chain propagation by the addition of acyclic ECL monomer to the terminal -OH

group of the propagating oligomer. It was obvious that active esterification of ECL and MGP occurred concurrently with propagation step of ECL oligomeric chain during early phase of the reaction as described earlier. However, no further esterification occurred when certain molecular weight values of the functionalised oligomer were attained. This could be attributed to (i) depletion of ECL monomers, and/or (ii) steric effect from the acyl chain of certain threshold molecular weight, impeding the formation of new ester bond between MGP and available free carboxyl terminal of ECL oligomer chain (Castano et al., 2014; Sen & Puskas, 2015).

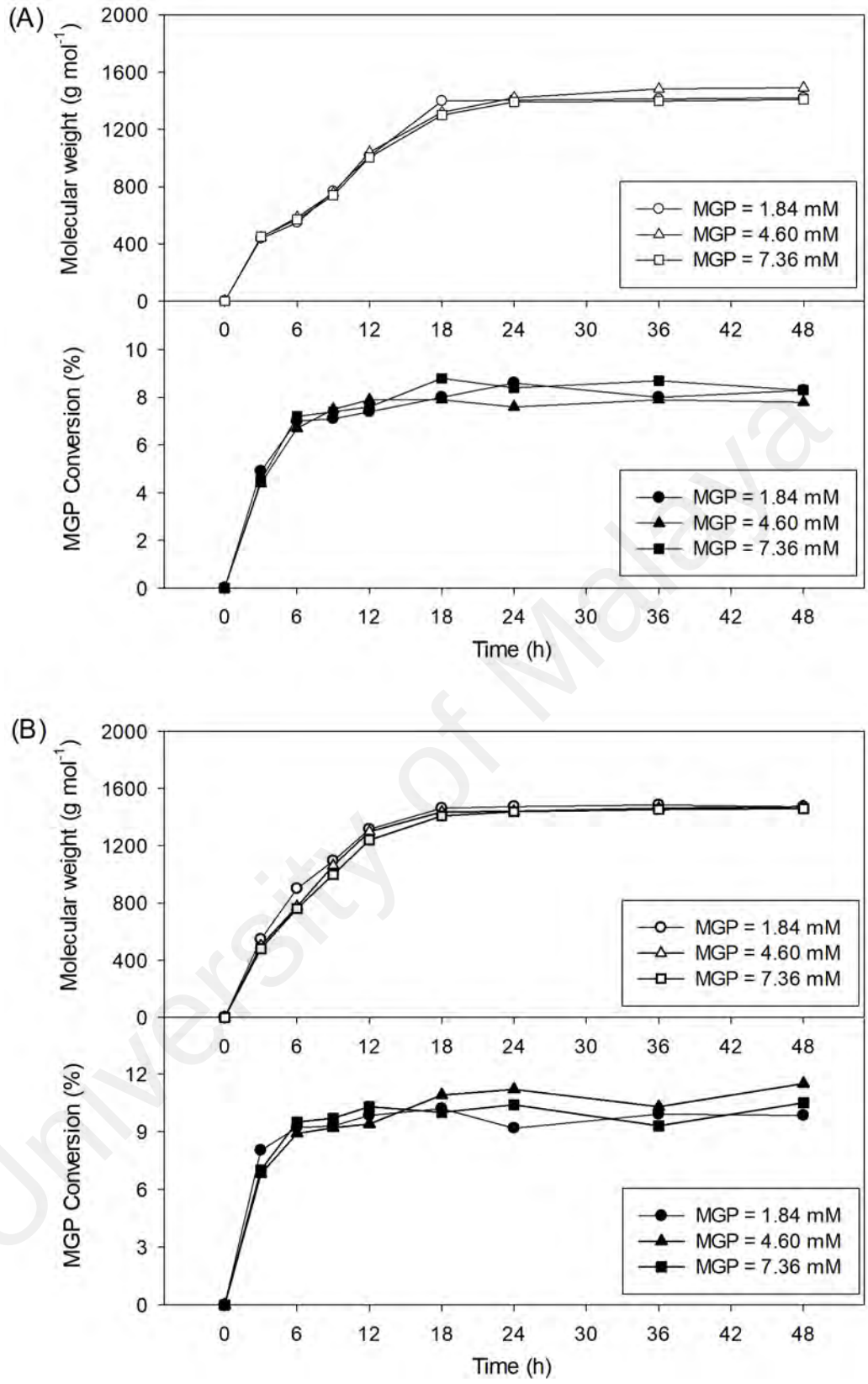

Figure 4.5: Effect of varied methyl-*D*-glucopyranoside (MGP) conversion (%) on molecular weight (g mol^{-1}) of functionalised oligomer at fixed ε-caprolactone (ECL) (A) 0.34 M of ECL; (B) 0.50 M of ECL; (C) 1.00 M of ECL

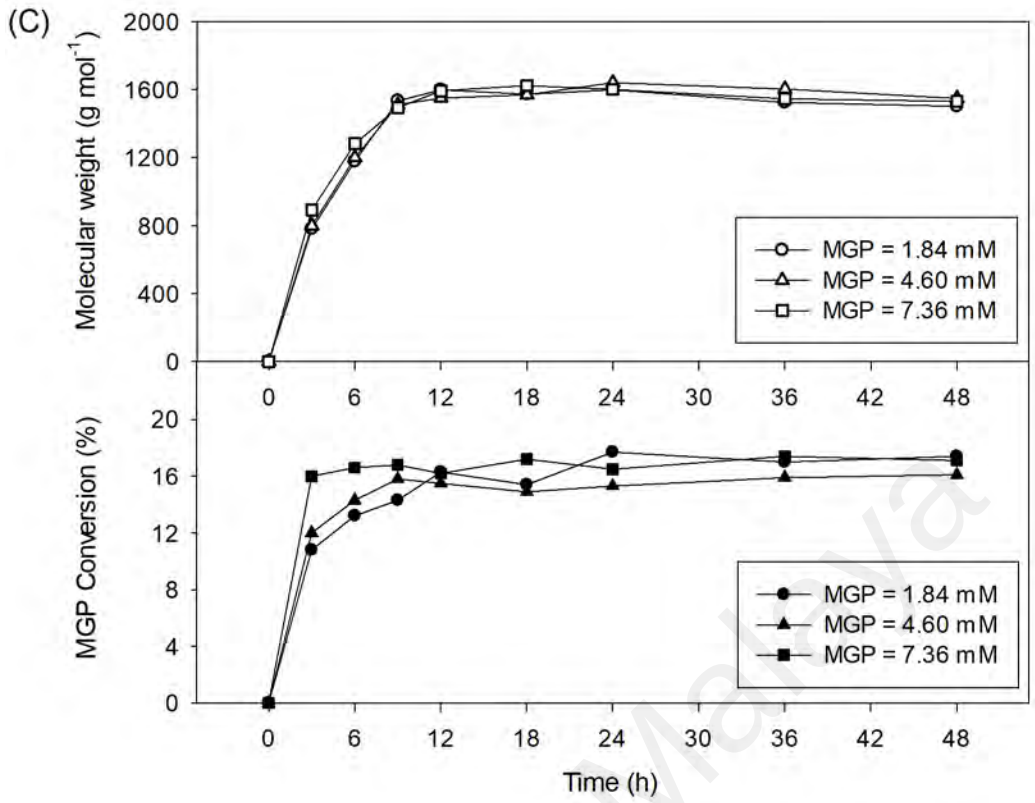

Figure 4.5, continued.

4.10 Initial Rate of Reaction

For the determination initial rate of reaction (v_0), experiments were carried out in round bottom glass reactor (Figure 3.1) for varied starting concentrations of ECL and MGP at 60 °C for 48 hours. The changes in v_0 as a function of varied initial ECL and MGP concentrations were shown in Figure 4.6. From the graph, the v_0 values increased with the concentration of ECL at fixed MGP concentration, and similarly for varied concentrations of MGP at fixed ECL concentration, respectively. It was observed that at fixed MGP concentration, the v_0 values apparently starting to reach a plateau when the ECL concentration was increased (Figure 4.6A). On the other hand, at fixed ECL concentration, the v_0 values increased steadily as MGP concentration become higher (Figure 4.6B).

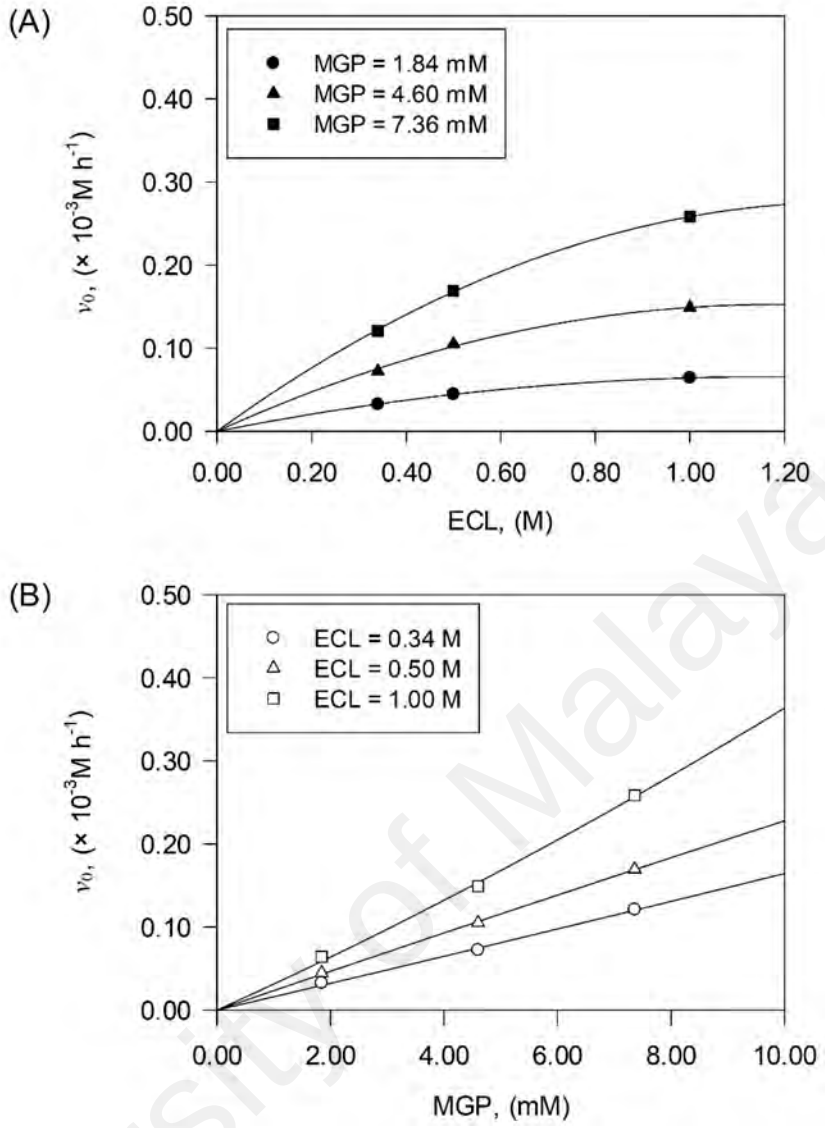

Figure 4.6: Initial rates (v_0) at varied initial substrate concentration (A) ε-Caprolactone (ECL); (B) Methyl-*D*-glucopyranoside (MGP)

4.11 Proposed Reaction Mechanism

In the current study, initiation route of terminal end functionalisation was proposed for the production of MGP-functionalised ECL oligomer (MGP-6-*O*-oligo-ECL). The reaction mechanism of lipase-catalysed formation of MGP-functionalised ECL oligomer was adopted and modified from previous studies (Albertsson & Varma, 2003; Barrera-Rivera et al., 2008; Duda et al., 2002; Kobayashi & Uyama, 2002; Mehta et al., 2007; Uyama et al., 1998). The overall reaction consists of two consecutive steps corresponding to (i) acylation of MGP by ECL followed by (ii) the chain propagation of the

functionalised oligomer. In the acylation step, ping-pong bi-bi mechanism of lipase-catalysed acylation of MGP was proposed. Subsequently, the reaction proceeds with chain propagation step of the acylated ECL monomer or oligomer *via* living polymerization mechanism.

4.11.1 Ping-pong Bi-bi Mechanism of Esterification

The first step of functionalisation involves the attachment of MGP with ECL. The ping-pong bi-bi mechanism was proposed for lipase-catalysed esterification of ECL with MGP. Sugar moiety from the functional group in MGP was attached to the terminal carboxyl group of ECL releasing two products sequentially along the way *viz.* water molecule and acylated MGP. The general reaction sequences describing ping-pong bi-bi mechanism without ternary complex is illustrated in Figure 4.7.

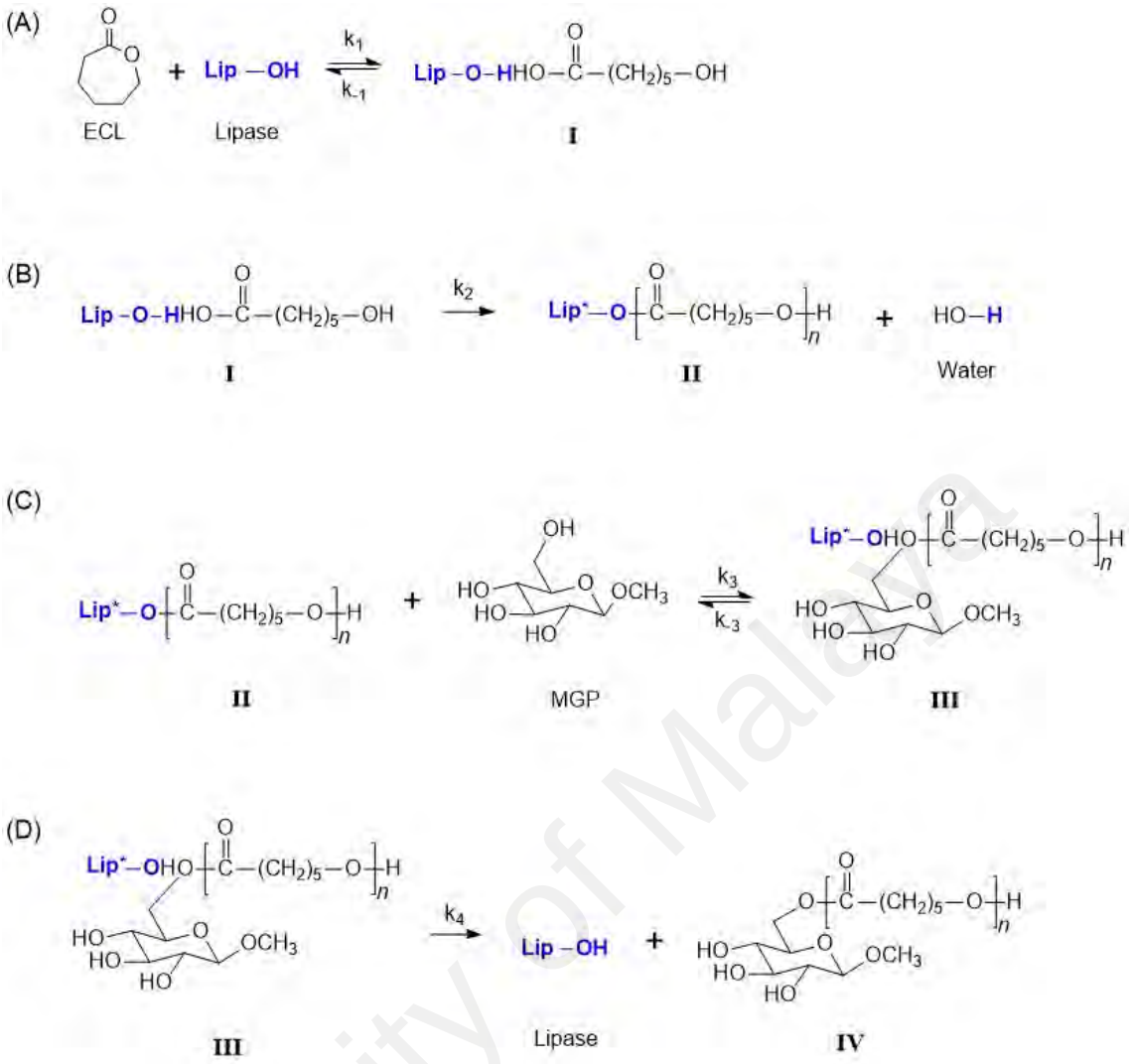

Figure 4.7: Reaction scheme of lipase-catalysed esterification of ECL with MGP (A) Ring opening of ECL; (B) Molecular rearrangement; (C) MGP acylation; (D) Regeneration of free enzyme

According to reaction scheme, the reaction between lipase and cyclic monomer ECL begins with nucleophilic attack of ester group of ECL by lipase –OH results in the opening of ECL ring system with the formation of intermediate (**I**) (Figure 4.7A). Next, the first molecular rearrangement of intermediate will lead to the release of first product e.g., water molecule and the formation of acylated lipase-hydroxyhexanoic acid complex (**II**) (Figure 4.7B). The proposed step of ring opening of ECL (Figure 4.7A) was characterized by the steady increased in ECL conversion profile (Figure 4.4). Then, deacylation of acylated lipase-hydroxyhexanoic acid by the nucleophilic attack of OH in the MGP,

producing the second intermediate (**III**) (Figure 4.7C). The proposed mechanism of MGP acylation (Figure 4.7C) was attributed to the esterification of activated lipase-acyl complex by the OH group of MGP indicated by the rapid increased in MGP conversion before reaching a constant value upon attaining a certain molecular weight (Figure 4.5). Followed by the second molecular rearrangement (Figure 4.7D), products include lipase and oligomeric sugar ester or methyl-6-*O*-(hydroxyhexanoyl)$_n$-*D*-glucopyranoside (**IV**) where *n* is the repeating unit hydroxyhexanoic acid obtained from the deacylation of acyl complex of lipase-hydroxyhexanoic acid. It is noted that both acyclic ECL monomer and ECL oligomers possess only a single available terminal carboxyl group for esterification.

4.11.2 Living Polymerization Mechanism of Chain Propagation

The general mechanism for lipase-catalysed chain propagation of MGP-functionalised ECL oligomer was described based on the given reaction scheme (Figure 4.8). After successful functionalisation, a chain propagation step was initiated by the regioselectivity of lipase. The general mechanism involved the reaction between acylated lipase-hydroxyhexanoic acid complex (**II**) and ECL monomeric/oligomeric sugar ester or methyl-6-*O*-(6-hydroxyhexanoyl)-*D*-glucopyranoside (**IV**) resulted in the addition of one unit hydroxyhexanoic acid unit into the main chain (Figure 4.8A). Propagation of initial ECL monomeric/oligomeric sugar ester (**V**) resulted in growing polymer chain before termination giving the final product of methyl-6-*O*-oligo(caprolactone)$_n$-*D*-glucopyranoside (**VI**) with regeneration of free lipase (Figure 4.8B). The acylation of sugar for a single acylated enzyme-substrate complex was hypothesized to occur subsequent to ring opening of ECL monomer. Then, the chain propagation step of free terminal carboxyl group ensued before the termination step. In this study, termination of propagation step is attributed to reduction in esterification activity from depletion in ECL monomer availability at high conversion rate. This was supported by the constant

molecular weight of functionalized oligomer when ECL conversion was higher than 80 % (Figure 4.4).

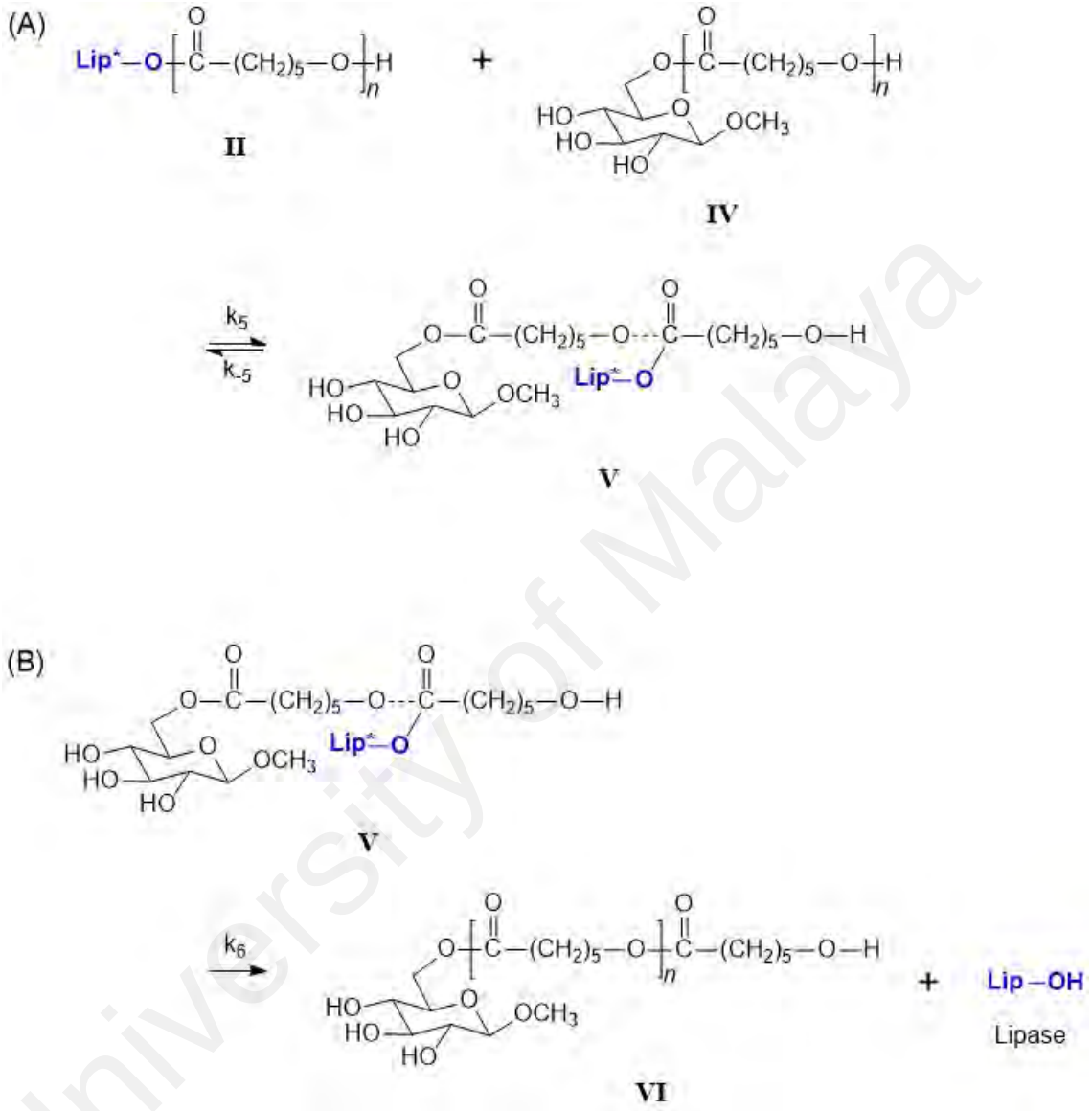

Figure 4.8: Reaction scheme of lipase-catalysed chain propagation step MGP-functionalised ECL oligomer (A) Nucleophilic attack of acyl complex; (B) Regeneration of free enzyme

4.12 Kinetic of Ping-pong Bi-bi Mechanism of Esterification

4.12.1 Linearization of Lineweaver-Burk Plot

Linearization analysis of initial velocity v_0 can be carried out using Lineweaver-Burk (LB) or double reciprocal plot. The linear plot can also be used to identify the presence substrate inhibition effects on the current experimental data according to ping-pong bi-bi mechanism (Figure 4.9). The reciprocal of initial rates ($1/v_0$) were plotted as a function of reciprocal of varied substrate concentrations (1/S). Since the slopes for each of linear lines were different, the uncompetitive inhibition can be ruled out. Competitive inhibition was also ruled out since no single intercept by the lines was observed at the abscissa (1/ECL = 0) with the increase in both MGP and ECL concentrations indicating that the V_{max} was unaffected. Intercepts at common point on *x*-axis were not possible for different values of *y*-intercept thus ruling out the ternary complex formation in the current study (Yadav & Devi, 2004).

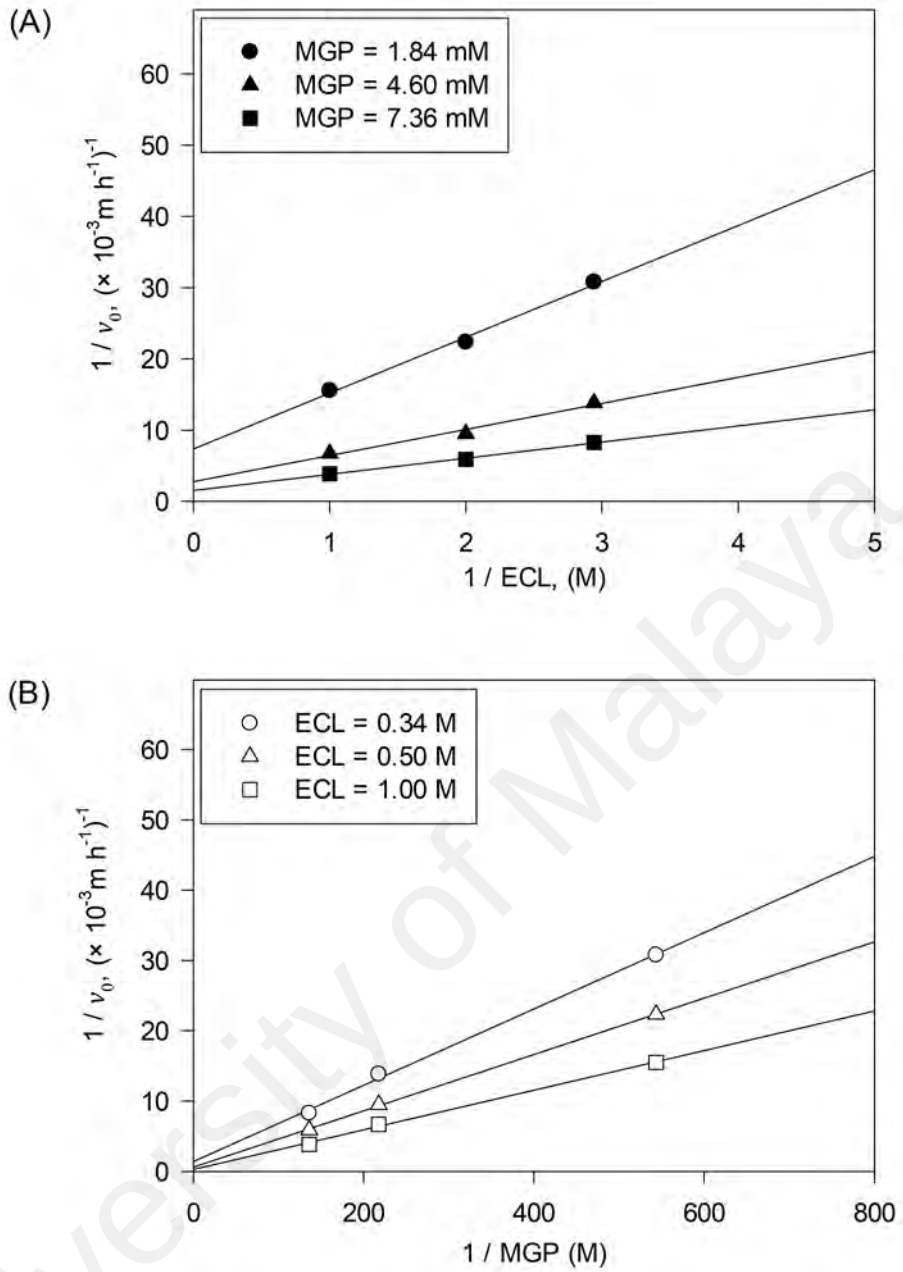

Figure 4.9: Lineweaver-Burk plots for varied substrate concentration (A) ε-Caprolactone (ECL); (B) Methyl-*D*-glucopyranoside (MGP)

4.12.2 Nonlinear Analysis of Ping-pong Bi-bi Model

The equation for initial velocity of ping-pong bi-bi model (Eq. 3.2) was solved using nonlinear regression analysis. Kinetic parameter values including V_{max}, K_{mMGP} and K_{mECL} in the equation were estimated using Polymath® 6.0. Levenberg-Marquardt algorithm was used in finding the global solution of parameter values. The estimated kinetic parameter values were summarized in Table 4.4. The 95% confidence interval of each of predicted kinetic parameter values (Table 4.4) must be significantly smaller than the respective parameter numerical values (in absolute term) (Bernaerts et al., 2002). Thus, the estimated kinetic model parameters were validated statistically, thus supporting ping-pong bi-bi model as a stable and valid proposition.

Table 4.4: Kinetic parameters for the ping-pong bi-bi model.

Kinetic Parameters	Predicted Value	95% confidence interval
V_{max} (M h^{-1})	3.848×10^{-3}	6.330×10^{-6}
K_{mMGP} (M)	8.189×10^{-2}	2.270×10^{-4}
K_{mECL} (M)	6.050	2.491×10^{-2}

It was found that for both substrates, the Michaelis-Menten constant values for ECL (K_{mECL}) was higher than MGP (K_{mMGP}), indicating strong affinity towards MGP by lipase compared to ECL. Thus, MGP is considered as the limiting substrate based on the predicted kinetic parameters in Table 4.4. According to the proposed mechanism (Section 4.11.1), the predicted V_{max} value (Table 4.4) is due to the acylation steps of acyl complex of lipase- hydroxyhexanoic acid (acyl donor) towards the OH group of MGP (acyl acceptor). Furthermore, the deacylation of acyl complex of lipase-hydroxyhexanoic acid by the OH group in MGP was proposed as the rate-determining step in lipase-catalysed functionalisation of MGP and ECL monomer/oligomer followed by the regeneration of free lipase. Similarly, the rate determining step of acyl-transfer from the catalyst-substrate complex to the alcohol has been proposed previously (Lee et al., 2012).

The kinetic model validation of ping-pong bi-bi mechanism for the lipase-catalysed MGP functionalisation of ECL oligomer was carried out. The predicted kinetic parameters from the nonlinear regression analysis were applied in Eq. 3.2 to obtain predicted initial velocity values. From Figure 4.10, the Pearson correlation coefficient, R^2 = 0.9708 indicated the predicted initial velocities agreed well with the experimental data. In addition, simulation of initial velocities was carried out for varied ECL concentrations at fixed MGP concentrations by using the obtained kinetic constants (Figure 4.11). The plotted graphs showed good agreement between the predicted values and experimental data. Thus, lipase-catalysed MGP functionalisation of ECL oligomer is adequately described using ping-pong bi-bi mechanism.

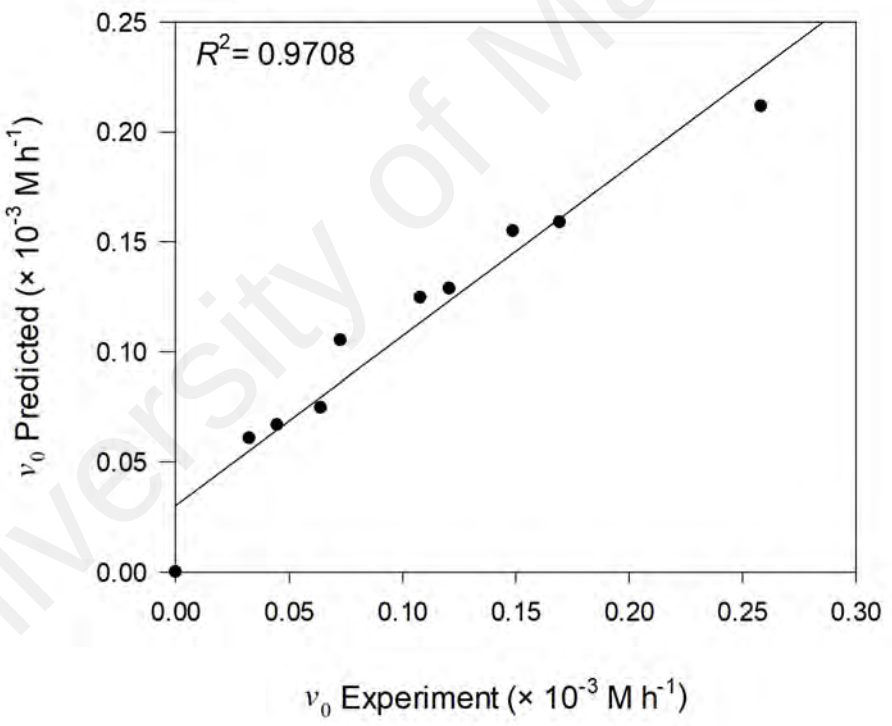

Figure 4.10: Plot of experimental and predicted initial velocities (v_0) determined from ping-pong bi-bi model (R^2 is Pearson correlation coefficient)

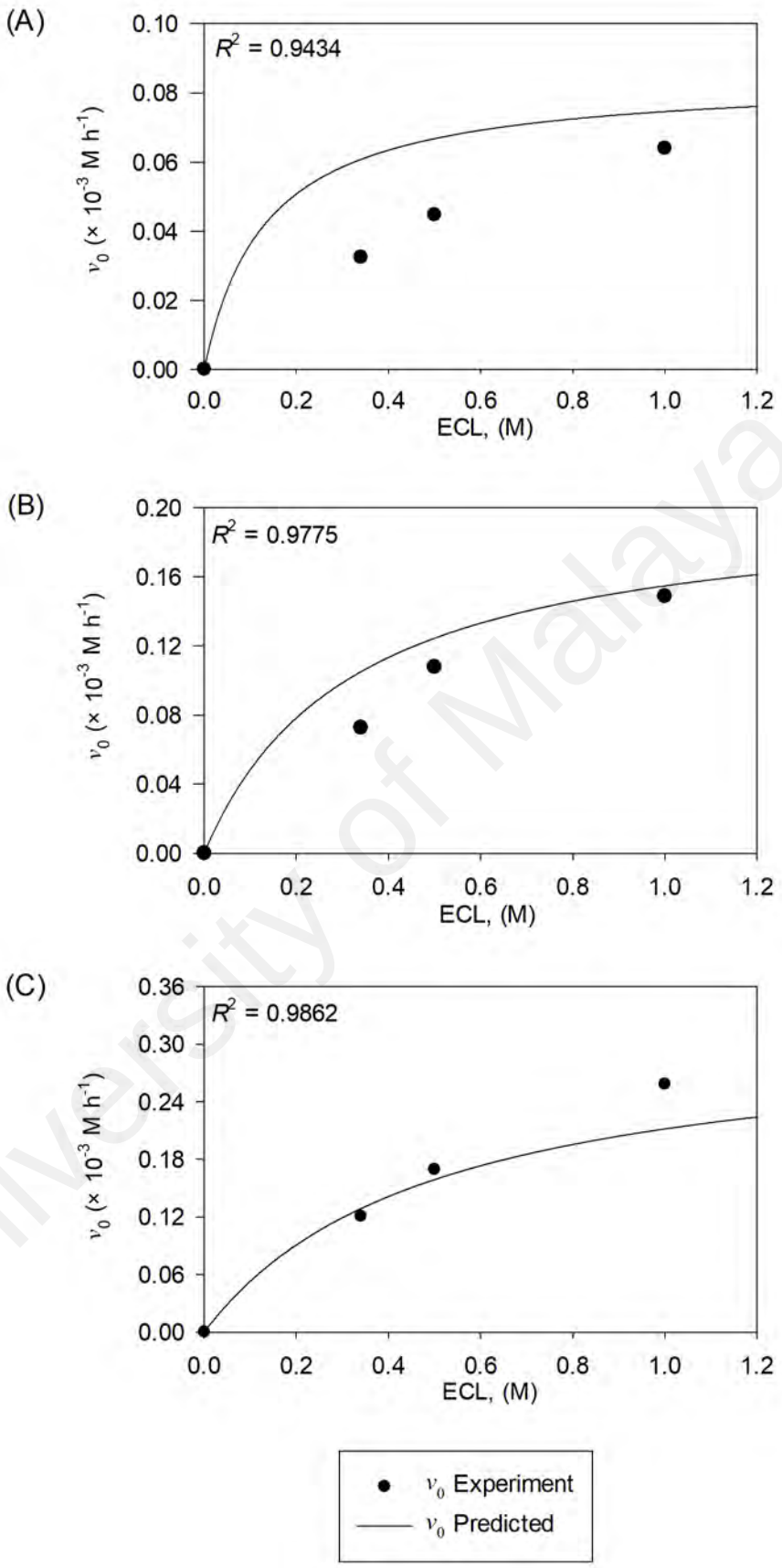

Figure 4.11: Plots of experimental and predicted initial velocities (v_0) as function of varied ECL concentrations (A) 1.84 mM of MGP; (B) 4.60 mM of MGP; (C) 7.36 mM of MGP (R^2 is Pearson correlation coefficient)

4.13 Kinetic of Living Polymerization Mechanism of Chain Propagation

The kinetic parameters describing the chain propagation was estimated from linear regression analysis e.g., plot *ln* (M_0/M) versus time where M_0 and M are monomer concentrations of starting and apparent, respectively. The apparent rate constant r_{App}, can be determined from the slope of *ln* (M_0/M) versus time, which was also used to demonstrate the living polymerization characteristic of the propagation step for MGP-functionalised ECL oligomer.

The apparent rate constant values determined from the linear regression analysis after 12 hours reaction were summarized in Table 4.5. At fixed MGP concentration of 1.84 mM, the conversion of ECL monomer increased with varied ECL concentration of 0.34, 0.50 and 1.00 M. Similar trend were observed when MGP concentration was fixed at 4.60 and 7.36 mM. The polymerization of MGP-functionalised ECL oligomer occurred with maximum conversion above 70 % was observed after 12 hours reaction at the highest starting ECL concentration. However, at the lowest starting ECL concentration of 0.34 M, the maximum conversion of ECL after 12 hours reaction was observed less than 50 %. The molecular weight of MGP-functionalised ECL oligomer after 12 hours reaction was increased corresponding to the increase in apparent rate constant values when starting ECL concentration was varied from 0.34 to 1.00 M. In the chain propagation step, regeneration of free lipase was considered the rate-limiting step if ECL is kept at saturating concentration.

The living or controlled polymerization is defined as any reaction which does not undergo chain termination or chain transfer step and the rate of monomer consumption in the propagation step follows the first-order rate law. The significance of living polymerization mechanism was due to its ability to control the macromolecular architecture of the polymer that leads to well-defined materials (Wei et al., 2018; Xu et al., 2014). The observed linearity from the plot of *ln* (M_0/M_t) versus time and molecular

weight (g mol^{-1}) versus conversion (%) can be used to establish the incidence of living polymerization based on the current kinetic data.

Table 4.5: Kinetic parameters of living polymerization for MGP-functionalised ECL oligomer.

MGP (mM)	ECL (M)	ECL conversion[a] (%)	Molecular weight[b] (g mol^{-1})	PDI	Apparent rate constant[c] (h^{-1})	95 % confidence interval
1.84	0.34	45.9	1013	1.433	0.0542	0.0027
	0.50	59.9	1316	1.532	0.0677	0.0049
	1.00	76.6	1599	1.462	0.0822	0.0085
4.60	0.34	44.9	1040	1.469	0.0554	0.0032
	0.50	56.4	1299	1.492	0.0619	0.0038
	1.00	71.0	1550	1.521	0.0771	0.0076
7.36	0.34	47.8	1005	1.438	0.0549	0.0025
	0.50	62.9	1240	1.522	0.0670	0.0043
	1.00	73.5	1593	1.491	0.0897	0.0119

[a] Dried weight analysis after 12 hours reaction
[b] GPC analysis MGP-functionalised ECL oligomer samples after 12 hours reaction
[c] Determined from the slope of ln (M_0/M_t) versus time

In the proposed chain propagation mechanism, the plot of ln (M_0/M_t) versus time was constructed for varied concentrations of ECL (Figure 4.12). From the linear regression analysis, the correlation coefficient (r^2) values were > 0.90 for all ECL concentrations within the reaction time range of 48 hours, which indicated that the polymerization proceeded under controlled or living mechanism. The r^2 values slightly decreased as the starting ECL concentration was increased up to 1.00 M. However, none of the r^2 values showed similar pattern when the starting MGP concentration was increased. Based on this observation, the controlled polymerization process was affected by the concentration of ECL substrate. It can be concluded that the propagation of ECL chain with free 6-hydroxyhexanoic monomer follows living polymerization mechanism without the chain termination step within the time range of interest.

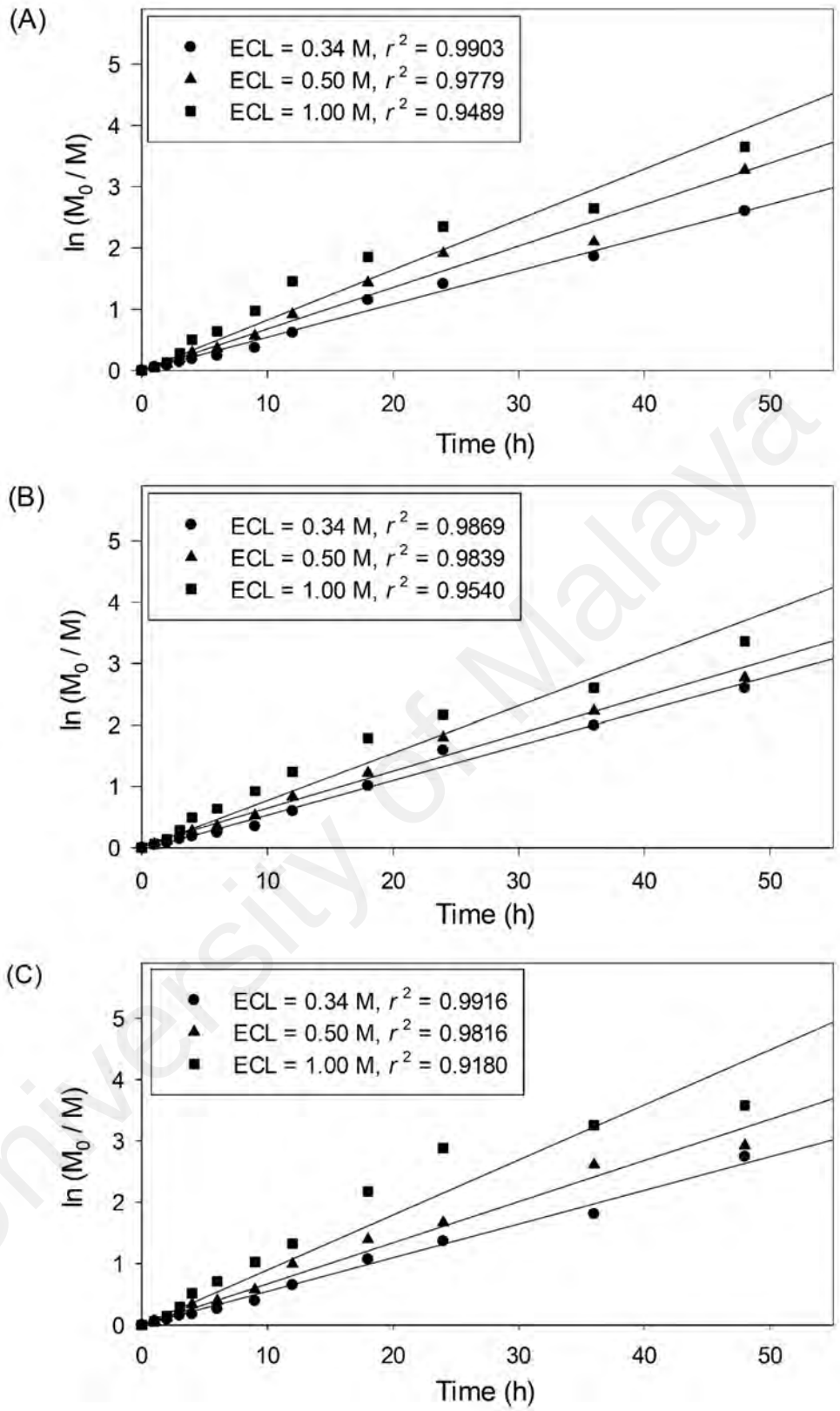

Figure 4.12: Plots of *ln* (M_0/M) versus time (h) for varied ECL concentrations at fixed MGP concentrations (A) 1.84 mM of MGP; (B) 4.60 mM of MGP; (C) 7.36 mM of MGP

Based on the plots in Figure 4.13, the molecular weight of functionalised oligomer increased rapidly with the ECL conversion (%) at the early stage of chain propagation step. As the reaction progress, the molecular weight remains unchanged after ECL conversion has reached 75 %. At varied starting ECL concentrations of 0.34, 0.50 and 1.00 M, there was insignificant different in the molecular weight observation at fixed initial MGP concentrations of 1.84, 4.60 and 7.36 mM. However, the observed maximum molecular weight did not exceeded 1,600 g mol^{-1}. Furthermore, the molecular weight was obtained at 90 % conversion after 48 hours reaction for all varied initial ECL concentrations, and for every fixed initial MGP concentration. The increase in the molecular weight suggested that the rate of chain propagation was significant than the chain termination rate. Based on linear regression analysis of the plots, the lowest r^2 value ($r^2 < 0.80$) was observed for the highest ECL concentration of 1.00 M (Figure 4.13C). However, for ECL concentrations of 0.34 (Figure 4.13A) and 0.50 M (Figure 4.13B), the r^2 showed considerably good correlation with values more than 0.80 ($r^2 > 0.80$). From the observation, an increase in starting ECL concentration may reduce the ability of the process to polymerize under living or controlled polymerization process. Based on the observed relationship between molecular weight (g mol^{-1}) and monomer conversion (%), the chain propagation of MGP-functionalised ECL oligomer was well controlled at least within the reaction time of interest.

The overall chain propagation step proceeds *via* living polymerization with no termination steps within the time range of interest, and monomer consumption obeyed first-order rate law. Living polymerization in the MGP-functionalised ECL oligomer production is desirable for the synthesis of tuneable functionalised polymer with narrow molecular weight range.

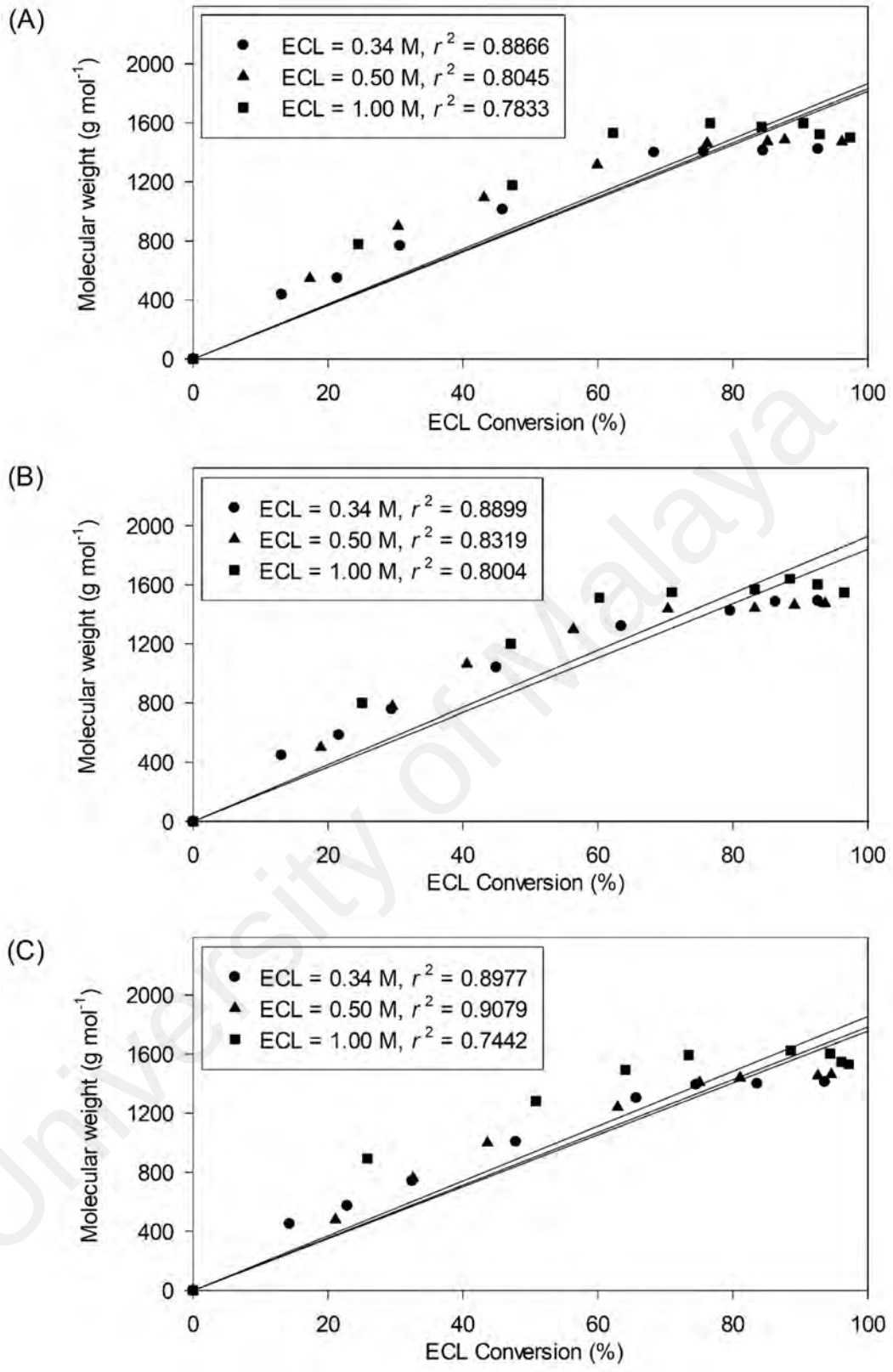

Figure 4.13: Plots of number average molecular weight (g mol^{-1}) versus ECL conversion (%) for varied ECL concentrations at fixed MGP concentrations (A) 1.84 mM of MGP; (B) 4.60 mM of MGP; (C) 7.36 mM of MGP

4.14 Product Characterization

4.14.1 FTIR Analysis

Dried samples obtained from the drying process (Section 3.5) were used for the FTIR analysis. FTIR spectrum was determined in the range of 4,000 to 400 cm^{-1} (Figure 4.14). Based on the spectrum, the presence of peaks at 1,402 and 1,210 cm^{-1} were attributed to stretching vibrations of –OCH group in C1 of MGP ring and $–COCH_3$ group in C1 of substituted methyl group in MGP, respectively (Ibrahim et al., 2006; Korolevich et al., 2007). Thus, the presence of sugar functional group in the ECL oligomer chain was indicated based on these two significant peaks. The highest peak intensity detected at 1,722 cm^{-1} was associated with -COO-R ester functional group, which is used as an indicator for repeating unit in the PCL main chain (Gumel et al., 2013; Li et al., 2013). The formation of broad peak around 3,420 cm^{-1} was attributed to -OH of terminal end ECL oligomer chain indicating the presence of linear polymer (Feng et al., 2012; He et al., 2015). The detected peaks at 2,945 cm^{-1} and 2,867 cm^{-1} were attributed to stretching vibration of –CH moieties of PCL, thus confirming the presence of linear main chain (He et al., 2015; Liu et al., 2004).

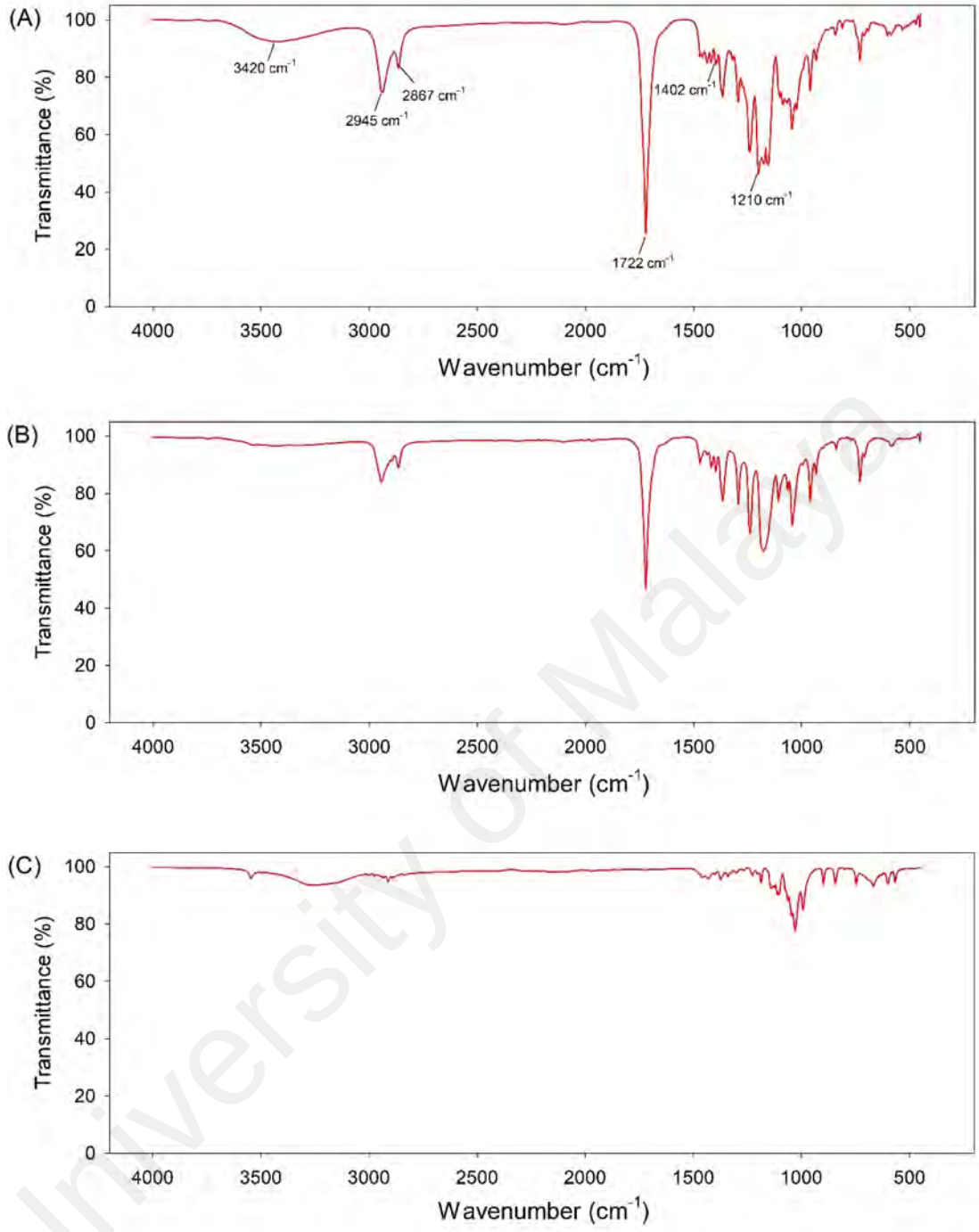

Figure 4.14: FTIR spectrum (A) MGP-functionalised ECL oligomer (MGP-6-*O*-oligo-ECL); (B) Neat ECL oligomer; (C) Commercial MGP

4.14.2 NMR Analysis

^{1}H NMR analysis was carried out for dried samples withdrawn from the reactor during early stages of the reaction to authenticate product formation, acylation and propagation mechanism. Figure 4.15 showed the spectrum for functionalisation product detailing the signals for (i) ECL monomeric sugar ester or methyl-6-*O*-(hydroxyhexanoyl)-*D*-glucopyranoside (MGP-6-*O*-ECL), (ii) ε-caprolactone (ECL), (iii) methyl-*D*-glucopyranoside (MGP) and (iv) ECL oligomeric sugar ester or methyl-6-*O*-(hydroxyhexanoyl)$_n$-*D*-glucopyranoside (MGP-6-*O*-oligo-ECL). The chemical assignments were in agreement to previous literature (Ariffin et al., 2014; Feng et al., 2015; Galia et al., 2016; Li et al., 1999; Saravanamoorthy et al., 2015; Song et al., 2016).

Figure 4.15A showed the proton spectrum for purified samples obtained at two hours of reaction. The chemical shift signals at 1.385 ppm and 1.653 ppm were assigned to methylene proton (-CH_2-) of ***c*** and ***b*** + ***d***, respectively. The signals at 2.313 ppm and 3.651 ppm were attributed to methylene proton assigned to ***a*** and ***e*** corresponding to the ester group (-CH_2-COO) and the terminal end of -OH group (-CH_2-OH) in the ECL monomeric sugar ester compound (methyl-6-*O*-(hydroxyhexanoyl)-*D*-glucopyranoside), respectively. The formation of terminal end -OH group is significant indicator for the nucleophilic attack of carbonyl carbon in ECL ring system by lipase resulting in the ring opening of the ECL monomer (Duchiron et al., 2015). The signal of methylene proton ***e*** corresponding to ester group was subjected to the nucleophilic attack of MGP indicating acylation step. The signal at 1.770 ppm from unreacted ECL was assigned to the methylene proton of ***n*** + ***o*** + ***p***. The signal at 2.646 ppm was attributed to methylene proton ***m*** adjacent to acyl group of (-CH_2-COO). The signal assigned to methylene proton ***q*** adjacent to oxygen atom (-CH_2-O) was detected at 4.250 ppm. The chemical shift signals for MGP at 3.431 ppm and 4.775 ppm were assigned to methyl group (-CH_3) ***x*** and H atom ***r*** respectively. The chemical shift at δ 4.200-4.300 ppm corresponded to

methylene proton ***w*** adjacent to the oxygen atom that bind to the 6-hydoxyhexanoic acid intermediate. Due to many overlapping signals in the region of δ 3.400-3.720 ppm, the signals for single proton ***u***, ***t*** and ***s*** in the MGP were difficult to observe (Ariffin et al., 2014).

After three hours reaction (Figure 4.15B), the spectrum shows additional chemical shift at δ 4.063 ppm attributed to methylene proton ***j*** located adjacent to oxygen of intra-chain repeating unit of ECL oligomer. There was no signal corresponding to the formation of ECL oligomer detected at the same chemical shift from samples obtained before or at two hours reaction. This suggests that the incidence of propagation step most likely initiated after two hours reaction as indicated in Figure 4.15B (Elomaa et al., 2011; Jikei et al., 2015). The intensity of signals detected at δ 2.313 ppm and δ 3.651 ppm assigned to the methylene proton ***f*** and ***k*** indicated the formation of repeating units of ECL monomer with the -OH group at the terminal end of ECL oligomer. By comparing with the signals assigned to methylene proton ***a*** and ***e*** (Figure 4.15A), the increase in signals intensity assigned to methylene proton ***f*** and ***k*** (Figure 4.15B) suggested the occurrence of chain propagation step in the proposed mechanism. The chemical shifts for MGP were detected at δ 3.431 ppm and δ 4.775 ppm corresponding to methyl group ***x*** and hydrogen atom ***r***, respectively. The signal at δ 4.250 ppm signifying the presence of methylene proton from the formation of covalent bond between -OH group of C6 in MGP and the carboxylic acid end group of the 6-hydroxyhexanoic acid consequent to the ring opening of ECL. It is hypothesized that sugar acylation step could occur for a single 6-hydroxyhexanoate monomer followed by propagation step, or for a nascent oligomer chain with free carboxyl terminal followed by further propagation before termination step in both cases (Ariffin et al., 2014; Gumel et al., 2013).

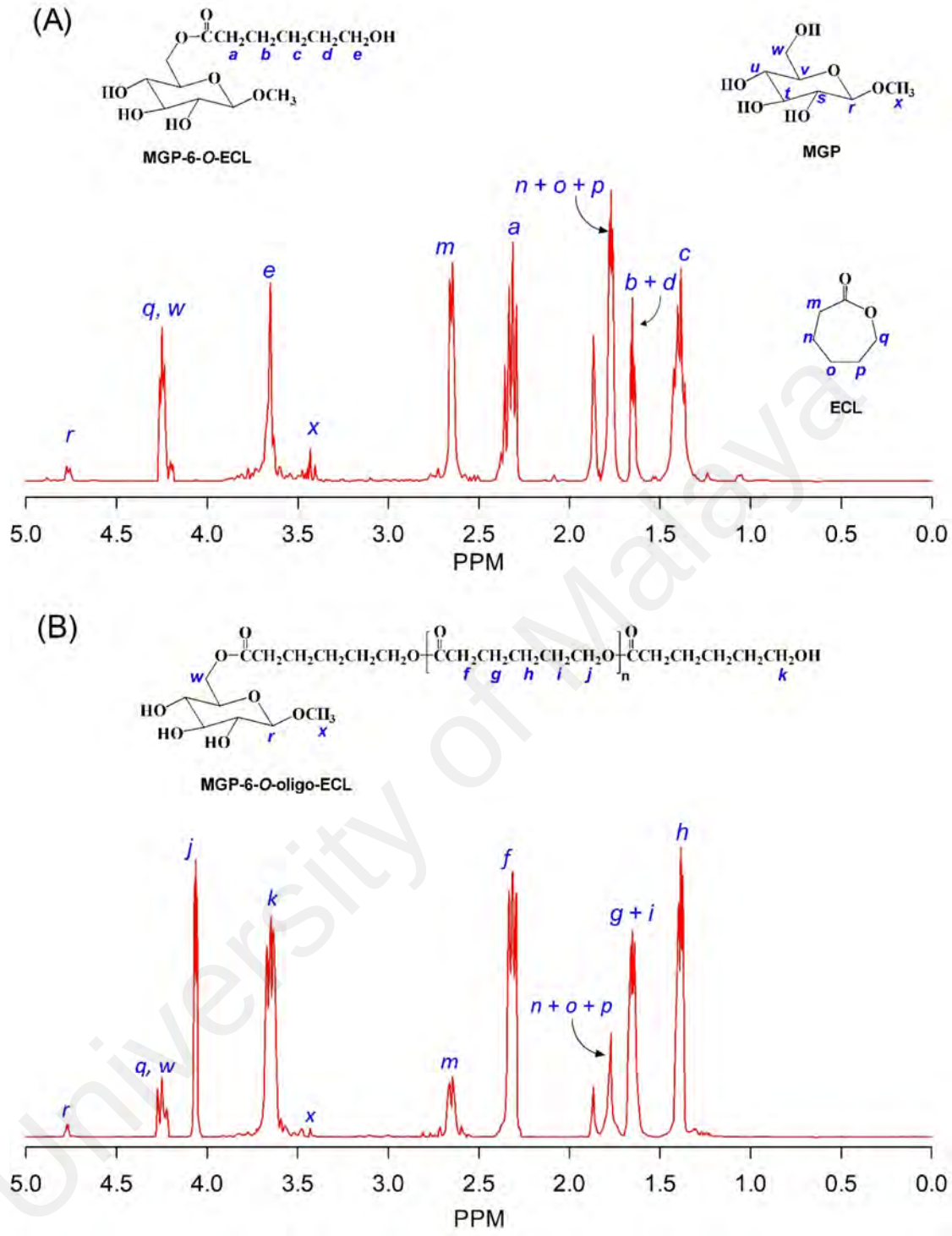

Figure 4.15: ^{1}H NMR spectrum of functionalisation product (A) Two hours reaction; (B) Three hours reaction

4.14.3 TGA Analysis

Samples from the validation experiment were subjected to thermal gravimetric analysis (TGA analysis). The thermogram of functionalised oligomer indicated its overall decomposition proceeded in three stages (Figure 4.16). The first stage was attributed to the loss of moisture at temperature range 35-140 °C which was due to water molecules in the samples. This was followed by the second degradation stage corresponding to the decomposition of sugar moiety at estimated temperature range of 150-240 °C (Figure 7). The decomposition of methyl-*D*-glucopyranoside (MGP) is due to cleavage between methoxy- and glucosyl group which further condensed with other sugar molecules has led to the formation of lower molecular mass of fragmented glycan (Ariffin et al., 2014). The third stage of decomposition corresponds to the degradation of PCL main chain at estimated temperature range of 240-520 °C (Figure 4.16). Constant percentage weight loss above 520 °C exhibits the complete thermal decomposition of functionalised oligomer.

In the case of neat PCL, the thermogram indicated two stages of degradation process including the first stage of moisture evaporation and followed by the PCL main chain degradation started at 240 ºC until constant weight loss above 500 ºC. The amount of sugar moiety was estimated to be less than 20 % based on the percentage of total weight loss during the degradation. Furthermore, the addition of sugar moiety has increased slightly the thermal stability of sugar-functionalised oligomer with initial decomposition temperature of the main chain at 240 ºC instead of 220 ºC as exhibited by the neat ECL oligomer. As previously reported, the addition of sugar moiety has increased the decomposition temperature of functionalised biodegradable polymer under constant heating rate (Gumel et al., 2013).

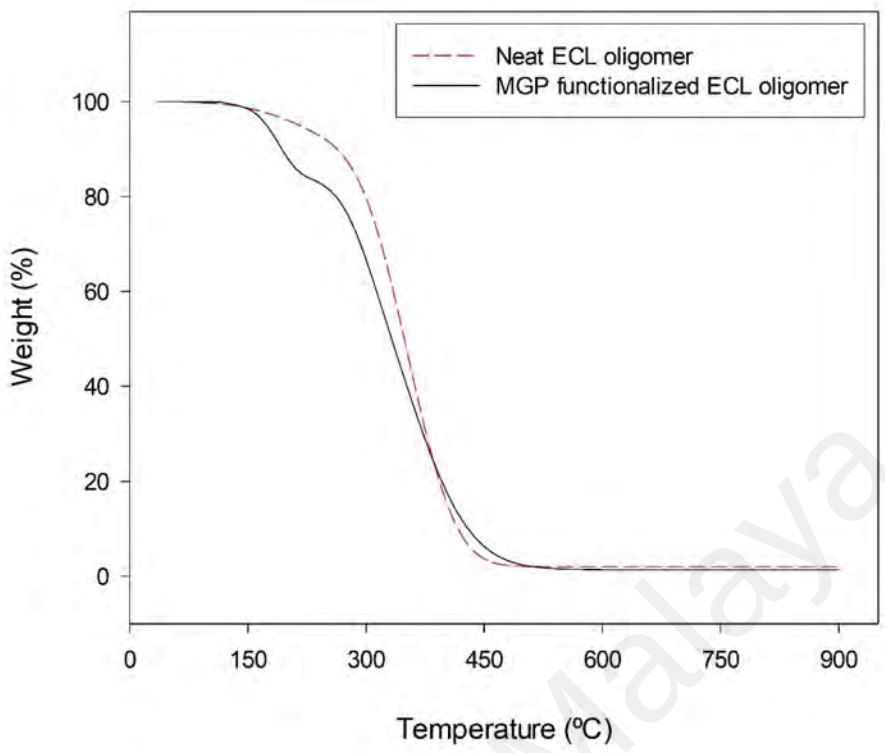

Figure 4.16: TGA curve of neat ECL oligomer and MGP-functionalised ECL oligomer

CHAPTER 5: CONCLUSION

In this study, one-pot synthesis of lipase-catalysed MGP-functionalised ECL oligomer was carried out in a bench-scale custom-fabricated enzymatic reactor. Reactions were performed in a batch mode in order to evaluate the effects of selected operating variables on the production of functionalised oligomer and its kinetic mechanism studies. Based on the finding, it is concluded that:

- The main effects of lipase, initial ECL concentration and temperature are significant with positive effect on the synthesis of functionalised oligomers whereas the effect of initial MGP concentration and agitation rate are insignificant;
- The effects of interaction between variables are significant suggesting the relationship between variables affects the final product yield;
- Kinetic model of ping-pong bi-bi without ternary complex and living polymerization mechanisms were proposed for the esterification and chain propagation, respectively, and they showed good correlation with experimental data;
- The estimated kinetic parameters of ping-pong bi-bi mechanism indicated that initial MGP concentration is the rate limiting substrate during the esterification step;
- Linear regression analysis indicates that living polymerization mechanism is applicable for chain propagation step of the functionalisation reaction;
- A linear relationship between conversion (%) and M_n was observed, indicating controlled rate of propagation in the absence of chain termination step;
- The functionalised oligomer are characterized by molecular weight of narrow polymer dispersity index (PDI) range from 1.30 to 1.70 with higher ECL monomer conversion rate signifying its potential for the production of carbohydrate-functionalised bio-oligomer with controllable molecular weight as platform chemicals.

REFERENCES

Abou-Zeid, D. M., Muller, R. J., & Deckwer, W. D. (2001). Degradation of natural and synthetic polyesters under anaerobic conditions. *Journal of Biotechnology*, *86*(2), 113-126.

Aguilar, A. R., & Guareno, E. O. (2000). Thermochemistry of methyl-D-glucopyranosides and methyl-D-galactopyranosides. *The Journal of Chemical Thermodynamics*, *32*(6), 767-775.

Ajellal, N., Carpentier, J. F., Guillaume, C., Guillaume, S. M., Helou, M., Poirier, V., . . . Trifonov, A. (2010). Metal-catalyzed immortal ring-opening polymerization of lactones, lactides and cyclic carbonates. *Dalton Transactions*, *39*(36), 8363-8376.

Al-Azemi T. F., & Bisht K. S. (2002). One-step synthesis of polycarbonates bearing pendant carboxyl groups by lipase-catalyzed ring-opening polymerization. *Journal of Polymer Science Part A: Polymer Chemistry*, *40*(9), 1267-1274.

Alamri, H., Zhao, J., Pahovnik, D., & Hadjichristidis, N. (2014). Phosphazene-catalyzed ring-opening polymerization of epsilon-caprolactone: influence of solvents and initiators. *Polymer Chemistry*, *5*(18), 5471-5478.

Albertsson, A. C., & Varma, I. K. (2003). Recent developments in ring opening polymerization of lactones for biomedical applications. *Biomacromolecules*, *4*(6), 1466-1486.

Aleman, C., Betran, O., Casanovas, J., Houk, K. N., & Hall, H. K. (2009). Thermodynamic control of the polymerizability of five-, six-, and seven-membered lactones. *The Journal of Organic Chemistry*, *74*(16), 6237-6244.

Ariffin, M. F. K., Annuar, M. S. M., & Heidelberg, T. (2014). Surfactant synthesis via lipase esterification of methyl α-D-glucopyranoside with selected aliphatic carboxylic acids. *Journal of Surfactants and Detergents*, *17*(4), 683-692.

Avella, M., Errico, M. E., Laurienzo, P., Martuscelli, E., Raimo, M., & Rimedio, R. (2000). Preparation and characterisation of compatibilised polycaprolactone/starch composites. *Polymer*, *41*(10), 3875-3881.

Averous, L., Moro, L., Dole, P., & Fringant, C. (2000). Properties of thermoplastic blends: starch-polycaprolactone. *Polymer*, *41*(11), 4157-4167.

Barrera-Rivera, K., & Martínez-Richa, A. (2017). Yarrowia lipolytica extracellular lipase Lip2 as biocatalyst for the ring-opening polymerization of epsilon-caprolactone. *Molecules*, *22*(11), 1917.

Barrera-Rivera, K. A., Flores-Carreon, A., & Martínez-Richa, A. (2008). Enzymatic ring-opening polymerization of epsilon-caprolactone by a new lipase from Yarrowia lipolytica. *Journal of Applied Polymer Science*, *109*(2), 708-719.

Barrera-Rivera, K. A., Marcos-Fernández, Á., Vera-Graziano, R., & Martínez-Richa, A. (2009). Enzymatic ring-opening polymerization of ε-caprolactone by *Yarrowia lipolytica* lipase in ionic liquids. *Journal of Polymer Science Part A: Polymer Chemistry, 47*(21), 5792-5805.

Belmessieri, D., Gozlan, C., Duclos, M. C., Molinier, V., Aubry, J. M., Dumitrescu, O., . . . Lemaire, M. (2017). Synthesis, surfactant properties and antimicrobial activities of methyl glycopyranoside ethers. *European Journal of Medicinal Chemistry*, *128*, 98-106.

Bernaerts, K., Servaes, R. D., Kooyman, S., Versyck, K. J., & Van Impe, J. F. (2002). Optimal temperature input design for estimation of the square root model parameters: parameter accuracy and model validity restrictions. *International Journal of Food Microbiology*, *73*(2), 145-157.

Bhangale, A. S., Beers, K. L., & Gross, R. A. (2012). Enzyme-catalyzed polymerization of end-functionalized polymers in a microreactor. *Macromolecules*, *45*(17), 7000-7008.

Bosworth, L. A., & Downes, S. (2010). Physicochemical characterisation of degrading polycaprolactone scaffolds. *Polymer Degradation and Stability*, *95*(12), 2269-2276

Bouyahyi, M., & Duchateau, R. (2014). Metal-based catalysts for controlled ring-opening polymerization of macrolactones: high molecular weight and well-defined copolymer architectures. *Macromolecules, 47*(2), 517-524.

Bouyahyi, M., Pepels, M. P. F., Heise, A., & Duchateau, R. (2012). Omega-pentandecalactone polymerization and omega-pentadecalactone/epsilon-caprolactone copolymerization reactions using organic catalysts. *Macromolecules*, *45*(8), 3356-3366.

Braud, C., Devarieux, R., Atlan, A., Ducos, C., & Vert, M. (1998). Capillary zone electrophoresis in normal or reverse polarity separation modes for the analysis of hydroxy acid oligomers in neutral phosphate buffer. *Journal of Chromatography B: Biomedical Sciences and Applications*, *706*(1), 73-82.

Bucko, M., Gemeiner, P., Schenkmayerova, A., Krajcovic, T., Rudroff, F., & Mihovilovic, M. D. (2016). Baeyer-villiger oxidations: Biotechnological approach. *Applied Microbiology and Biotechnology*, *100*(15), 6585-6599.

Carrot, G., Hilborn, J. G., Trollsas, M., & Hedrick, J. L. (1999). Two general methods for the synthesis of thiol-functional polycaprolactones. *Macromolecules*, *32*(16), 5264-5269.

Castano, M., Zheng, J. K., Puskas, J. E., & Becker, M. L. (2014). Enzyme-catalyzed ring-opening polymerization of epsilon-caprolactone using alkyne functionalized initiators. *Polymer Chemistry*, *5*(6), 1891-1896.

Cava, D., Gavara, R., Lagaron, J. M., & Voelkel, A. (2007). Surface characterization of poly(lactic acid) and polycaprolactone by inverse gas chromatography. *Journal of Chromatography A*, *1148*(1), 86-91.

Chamouleau, F., Coulon, D., Girardin, M., & Ghoul, M. (2001). Influence of water activity and water content on sugar esters lipase-catalyzed synthesis in organic media. *Journal of Molecular Catalysis B: Enzymatic*, *11*(4-6), 949-954.

Champagne, E., Strandman, S., & Zhu, X. X. (2016). Recent developments and optimization of lipase-catalyzed lactone formation and ring-opening polymerization. *Macromolecular Rapid Communications*, *37*(24), 1986-2004.

Charoensapyanan, R., Ito, K., Rudeekulthamrong, P., & Kaulpiboon, J. (2016). Enzymatic synthesis of propyl-alpha-glycosides and their application as emulsifying and antibacterial agents. *Biotechnology and Bioprocess Engineering*, *21*(3), 389-401.

Chen, C. X., Peng, J. S., Li, B., & Wang, L. L. (2009). The catalytic Baeyer–Villiger oxidation of cyclohexanone to epsilon-caprolactone over stibium-containing hydrotalcite. *Catalysis Letters*, *131*(3), 618-623.

Cheng, M., Angkawidjaja, C., Koga, Y., & Kanaya, S. (2012). Requirement of lid2 for interfacial activation of a family I.3 lipase with unique two lid structures. *FEBS Journal*, *279*(19), 3727-3737.

Cooke, S. L., & Whittington, A. R. (2016). Influence of therapeutic radiation on polycaprolactone and polyurethane biomaterials. *Materials Science and Engineering: C*, *60*, 78-83.

Correlo, V. M., Boesel, L. F., Bhattacharya, M., Mano, J. F., Neves, N. M., & Reis, R. L. (2005). Hydroxyapatite reinforced chitosan and polyester blends for biomedical applications. *Macromolecular Materials and Engineering, 290*(12), 1157-1165.

Darensbourg, D. J., & Yeung, A. D. (2014). Kinetics and thermodynamics of the decarboxylation of 1,2-glycerol carbonate to produce glycidol: computational insights. *Green Chemistry*, *16*(1), 247-252.

Lux, C. D., Joshi-Barr, S., Nguyen, T., Mahmoud, E., Schopf, E., Fomina, N., & Almutairi, A. (2012). Biocompatible polymeric nanoparticles degrade and release cargo in response to biologically relevant levels of hydrogen peroxide. *Journal of the American Chemical Society*, *134*(38), 15758-15764.

Deffieux, A., & Schappacher, M. (1998). Design of new polymer architectures by combination of anionic and cationic living polymerization techniques. *Macromolecular Symposia*, *132*(1), 45-55.

del Rosal, I., Brignou, P., Guillaume, S. M., Carpentier, J. F., & Maron, L. (2015). DFT investigations on the ring-opening polymerization of substituted cyclic carbonates catalyzed by zinc-(beta-diketiminate) complexes. *Polymer Chemistry*, *6*(17), 3336-3352.

Deng, F., & Gross, R. A. (1999). Ring-opening bulk polymerization of epsilon-caprolactone and trimethylene carbonate catalyzed by lipase Novozym 435. *International Journal of Biological Macromolecules*, *25*(1), 153-159.

Detrembleur, C., Mazza, M., Halleux, O., Lecomte, P., Mecerreyes, D., Hedrick, J. L., & Jerome, R. (2000). Ring-opening polymerization of gamma-bromo-epsilon-caprolactone: A Novel route to functionalized aliphatic polyesters. *Macromolecules*, *33*(1), 14-18.

Drozdz, A., Chrobok, A., Baj, S., Szymanska, K., Mrowiec-Bialon, J., & Jarzebski, A. B. (2013). The chemo-enzymatic Baeyer-Villiger oxidation of cyclic ketones with an efficient silica-supported lipase as a biocatalyst. *Applied Catalysis A: General*, *467*, 163-170.

Duchiron, S. W., Pollet, E., Givry, S., & Averous, L. (2015). Mixed systems to assist enzymatic ring opening polymerization of lactide stereoisomers. *RSC Advances*, *5*(103), 84627-84635.

Duda, A., Kowalski, A., Libiszowski, J., & Penczek, S. (2005). Thermodynamic and kinetic polymerizability of cyclic esters. *Macromolecular Symposia*, *224*(1), 71-84.

Duda, A., Kowalski, A., Penczek, S., Uyama, H., & Kobayashi, S. (2002). Kinetics of the ring-opening polymerization of 6-, 7-, 9-, 12-, 13-, 16-, and 17-membered lactones. Comparison of chemical and enzymatic polymerizations. *Macromolecules*, *35*(11), 4266-4270.

Dzienia, A., Maksym, P., Tarnacka, M., Grudzka-Flak, I., Golba, S., Zięba, A., . . . Paluch, M. (2017). High pressure water-initiated ring opening polymerization for the synthesis of well-defined alpha-hydroxy-omega-(carboxylic acid) polycaprolactones. *Green Chemistry*, *19*(15), 3618-3627.

Elling, B. R., & Xia, Y. (2015). Living alternating ring-opening metathesis polymerization based on single monomer additions. *Journal of the American Chemical Society*, *137*(31), 9922-9926.

Elomaa, L., Teixeira, S., Hakala, R., Korhonen, H., Grijpma, D. W., & Seppala, J. V. (2011). Preparation of poly(epsilon-caprolactone)-based tissue engineering scaffolds by stereolithography. *Acta Biomaterialia, 7*(11), 3850-3856.

Endo, T. (2009). General mechanisms in ring-opening polymerization. In P. Dubois, O. Coulembier & J. M. Raquez (Eds.), Handbook of ring opening polymerization (pp. 53-63). Weinheim, GER: Wiley-VCH.

Endo, T., & Sudo, A. (2016). Special issue “ring-opening polymerization”. *Molecules*, *21*(12), Article#1720.

Ericsson, D. J., Kasrayan, A., Johansson, P., Bergfors, T., Sandstrom, A. G., Backvall, J.-E., & Mowbray, S. L. (2008). X-ray structure of Candida antarctica lipase A shows a novel lid structure and a likely mode of interfacial activation. *Journal of Molecular Biology*, *376*(1), 109-119.

Estelles, J. M., Vidaurre, A., Duenas, J. M. M., & Cortazar, I. C. (2008). Physical characterization of polycaprolactone scaffolds. *Journal of Materials Science: Materials in Medicine*, *19*(1), 189-195.

Feng, J., Jiang, J., Xu, J., & Yang, Z. (2015). One-step method to produce methyl-D-glucoside from lignocellulosic biomass. *RSC Advances*, *5*(48), 38783-38791.

Feng, R., Song, Z., & Zhai, G. (2012). Preparation and in vivo pharmacokinetics of curcumin-loaded PCL-PEG-PCL triblock copolymeric nanoparticles. *International Journal of Nanomedicine*, *7*, 4089-4098.

Fereshteh, Z., Fathi, M., Bagri, A., & Boccaccini, A. R. (2016). Preparation and characterization of aligned porous PCL/zein scaffolds as drug delivery systems via improved unidirectional freeze-drying method. *Materials Science and Engineering: C*, *68*, 613-622.

Ferrario, V., Ebert, C., Knapic, L., Fattor, D., Basso, A., Spizzo, P., & Gardossi, L. (2011). Conformational changes of lipases in aqueous media: A comparative computational study and experimental implications. *Advanced Synthesis & Catalysis*, *353*(13), 2466-2480.

Galia, A., Scialdone, O., Spano, T., Valenti, M. G., Grignard, B., Lecomte, P., . . . Rousseau, C. (2016). Ring opening polymerization of epsilon-caprolactone in the presence of wet beta-cyclodextrin: effect of the operative pressure and of water molecules in the beta-cyclodextrin cavity. *RSC Advances*, *6*(93), 90290-90299.

García-Arguelles, S., García, C., Serrano, M. C., Gutierrez, M. C., Ferrer, M. L., & del Monte, F. (2015). Near-to-eutectic mixtures as bifunctional catalysts in the low-temperature-ring-opening-polymerization of epsilon-caprolactone. *Green Chemistry*, *17*(6), 3632-3643.

Gopinath, S., & Sugunan, S. (2007). Enzymes immobilized on montmorillonite K 10: Effect of adsorption and grafting on the surface properties and the enzyme activity. *Applied Clay Science*, *35*(1), 67-75.

Granado, A., Eguiazabal, J. I., & Nazabal, J. (2008). Structure and mechanical properties of blends of poly(epsilon-caprolactone) with a poly(amino ether). *Journal of Applied Polymer Science*, *109*(6), 3892-3899.

Gumel, A. M., Annuar, M. S. M., & Heidelberg, T. (2013). Enzymatic synthesis of 6-O-glucosyl-poly(3-hydroxyalkanoate) in organic solvents and their binary mixture. *International Journal of Biological Macromolecules*, *55*, 127-136.

Gumel, A. M., Annuar, M. S. M., & Heidelberg, T. (2013). Single-step lipase-catalyzed functionalization of medium-chain-length polyhydroxyalkanoates. *Journal of Chemical Technology & Biotechnology*, *88*(7), 1328-1335.

Guo, J., Chen, C. P., Wang, S. G., & Huang, X. J. (2015). A convenient test for lipase activity in aqueous-based solutions. *Enzyme and Microbial Technology*, *71*, 8-12.

Habeych, D. I., Eggink, G., & Boeriu, C. G. (2011). Linear and cyclic ester oligomers of succinic acid and 1, 4-butanediol: Biocatalytic synthesis and characterization. *Biocatalysis and Biotransformation*, *29*(6), 299-310.

Hans, M., Gasteier, P., Keul, H., & Moeller, M. (2006). Ring-opening polymerization of epsilon-caprolactone by means of mono- and multifunctional Initiators: comparison of chemical and enzymatic catalysis. *Macromolecules*, *39*(9), 3184-3193.

Hans, M., Keul, H., & Moeller, M. (2009). Ring-opening polymerization of DD-Lactide catalyzed by Novozyme 435. *Macromolecular Bioscience, 9*(3), 239-247.

Hasan, F., Shah, A. A., & Hameed, A. (2006). Industrial applications of microbial lipases. *Enzyme and Microbial Technology*, *39*(2), 235-251.

He, W., Fang, Z., Zhu, N., Ji, D., Li, Z. J., & Guo, K. (2015). Ring-opening polymerization of e-caprolactone catalyzed by a novel lipase Candida sp. 99-125. *Biocatalysis and Biotransformation*, *33*(3), 150-155.

Henini, G., Souahi, F., & Laidani, Y. (2012). Tracking offline conversion solution polymerization of methyl methacrylate/vinyl acetate in toluene in a reactor calorimeter. *Procedia Engineering*, *33*, 225-233.

Herrera-Kao, W., Cervantes-Uc J, M., Lara-Ceniceros, T., & Aguilar-Vega, M. (2015). Effect of reaction temperature on the physicochemical properties of poly(pentadecanolide) obtained by enzyme-catalyzed ring-opening polymerization. *Polymer Bulletin*, *72*(3), 441-452.

Huang, X. J, Xiao, Y., & Lang, M. D. (2011). Synthesis and self-assembly behavior of six-armed block copolymers with pH- and thermo-responsive properties. *Macromolecular Research*, *19*(2), 113-121.

Huang, Y. G., Li, L. Y., & Li, G. J. (2015). An enzyme-catalysed access to amphiphilic triblock copolymer of PCL-b-PEG-b-PCL: synthesis, characterization and self-assembly properties. *Designed Monomers and Polymers*, *18*(8), 799-806.

Hudson, S., Magner, E., Cooney, J., & Hodnett, B. K. (2005). Methodology for the immobilization of enzymes onto mesoporous materials. *The Journal of Physical Chemistry B*, *109*(41), 19496-19506.

Humeau, C., Girardin, M., Rovel, B., & Miclo, A. (1998). Effect of the thermodynamic water activity and the reaction medium hydrophobicity on the enzymatic synthesis of ascorbyl palmitate. *Journal of Biotechnology*, *63*(1), 1-8.

Ibrahim, M., Alaam, M., El-Haes, H., Jalbout, A. F., & de Leon, A. (2006). Analysis of the structure and vibrational spectra of glucose and fructose. *Ecletica Química*, *31*(3), 15-21.

Jankowski, K. J., Budzyński, W. S., Załuski, D., Hulanicki, P. S., & Dubis, B. (2016). Using a fractional factorial design to evaluate the effect of the intensity of agronomic practices on the yield of different winter oilseed rape morphotypes. *Field Crops Research*, *188*, 50-61.

Jenkins, A. D., Jones, R. G., & Moad, G. (2010). Terminology for reversible-deactivation radical polymerization previously called "controlled" radical or "living" radical polymerization (IUPAC Recommendations 2010). *Pure and Applied Chemistry*, *82*(2), 483-491.

Jeon, S. J., Jung, M. Y., & Do, J. Y. (2016). Anionic ring-opening polymerization of cyclic 1,3-dithiocarbonate and thermal depolymerization. *Reactive and Functional Polymers*, *100*, 37-43.

Jérôme, C., & Lecomte, P. (2008). Recent advances in the synthesis of aliphatic polyesters by ring-opening polymerization. *Advanced Drug Delivery Reviews*, *60*(9), 1056-1076.

Jiang, Y., Zhang, Y., Banks, C., Heaven, S., & Longhurst, P. (2017). Investigation of the impact of trace elements on anaerobic volatile fatty acid degradation using a fractional factorial experimental design. *Water Research*, *125*, 458-465.

Jikei, M., Takeyama, Y., Yamadoi, Y., Shinbo, N., Matsumoto, K., Motokawa, M., . . . Yamamoto, F. (2015). Synthesis and properties of poly(L-lactide)-poly(epsilon-caprolactone) multiblock copolymers by the self-polycondensation of diblock macromonomers. *Polymer Journal*, *47*(10), 657-665.

Junior, I. I., Flores, M. C., Sutili, F. K., Leite, S. G. F., Miranda, L. S. D., Leal, I. C. R., & de Souza, R. O. M. A. (2012). Lipase-catalyzed monostearin synthesis under continuous flow conditions. *Organic Process Research & Development*, *16*(5), 1098-1101.

Kang, B., Opatz, T., Landfester, K., & Wurm, F. R. (2015). Carbohydrate nanocarriers in biomedical applications: functionalization and construction. *Chemical Society Reviews*, *44*(22), 8301-8325.

Ketelaars, A. A. J., Papantoniou, Y., & Nakayama, K. (1997). Analysis of the density and the enthalpy of poly(epsilon-caprolactone)-polycarbonate blends: Amorphous phase compatibility and the effect of secondary crystallization. *Journal of Applied Polymer Science*, *66*(5), 921-927.

Kikuchi, H., Uyama, H., & Kobayashi, S. (2002). Lipase-catalyzed ring-opening polymerization of substituted lactones. *Polymer Journal, 34*(11), 835-840.

Kim, J., Haam, S., Park, D. W., Ahn, I. S., Lee, T. G., Kim, H. S., & Kim, W. S. (2004). Biocatalytic esterification of beta-methylglucoside for synthesis of biocompatible sugar-containing vinyl esters. *Chemical Engineering Journal*, *99*(1), 15-22.

Kobayashi, S. (2010). Lipase-catalyzed polyester synthesis - A green polymer chemistry. *Proceedings of the Japan Academy, Series B*, *86*(4), 338-365.

Kobayashi, S. (2015). Enzymatic ring-opening polymerization and polycondensation for the green synthesis of polyesters. *Polymers for Advanced Technologies*, *26*(7), 677-686.

Kobayashi, S., Takeya, K., Suda, S., & Uyama, H. (1998). Lipase-catalyzed ring-opening polymerization of medium-size lactones to polyesters. *Macromolecular Chemistry and Physics*, *199*(8), 1729-1736.

Kobayashi, S., & Uyama, H. (2002). In vitro polyester synthesis via enzymatic polymerization. *Current Organic Chemistry*, *6*(2), 209-222.

Kobayashi, S., Uyama, H., & Namekawa, S. (1998). In vitro biosynthesis of polyesters with isolated enzymes in aqueous systems and organic solvents. *Polymer Degradation and Stability*, *59*(1), 195-201.

Kooy, F. K., Beeftink, H. H., Eppink, M. H. M., Tramper, J., Eggink, G., & Boeriu, C. G. (2014). Kinetic and structural analysis of two transferase domains in Pasteurella multocida hyaluronan synthase. *Journal of Molecular Catalysis B: Enzymatic*, *102*, 138-145.

Korolevich, F. V., Zhbankova, M. R., Piottukh-Peletskii, V. N., & Zhbankov, R. G. (2007). Interpretation of the IR spectrum of methyl-beta-D-glucopyranoside based on the theoretical calculation of frequencies and intensities of normal vibrations. *Journal of Structural Chemistry*, *48*(5), 821-830.

Korzhikov, V. A., Gusevskaya, K. V., Litvinchuk, E. N., Vlakh, E. G., & Tennikova, T. B. (2013). Enzyme-mediated ring-opening polymerization of pentadecalactone to obtain biodegradable polymer for fabrication of scaffolds for bone tissue engineering. *International Journal of Polymer Science*, Article#476748.

Labet, M., & Thielemans, W. (2009). Synthesis of polycaprolactone: a review. *Chemical Society Reviews*, *38*(12), 3484-3504.

Lam, C. X. F., Teoh, S. H., & Hutmacher, D. W. (2007). Comparison of the degradation of polycaprolactone and polycaprolactone-(beta-tricalcium phosphate) scaffolds in alkaline medium. *Polymer International*, *56*(6), 718-728.

Lambermont-Thijs, H. M. L., van der Woerdt, F. S., Baumgaertel, A., Bonami, L., Du Prez, F. E., Schubert, U. S., & Hoogenboom, R. (2010). Linear poly(ethylene imine)s by acidic hydrolysis of poly(2-oxazoline)s: Kinetic screening, thermal properties, and temperature-induced solubility transitions. *Macromolecules*, *43*(2), 927-933.

Leisch, H., Morley, K., & Lau, P. C. K. (2011). Baeyer−Villiger monooxygenases: more than just green chemistry. *Chemical Reviews*, *111*(7), 4165-4222.

Li, F., Yu, D., Lin, X. M., Liu, D. B., Xia, H. M., & Chen, S. (2012). Biodegradation of poly(epsilon-caprolactone) (PCL) by a new Penicillium oxalicum strain DSYD05-1. *World Journal of Microbiology and Biotechnology*, *28*(10), 2929-2935.

Li, H., Peng, L. C., Lin, L., Chen, K. L., & Zhang, H. (2013). Synthesis, isolation and characterization of methyl levulinate from cellulose catalyzed by extremely low concentration acid. *Journal of Energy Chemistry*, *22*(6), 895-901.

Li, J., Xie, W. H., Cheng, H. N., Nickol, R. G., & Wang, P. G. (1999). Polycaprolactone-modified hydroxyethylcellulose films prepared by lipase-catalyzed ring-opening polymerization. *Macromolecules*, *32*(8), 2789-2792.

Li, Q. S., Li, G. Q., Yu, S. S., Zhang, Z. M., Ma, F. Q., & Feng, Y. (2011). Ring-opening polymerization of epsilon-caprolactone catalyzed by a novel thermophilic lipase from Fervidobacterium nodosum. *Process Biochemistry*, *46*(1), 253-257.

Liese, A., & Villela, M. (1999). Production of fine chemicals using biocatalysis. *Current Opinion in Biotechnology*, *10*(6), 595-603.

Lin, G. Y., Cosimbescu, L., Karin, N. J., Gutowska, A., & Tarasevich, B. J. (2013). Injectable and thermogelling hydrogels of PCL-g-PEG: mechanisms, rheological and enzymatic degradation properties. *Journal of Materials Chemistry B*, *1*(9), 1249-1255.

Liu, L., Li, Y., Liu, H., & Fang, Y. (2004). Synthesis and characterization of chitosan-graft-polycaprolactone copolymers. *European Polymer Journal*, *40*(12), 2739-2744.

Liu, S., Srinivasan, S., Grady, M. C., Soroush, M., & Rappe, A. M. (2014). Backbiting and beta-scission reactions in free-radical polymerization of methyl acrylate. *International Journal of Quantum Chemistry*, *114*(5), 345-360.

Liu, Y. C., Ko, B. T., & Lin, C. C. (2001). A highly efficient catalyst for the "Living" and "Immortal" polymerization of epsilon-caprolactone and l-lactide. *Macromolecules*, *34*(18), 6196-6201.

Lou, X. D., Detrembleur, C., & Jerome, R. (2003). Novel aliphatic polyesters based on functional cyclic (di)esters. *Macromolecular Rapid Communications*, *24*(2), 161-172.

Ma, J. T., Li, Q. S., Song, B., Liu, D. L., Zheng, B. S., Zhang, Z. M., & Feng, Y. (2009). Ring-opening polymerization of epsilon-caprolactone catalyzed by a novel thermophilic esterase from the archaeon Archaeoglobus fulgidus. *Journal of Molecular Catalysis B: Enzymatic*, *56*(2), 151-157.

Makiguchi, K., Satoh, T., & Kakuchi, T. (2011). Diphenyl phosphate as an efficient cationic organocatalyst for controlled/living ring-opening polymerization of delta-valerolactone and epsilon-caprolactone. *Macromolecules*, *44*(7), 1999-2005.

Manavitehrani, I., Fathi, A., Badr, H., Daly, S., Shirazi, A. N., & Dehghani, F. (2016). Biomedical applications of biodegradable polyesters. *Polymers*, *8*(1), Article#20.

Marcilla, R., de Geus, M., Mecerreyes, D., Duxbury, C. J., Koning, C. E., & Heise, A. (2006). Enzymatic polyester synthesis in ionic liquids. *European Polymer Journal*, *42*(6), 1215-1221.

Marten, E., Muller, R. J., & Deckwer, W. D. (2003). Studies on the enzymatic hydrolysis of polyesters I. Low molecular mass model esters and aliphatic polyesters. *Polymer Degradation and Stability*, *80*(3), 485-501.

Matsumoto, M., Odachi, D., & Kondo, K. (1999). Kinetics of ring-opening polymerization of lactones by lipase. *Biochemical Engineering Journal*, *4*(1), 73-76.

Matsumura, S. (2006). Enzymatic synthesis of polyesters via ring-opening polymerization. In S. Kobayashi, H. Ritter & D. Kaplan (Eds.), Enzyme-Catalyzed Synthesis of Polymers (pp. 95-132). Berlin, Heidelberg: Springer Berlin Heidelberg.

Matsumura, S., Ebata, H., Kondo, R., & Toshima, K. (2001). Organic solvent-free enzymatic transformation of poly(epsilon-caprolactone) into repolymerizable oligomers in supercritical carbon dioxide. *Macromolecular Rapid Communications, 22*(16), 1325-1329.

Medina, D. A., Contreras, J. M., Lopez-Carrasquero, F. J., Cardozo, E. J., & Contreras, R. R. (2018). Use of samarium(III)–amino acid complexes as initiators of ring-opening polymerization of cyclic esters. *Polymer Bulletin*, *75*(3), 1253-1263.

Meek, M. F., & Jansen, K. (2009). Two years after in vivo implantation of poly(DL-lactide-epsilon-caprolactone) nerve guides: Has the material finally resorbed? *Journal of Biomedical Materials Research Part A*, *89A*(3), 734-738.

Mehta, R., Kumar, V., & Upadhyay, S. N. (2007). Mathematical modeling of the poly(lactic acid) ring–opening polymerization kinetics. *Polymer-Plastics Technology and Engineering*, *46*(3), 257-264.

Mei, Y., Kumar, A., & Gross, R. (2003). Kinetics and mechanism of Candida antarctica lipase B catalyzed solution polymerization of epsilon-caprolactone. *Macromolecules*, *36*(15), 5530-5536.

Mei, Y., Kumar, A., & Gross, R. A. (2002). Probing water-temperature relationships for lipase-catalyzed lactone ring-opening polymerizations. *Macromolecules*, *35*(14), 5444-5448.

Mendes, A. A., Oliveira, P. C., & de Castro, H. F. (2012). Properties and biotechnological applications of porcine pancreatic lipase. *Journal of Molecular Catalysis B: Enzymatic*, *78*, 119-134.

Mezzasalma, L., Dove, A. P., & Coulembier, O. (2017). Organocatalytic ring-opening polymerization of l-lactide in bulk: A long standing challenge. *European Polymer Journal*, *95*, 628-634.

Molinier, V., Kouwer, P. H. J., Fitremann, J., Bouchu, A., Mackenzie, G., Queneau, Y., & Goodby, J. W. (2006). Self-organizing properties of monosubstituted sucrose fatty acid esters: the effects of chain length and unsaturation. *Chemistry*, *12*(13), 3547-3557.

Namekawa, S., Suda, S., Uyama, H., & Kobayashi, S. (1999). Lipase-catalyzed ring-opening polymerization of lactones to polyesters and its mechanistic aspects. *International Journal of Biological Macromolecules, 25*(1), 145-151.

Namekawa, S., Uyama, H., & Kobayashi, S. (1998). Lipase-catalyzed ring-opening polymerization of 16-hexadecanolide. *Proceedings of the Japan Academy, Series B*, *74*(4), 65-68.

Natta, F. J. v., Hill, J. W., & Carothers, W. H. (1934). Studies of polymerization and ring formation. XXIII.1 epsilon-caprolactone and its polymers. *Journal of the American Chemical Society*, *56*(2), 455-457.

Neitzel, A. E., Haversang, T. J., & Hillmyer, M. A. (2016). Organocatalytic cationic ring-opening polymerization of a cyclic hemiacetal ester. *Industrial & Engineering Chemistry Research*, *55*(45), 11747-11755.

Ortega-Toro, R., Contreras, J., Talens, P., & Chiralt, A. (2015). Physical and structural properties and thermal behaviour of starch-poly(epsilon-caprolactone) blend films for food packaging. *Food Packaging and Shelf Life*, *5*, 10-20.

Panova, A. A., & Kaplan, D. L. (2003). Mechanistic limitations in the synthesis of polyesters by lipase-catalyzed ring-opening polymerization. *Biotechnology and Bioengineering*, *84*(1), 103-113.

Penczek, S., & Moad, G. (2009). Glossary of terms related to kinetics, thermodynamics, and mechanisms of polymerization (IUPAC Recommendations 2008). *Pure and Applied Chemistry*, *80*(10), 2163-2193.

Piotrowska, U., & Sobczak, M. (2015). Enzymatic polymerization of cyclic monomers in ionic liquids as a prospective synthesis method for polyesters used in drug delivery systems. *Molecules*, *20*(1), 1-23.

Polloni, A. E., Veneral, J. G., Rebelatto, E. A., de Oliveira, D., Oliveira, J. V., Araujo, P. H. H., & Sayer, C. (2017). Enzymatic ring opening polymerization of omega-pentadecalactone using supercritical carbon dioxide. *The Journal of Supercritical Fluids*, *119*, 221-228.

Pulkkinen, M., Malin, M., Bohm, J., Tarvainen, T., Wirth, T., Seppala, J., & Jarvinen, K. (2009). In vivo implantation of 2,2'-bis(oxazoline)-linked poly-epsilon-caprolactone: Proof for enzyme sensitive surface erosion and biocompatibility (vol 36, pg 310, 2009). *European Journal of Pharmaceutical Sciences*, *37*(2), 183-183.

Qi, W., Ghoroghchian, P. P., Li, G. Z., Hammer, D. A., & Therien, M. J. (2013). Aqueous self-assembly of poly(ethylene oxide)-block-poly(epsilon-caprolactone) (PEO-b-PCL) copolymers: disparate diblock copolymer compositions give rise to nano- and meso-scale bilayered vesicles. *Nanoscale*, *5*(22), 10908-10915.

Reichert, J. C., Wullschleger, M. E., Cipitria, A., Lienau, J., Cheng, T. K., Schutz, M. A., . . . Hutmacher, D. W. (2011). Custom-made composite scaffolds for segmental defect repair in long bones. *International Orthopaedics*, *35*(8), 1229-1236.

Romero, C. M., Pera, L. M., Loto, F., Vallejos, C., Castro, G., & Baigori, M. D. (2012). Purification of an organic solvent-tolerant lipase from Aspergillus niger MYA 135 and its application in ester synthesis. *Biocatalysis and Agricultural Biotechnology*, *1*(1), 25-31.

Rosa, D. S., Neto, I. C., Calil, M. R., Pedroso, A. G., Fonseca, C. P., & Neves, S. (2004). Evaluation of the thermal and mechanical properties of poly(epsilon-caprolactone), low-density polyethylene, and their blends. *Journal of Applied Polymer Science*, *91*(6), 3909-3914.

Santos, R. D., Rosso Comim, S. R., Oliveira, D. d., Treichel, H., Di Luccio, M., Ferreira, S. R. S., & Vladimir Oliveira, J. (2012). Lipase-catalyzed synthesis of poly(ε-caprolactone) in supercritical carbon dioxide. *Biocatalysis and Agricultural Biotechnology, 1*(4), 280-283.

Saravanamoorthy, S., Muneeswaran, M., Giridharan, N., & Velmathi, S. (2015). Solvent-free ring opening polymerization of epsilon-caprolactone and electrical properties of polycaprolactone blended BiFeO3 nanocomposites. *RSC Advances, 5*(54), 43897-43905.

Sarvari, R., Akbari-Alanjaraghi, M., Massoumi, B., Beygi-Khosrowshahi, Y., & Agbolaghi, S. (2017). Conductive and biodegradable scaffolds based on a five-arm and functionalized star-like polyaniline–polycaprolactone copolymer with a D-glucose core. *New Journal of Chemistry*, *41*(14), 6371-6384.

Sattayanon, C., Sontising, W., Limwanich, W., Meepowpan, P., Punyodom, W., & Kungwan, N. (2015). Effects of alkoxide alteration on the ring-opening polymerization of epsilon-caprolactone initiated by n-Bu3SnOR: a DFT study. *Structural Chemistry*, *26*(3), 695-703.

Save, M., Schappacher, M., & Soum, A. (2002). Controlled ring-opening polymerization of lactones and lactides initiated by lanthanum isopropoxide, 1 - General aspects and kinetics. *Macromolecular Chemistry and Physics*, *203*(5-6), 889-899.

Scherkus, C., Schmidt, S., Bornscheuer, U. T., Groger, H., Kara, S., & Liese, A. (2016). A fed-batch synthetic strategy for a three-step enzymatic synthesis of poly-epsilon-caprolactone. *ChemCatChem, 8*(22), 3446-3452.

Secundo, F., Carrea, G., Tarabiono, C., Gatti-Lafranconi, P., Brocca, S., Lotti, M., . . . Eggert, T. (2006). The lid is a structural and functional determinant of lipase activity and selectivity. *Journal of Molecular Catalysis B: Enzymatic*, *39*(1–4), 166-170.

Sen, S., & Puskas, J. (2015). Green polymer chemistry: Enzyme catalysis for polymer functionalization. *Molecules*, *20*(5), 9358-9379.

Sha, K., Qin, L., Li, D. S., Liu, X. T., & Wang, J. Y. (2005). Synthesis and characterization of diblock and triblock copolymer by enzymatic ring-opening polymerization of epsilon-caprolactone and ATRP of styrene. *Polymer Bulletin*, *54*(1-2), 1-9.

Shah, A. A., Nawaz, A., Kanwal, L., Hasan, F., Khan, S., & Badshah, M. (2015). Degradation of poly(epsilon-caprolactone) by a thermophilic bacterium Ralstonia sp. strain MRL-TL isolated from hot spring. *International Biodeterioration & Biodegradation*, *98*, 35-42.

Shoda, S. I., Uyama, H., Kadokawa, J., Kimura, S., & Kobayashi, S. (2016). Enzymes as green catalysts for precision macromolecular synthesis. *Chemical Reviews*, *116*(4), 2307-2413.

Singh, R., Kumar, M., Mittal, A., & Mehta, P. K. (2016). Microbial enzymes: industrial progress in 21st century. *3 Biotech*, *6,* Article#174.

Sisson, A. L., Ekinci, D., & Lendlein, A. (2013). The contemporary role of epsilon-caprolactone chemistry to create advanced polymer architectures. *Polymer*, *54*(17), 4333-4350.

Skjold-Jorgensen, J., Bhatia, V. K., Vind, J., Svendsen, A., Bjerrumt, M. J., & Farrens, D. (2015). The enzymatic activity of lipases correlates with polarity-induced conformational changes: A trp-induced quenching fluorescence study. *Biochemistry*, *54*(27), 4186-4196.

Sobczak, M. (2012). Enzyme-catalyzed ring-opening polymerization of cyclic esters in the presence of poly(ethylene glycol). *Journal of Applied Polymer Science*, *125*(5), 3602-3609.

Song, P., Jiang, S. C., Ren, Y. J., Zhang, X., Qiao, T. K., Song, X. F., . . . Chen, X. S. (2016). Synthesis and characterization of tannin grafted polycaprolactone. *Journal of Colloid and Interface Science*, *479*, 160-164.

Song, R., Murphy, M., Li, C. S., Ting, K., Soo, C., & Zheng, Z. (2018). Current development of biodegradable polymeric materials for biomedical applications. *Drug Design Development and Therapy*, *12*, 3117-3145.

Srivastava, R. K., & Albertsson, A. C. (2006). Enzyme-catalyzed ring-opening polymerization of seven-membered ring lactones leading to terminal-functionalized and triblock polyesters. *Macromolecules*, *39*(1), 46-54.

Stanley, N., Bucataru, G., Miao, Y., Favrelle, A., Bria, M., Stoffelbach, F., . . . Zinck, P. (2014). Brønsted acid-catalyzed polymerization of epsilon-caprolactone in water: A mild and straight forward route to poly(epsilon-caprolactone)-graft-water-soluble polysaccharides. *Journal of Polymer Science Part A: Polymer Chemistry*, *52*(15), 2139-2145.

Stergiou, P. Y., Foukis, A., Filippou, M., Koukouritaki, M., Parapouli, M., Theodorou, L. G., . . . Papamichael, E. M. (2013). Advances in lipase-catalyzed esterification reactions. *Biotechnology Advances*, *31*(8), 1846-1859.

Sun, Y. Y., Cui, Y. Q., Xiong, J., Dai, Z. R., Tang, N., & Wu, J. C. (2015). Different mechanisms at different temperatures for the ring-opening polymerization of lactide catalyzed by binuclear magnesium and zinc alkoxides. *Dalton Transactions, 44*(37), 16383-16391.

Szwarc, M. (1998). Living polymers. Their discovery, characterization, and properties. *Journal of Polymer Science Part A: Polymer Chemistry*, *36*(1), IX-XV.

Takwa, M., Xiao, Y., Simpson, N., Malmstrom, E., Hult, K., Koning, C. E., . . . Martinelle, M. (2008). Lipase catalyzed HEMA initiated ring-opening polymerization: In situ formation of mixed polyester methacrylates by transesterification. *Biomacromolecules*, *9*(2), 704-710.

Thurecht, K. J., Heise, A., deGeus, M., Villarroya, S., Zhou, J. X., Wyatt, M. F., & Howdle, S. M. (2006). Kinetics of enzymatic ring-opening polymerization of epsilon-caprolactone in supercritical carbon dioxide. *Macromolecules*, *39*(23), 7967-7972.

Tian, H. Y., Tang, Z. H., Zhuang, X. L., Chen, X. S., & Jing, X. B. (2012). Biodegradable synthetic polymers: Preparation, functionalization and biomedical application. *Progress in Polymer Science*, *37*(2), 237-280.

Todea, A., Aparaschivei, D., Badea, V., Boeriu, C. G., & Peter, F. (2018). Biocatalytic route for the synthesis of oligoesters of hydroxy-fatty acids and e-caprolactone. *Biotechnology Journal*, *13*(6), Article#1700629.

Tokiwa, Y., Calabia, B. P., Ugwu, C. U., & Aiba, S. (2009). Biodegradability of plastics. *International Journal of Molecular Sciences*, *10*(9), 3722-3742.

Tsai, S. W., & Chang, C. S. (1993). Kinetics of lipase-catalyzed hydrolysis of lipids in biphasic organic-aqueous systems. *Journal of Chemical Technology & Biotechnology*, *57*(2), 147-154.

Uscátegui, Y. L., Arévalo, F. R., Díaz, L. E., Cobo, M. I., & Valero, M. F. (2016). Microbial degradation, cytotoxicity and antibacterial activity of polyurethanes based on modified castor oil and polycaprolactone. *Journal of Biomaterials Science, Polymer Edition*, *27*(18), 1860-1879.

Uyama, H., Kikuchi, H., & Kobayashi, S. (1995). One-shot synthesis of polyester macromonomer by enzymatic ring-opening polymerization of lactone in the presence of vinyl ester. *Chemistry Letters*, *24*(11), 1047-1048.

Uyama, H., Suda, S., Kikuchi, H., & Kobayashi, S. (1997). Extremely efficient catalysis of immobilized lipase in ring-opening polymerization of lactones. *Chemistry Letters, 26*(11), 1109-1110.

Uyama, H., Suda, S., & Kobayashi, S. (1998). Enzymatic synthesis of terminal-functionalized polyesters by initiator method. *Acta Polymerica*, *49*(12), 700-703.

Van de Velde, K., & Kiekens, P. (2002). Biopolymers: overview of several properties and consequences on their applications. *Polymer Testing*, *21*(4), 433-442.

van der Mee, L., Helmich, F., de Bruijn, R., Vekemans, J. A. J. M., Palmans, A. R. A., & Meijer, E. W. (2006). Investigation of lipase-catalyzed ring-opening polymerizations of lactones with various ring sizes: Kinetic evaluation. *Macromolecules*, *39*(15), 5021-5027.

Varma, A. J., Kennedy, J. F., & Galgali, P. (2004). Synthetic polymers functionalized by carbohydrates: A review. *Carbohydrate Polymers*, *56*(4), 429-445.

Vert, M. (2009). Degradable and bioresorbable polymers in surgery and in pharmacology: beliefs and facts. *Journal of Materials Science: Materials in Medicine*, *20*(2), 437-446.

Villadsen, J., Nielsen, J., & Liden, G. (2011). Bioreaction engineering principles. New York, NY: Springer Science & Business Media.

Walter, E., & Pronzato, L. (1997). Identification of parametric models from experimental data. London (UK): Springer Verlag.

Wang, G. W., & Huang, J. L. (2008). Synthesis and characterization of well-defined ABC 3-Miktoarm star-shaped terpolymers based on poly(styrene), poly(ethylene oxide), and poly(epsilon-caprolactone) by combination of the "living" anionic polymerization with the ring-opening polymerization. *Journal of Polymer Science Part A: Polymer Chemistry*, *46*(3), 1136-1150.

Wang, S. F., Lu, L. C., Gruetzmacher, J. A., Currier, B. L., & Yaszemski, M. J. (2005). A biodegradable and cross-linkable multiblock copolymer consisting of poly (propylene fumarate) and poly (epsilon-caprolactone): synthesis, characterization, and physical properties. *Macromolecules*, *38*(17), 7358-7370.

Wang, X. M., Li, D. M., Qu, M., Durrani, R., Yang, B., & Wang, Y. H. (2017). Immobilized MAS1 lipase showed high esterification activity in the production of triacylglycerols with n-3 polyunsaturated fatty acids. *Food Chemistry*, *216*, 260-267.

Wang, Y. M., Rodriguez-Perez, M. A., Reis, R. L., & Mano, J. F. (2005). Thermal and thermomechanical behaviour of polycaprolactone and starch/polycaprolactone blends for biomedical applications. *Macromolecular Materials and Engineering, 290*(8), 792-801.

Wang, Y., Zhao, W., Liu, D. T., Li, S. H., Liu, X. L., Cui, D. M., & Chen, X. S. (2012). Magnesium and zinc complexes supported by N,O-bidentate pyridyl functionalized alkoxy ligands: Synthesis and immortal ROP of epsilon-CL and L-LA. *Organometallics*, *31*(11), 4182-4190.

Wei, C., Xu, Y., Yan, B. K., Hou, J. Q., Du, Z. Z., & Lang, M. D. (2018). Well-defined selenium-containing aliphatic polycarbonates via lipase-catalyzed ring-opening polymerization of selenic macrocyclic carbonate monomer. *ACS Macro Letters, 7*(3), 336-340.

Williams, D. (2003). Revisiting the definition of biocompatibility. *Medical Device Technology*, *14*(8), 10-13.

Wong, W. H., Lee, W. X., Ramanan, R. N., Tee, L. H., Kong, K. W., Galanakis, C. M., . . . Prasad, K. N. (2015). Two level half factorial design for the extraction of phenolics, flavonoids and antioxidants recovery from palm kernel by-product. *Industrial Crops and Products*, *63*, 238-248.

Woodruff, M. A., & Hutmacher, D. W. (2010). The return of a forgotten polymer - Polycaprolactone in the 21st century. *Progress in Polymer Science*, *35*(10), 1217-1256.

Wu, D., Lv, Y., Guo, R., Li, J., Habadati, A., Lu, B. W., . . . Wei, Z. (2017). Kinetics of $Sn(Oct)_2$-catalyzed ring opening polymerization of epsilon-caprolactone. *Macromolecular Research*, *25*(11), 1070-1075.

Xia, Y., Cao, D., Sun, Y., Li, F. F., & Qi, Z. J. (2016). Cationic ring opening polymerization of octamethylcyclotetrasiloxane initiated by solid superacid. *Glass Physics and Chemistry*, *42*(3), 307-311.

Xu, J. T., Jung, K., Atme, A., Shanmugam, S., & Boyer, C. (2014). A robust and versatile photoinduced living polymerization of conjugated and unconjugated monomers and its oxygen tolerance. *Journal of the American Chemical Society*, *136*(14), 5508-5519.

Yadav, G. D., & Devendran, S. (2012). Lipase catalyzed synthesis of cinnamyl acetate via transesterification in non-aqueous medium. *Process Biochemistry*, *47*(3), 496-502.

Yadav, G. D., & Devi, K. M. (2004). Immobilized lipase-catalysed esterification and transesterification reactions in non-aqueous media for the synthesis of tetrahydrofurfuryl butyrate: Comparison and kinetic modeling. *Chemical Engineering Science, 59*(2), 373-383.

Yan, H. D., Zhang, Q., & Wang, Z. (2014). Biocatalytic synthesis of short-chain flavor esters with high substrate loading by a whole-cell lipase from Aspergillus oryzae. *Catalysis Communications*, *45*, 59-62.

Yang, H. J., Xu, J. B., Pispas, S., & Zhang, G. Z. (2012). Hybrid copolymerization of epsilon-caprolactone and methyl methacrylate. *Macromolecules, 45*(8), 3312-3317.

Yang, J. B., Liu, Y., Liang, X., Yang, Y., & Li, Q. S. (2018). Enantio-, regio-, and chemoselective lipase-catalyzed polymer synthesis. *Macromolecular Bioscience, 18*(7), Article#1800131.

Yang, Y., Ge, Y. K., Zhao, H., Shi, W., & Li, Q. S. (2011). Lipase-catalyzed synthesis of poly(epsilon-caprolactone) and characterization of its solid-state properties. *Biocatalysis and Biotransformation*, *29*(6), 337-343.

Yang, Y., Zhang, J. X., Wu, D., Xing, Z., Zhou, Y. L., Shi, W., & Li, Q. S. (2014). Chemoenzymatic synthesis of polymeric materials using lipases as catalysts: A review. *Biotechnology Advances*, *32*(3), 642-651.

Yao, C. G., Liu, D. T., Li, P., Wu, C. J., Li, S. H., Liu, B., & Cui, D. M. (2014). Highly 3,4-selective living polymerization of isoprene and copolymerization with epsilon-caprolactone by an amidino N-heterocyclic carbene ligated lutetium bis(alkyl) complex. *Organometallics*, *33*(3), 684-691.

Yao, Q. Q., Cosme, J. G. L., Xu, T., Miszuk, J. M., Picciani, P. H. S., Fong, H., & Sun, H. L. (2017). Three dimensional electrospun PCL/PLA blend nanofibrous scaffolds with significantly improved stem cells osteogenic differentiation and cranial bone formation. *Biomaterials*, *115*, 115-127.

Ye, R., Pyo, S. H., & Hayes, D. G. (2010). Lipase-catalyzed synthesis of saccharide-fatty acid esters using suspensions of saccharide crystals in solvent-free media. *Journal of the American Oil Chemists Society*, *87*(3), 281-293.

Yoshida, E., & Osagawa, Y. (1998). Synthesis of poly(epsilon-caprolactone) with a stable nitroxyl radical as an end-functional group and its application to a counter radical for living radical polymerization. *Macromolecules*, *31*(5), 1446-1453.

Yoshida, Y., Kimura, Y., Kadota, M., Tsuno, T., & Adachi, S. (2006). Continuous synthesis of alkyl ferulate by immobilized Candida antarctica lipase at high temperature. *Biotechnology Letters*, *28*(18), 1471-1474.

Zaks, A. (2001). Industrial biocatalysis. *Current Opinion in Chemical Biology*, *5*(2), 130-136.

Zaleska, I. M., Kitagawa, M., Sugihara, S., & Ikeda, I. (2009). Synthesis of biocompatible and biodegradable block copolymers of polyvinyl alcohol-block-poly(epsilon-caprolactone) using metal-free living cationic polymerization. *Journal of Polymer Science Part A: Polymer Chemistry*, *47*(19), 5169-5179.

Zhang, M. J., Su, E. Z., Lin, J. P., & Wei, D. Z. (2012). Lipase-catalyzed continuous ring-opening polymerization of epsilon-caprolactone in a packed-bed reactor. *Chemical and Biochemical Engineering Quarterly, 26*(1), 1-6.

Zhang, Y. Y., Lu, P. Y., Sun, Q. H., Li, T., Zhao, L. J., Gao, X., . . . Liu, J. H. (2018). Lipase-mediated direct in situ ring-opening polymerization of epsilon-caprolactone formed by a chemo-enzymatic method. *Journal of Biotechnology*, *281*, 74-80.

Zhao, H. (2018). Enzymatic ring-opening polymerization (ROP) of polylactones: roles of non-aqueous solvents. *Journal of Chemical Technology and Biotechnology*, *93*(1), 9-19.

Zhao, H., Nathaniel, G. A., & Merenini, P. C. (2017). Enzymatic ring-opening polymerization (ROP) of lactides and lactone in ionic liquids and organic solvents: digging the controlling factors. *RSC Advances*, *7*(77), 48639-48648.

Zhu, N., Huang, W. J., Hu, X., Liu, Y. H., Fang, Z., & Guo, K. (2018). Chemoselective polymerization platform for flow synthesis of functional polymers and nanoparticles. *Chemical Engineering Journal, 333*, 43-48.

Zhu, N., Zhang, Z.-L., He, W., Geng, X.-C., Fang, Z., Li, X., . . . Guo, K. (2015). Highly chemoselective lipase from Candida sp. 99-125 catalyzed ring-opening polymerization for direct synthesis of thiol-terminated poly(epsilon-caprolactone). *Chinese Chemical Letters*, *26*(3), 361-364.